NASA Contractor Report 3691

Aircraft Measurements of Trace Gases and Particles Near the Tropopause

P. Falconer, R. Pratt, A. Detwiler,
C-S. Chen, A. Hogan, S. Bernard,
K. Krebschull, and W. Winters

GRANT NSG-3138
JUNE 1983

25th Anniversary
1958-1983

NASA

NASA Contractor Report 3691

Aircraft Measurements of Trace Gases and Particles Near the Tropopause

P. Falconer, R. Pratt, A. Detwiler,
C-S. Chen, A. Hogan, S. Bernard,
K. Krebschull, and W. Winters
State University of New York at Albany
Albany, New York

Prepared for
Lewis Research Center
under Grant NSG-3138

National Aeronautics
and Space Administration

**Scientific and Technical
Information Branch**

1983

Page intentionally left blank

TABLE OF CONTENTS

INTRODUCTION

The five independent contributions which constitute this report describe various research activities that were supported by the Global Atmospheric Sampling Program under Grant NSG-3138, or which developed independently, using the GASP data base. Chapter 1 was written as a Master of Science thesis by C. S. Chen. Under the direction of R. Pratt, Chen surveyed the characteristics of the particle size spectrum in various meteorological settings from a special collection of GASP data taken near the end of the program. Chapter 2 describes further analysis of that subset of data performed by A. Detwiler, whose specific interest was the relationships between humidity and cloud particles. In Chapter 3, P. Falconer and R. Pratt report climatological and case studies of tropical ozone distributions measured on a large number of flights over the course of the entire program. Finally, Chapters 4 and 5 by A. Hogan and colleagues discuss particle counter calibrations, as well as the comparison of GASP particle data in the upper troposphere with other measurements at lower altitudes, over the Pacific Ocean.

This final report, together with previous publications, completes the documentation of GASP research at the Atmospheric Sciences Research Center. A complete listing of reports and publications resulting from this program is given in the following table.

GASP Bibliography

Holdeman, J. D., G. D. Nastrom, and P. D. Falconer, 1977: An Analysis of the First Two Years of GASP Data, NASA TM-73817, Lewis Research Center, Cleveland, OH. 4 pp.

Falconer, P. D., 1978: Global Atmospheric Sampling Program: Prospects for Establishing a Tropospheric Ozone Budget from Commercial Aircraft Data. Air Quality Meteorology and Atmospheric Ozone, ASTM STP 653 (A. L. Morris and R. C. Barras, editors), Amer. Soc. for Testing and Materials, pp. 479-490.

Falconer, P. D., R. W. Pratt, and V. A. Mohnen, 1978: The Transport Cycle of Atmospheric Ozone and Its Measurement from Aircraft and at the Earth's Surface. Man's Impact on the Troposphere: Lectures in Tropospheric Chemistry (J. S. Levine and D. R. Shryer, editors), NASA Ref. Publ. 1022, Langley Research Center, Hampton, VA. pp. 109-147.

Pratt, R. W. and P. D. Falconer, 1978: Report of Research Activities on the NASA-Global Atomspheric Sampling Program for the Period January 1977 to July 1978. A.S.R.C. Publ. No. 673, Atmospheric Sciences Research Center, State University of New York, Albany, NY, 20 pp.

Pratt, R., and P. Falconer, 1979: Circumpolar Measurements of Ozone, Particles, and Carbon Monoxide from a Commercial Airliner. J. Geophys. Res., 84, pp. 7876-7882.

Hogan, A., and V. Mohnen, 1979: On the Global Distribution of Aerosols. Science, 205, pp. 1373-1375.

Falconer, P., and R. Pratt, 1979: A Summary of Research on the NASA - Global Atmospheric Sampling Program Performed by the Atmospheric Sciences Research Center, NASA CR-159614, Lewis Research Center, OH, 57 pp.

Falconer, P., and R. Pratt, 1980: Comments on "Experimental Evidence for Interhemispheric Transport from Airborne Carbon Monoxide Measurements." J. Appl. Meteor., 19, pp. 338-339.

CHAPTER 1

AIRCRAFT MEASUREMENTS OF THE PARTICLE SIZE SPECTRUM NEAR THE TROPOPAUSE

Cheng-Shih Chen*

1.1 INTRODUCTION

In the atmosphere, particles are related to weather processes and determine the radiative and optical properties of the atmosphere. Previous stratospheric particle research has been described in major references such as Junge (1963), Green and Lane (1964), and Friedlander (1977). But little research has dealt extensively with the upper troposphere and lower stratosphere, i.e. around the tropopause. Atmospheric particle observations have usually been obtained in three ways. First, there are near-surface measurements like those of Junge (1961). More recently, Rosen and Hofmann, (1976) and Ehhalt (1975) have carried out balloon-borne observations. Finally, there are aircraft measurements such as Cadle and Langer (1979) and GAMETAG (1977). In the latter category, most flight measurements are rich in detail but limited in number of cases studied.

During the past 4 years the Global Atmospheric Sampling Program (GASP) of the National Aeronautics and Space Administration (NASA) has acquired an extensive aircraft derived data base. Constituents measured include ozone, water vapor mixing ratio, carbon monoxide, particles, and meteorological data, from automated instrumentation installed on commercial airliners. The simultaneous observation of several such trace constituents, in addition to the meteorological variables, greatly aids interpretation of the data. Since the data are measured and recorded by automated instruments, they cover many parts of the earth over a long period of time. Thus the GASP has obtained a large and geographically extensive data base. However, it is limited in flight level to altitudes around the tropopause, because of the typical flight level of commercial airliners.

The GASP data described in this study also include particularly extensive measurements of condensation nuclei and light-scattering particles. Furthermore, there are data from a special filter modification to the condensation nuclei instrument which permits a rough characterization of the size spectrum of the smallest particles. The size spectrum is related to the age of a particular particle population as discussed in Section 1.4. Such information has never before been collected in such a routine and widespread manner.

* Graduate Student, Department of Atmospheric Science, State University of New York at Albany.

The goal of this chapter is to describe the particle concentrations and size distributions near the tropopause over various synoptic situations and geographical locations, using the GASP data base. This information is of interest in itself, but also permits some general conclusions concerning particle removal processes, as well as cross-tropopause transport of air.

1.2 INSTRUMENTATION

The atmospheric trace constituents used in this study were measured from October 1978 through February 1979. The details of instrumentation and data recording are for the most part covered by Briehl et al., (1980). The usual, and minimum time resolution for all constituents in this study is 5 minutes, or a horizontal distance of about 70 km. at flight velocity.

1.2.1 Ozone

GASP ozone measurements are made using an ultraviolet absorption ozone photometer (Tiefermann, 1979). The concentration of atmospheric ozone is determined by measuring the difference in intensity of an ultraviolet light beam which alternately passes through the sample gas and an ozone-free gas (generated within the instrument). The range of this instrument is from 3 to 20,000 ppbv (parts per billion by volume), with a sensitivity of 3 ppbv.

Laboratory calibrations indicate that the published ozone measurements are probably 9 percent too high. In this study, the relative changes in ozone are of most interest, and no correction has been applied. The random error of the ambient ozone measurement is 3 percent of reading or 3 ppbv, whichever is greater.

1.2.2 Water Vapor

Atmospheric water vapor is measured with a chilled mirror dew/frost point hygrometer (Englund and Dudzinski, 1981). The hygrometer consists of an electronics package, and a thermo-electrically-cooled mirror sensor remotely mounted at the aircraft skin. The hygrometer operates by optically detecting the formation of condensate on the mirror surface as the mirror is cooled to the dew/frost point temperature of the ambient air. The instrument can track dew/frost point changes of about 1.5 deg C per second.

Water vapor data are reported as both dew/frost point temperature and water vapor mixing ratio. Data have been edited out whenever the indicated dew/frost point was more than 10 percent warmer than the ambient air temperature on the ground that this would exceed physically realistic supersaturation values (P. Falconer, private communication referenced by Briehl et al., 1980). The water vapor measurement is not calibrated during flights, but laboratory calibrations indicate a measurement error with a standard deviation of 1.2 deg C, over a range from -68 to +17 deg C.

1.2.3. Light-Scattering Particles

A Royco light-scattering particle detector modified for high altitude use measured the concentrations of particles whose scattering area was equivalent to that of water drops whose minimum diameter equals 0.45 micron. Measured particle densities, in particles per ambient m^3 are reported for particles greater than 0.45, greater than 1.4, and greater than 3.0 micron in diameter (hereafter referred to as PD2, PD4, and PD5, respectively). However PD2 has a high noise to signal ratio, so little emphasis is put on PD2 in this study.

Experience has indicated that flight through clouds results in a significantly greater count of the largest size particles than is obtained in clear air (Reck et al., 1977). A simple cloud detector is thus available by observing the counting rate of the particle size range which yields the PD5 data. This signal is monitored for 255 seconds prior to each data recording. The time (in seconds) during which the signal is greater than a preset level is interpreted as time in clouds. This level was based on visual observation of a light haze, and corresponds to a local particle density in the PD5 range of 66,000 particles per m^3.

1.2.4 Condensation Nuclei

The condensation nuclei concentration measurement (hereafter referred to as CN) is made when an air sample is brought from the GASP inlet probe to the monitor through an 8 m length of 17 mm internal diameter tubing. In the detector system, the pressurized sample is humidified and enters a cloud chamber. An adiabatic expansion process then creates conditions such that the particles act as nucleation sites for the formation of a water droplet cloud. The density of the cloud, assumed to be proportional to the number of particles present, is measured by a light attenuation instrument. The instrument has a full scale of 1000 particles per cm^3 at flight level. The overall accuracy of a concentration measurement is estimated to be better than 10 percent of a reading at concentrations greater than 100 particles per cm^3, for a given type of particle. Noise level in the monitor's output signal is equivalent to less than 10 particles per cm^3 at flight conditions. The time constant (63 percent change) for a step change in inlet concentrations is 6 seconds, which permits high spatial resolution of meteorological conditions. Additional details are given by Nyland (1979).

A local value of CN as well as an average over the previous 240 seconds is recorded at each observation time. The concentration is given in particles per cm^3 at ambient conditions.

1.2.5 Filtered Condensation Nuclei

In addition to the measurement of total CN described above, an independent measurement was made with another CN instrument which drew its sample through a Nuclepore filter. This filter selectively transmits particles of certain ranges proportional to poresize and flow rate. Theory behind this modification is discussed in Section 1.4. The transmission characteristics of the filter for different sizes of particles is affected by particle diffusion, impaction, and interception. These factors are expressed in equations developed by Spurny (1969) which are applied here.

The transmission efficiency ε of a Nuclepore filter is a function of partial efficiency of impaction ε_i, partial efficiency of diffusion ε_D and partial efficiency of interception ε_R. Thus transmission efficiency can be written as:

$$\varepsilon = \varepsilon_i + \varepsilon_D + \delta \cdot \varepsilon_R - \varepsilon_i \cdot \varepsilon_D - \delta \cdot \varepsilon_i \cdot \varepsilon_R$$

$$\varepsilon_i = \frac{2\varepsilon_i'}{1+\xi} - \frac{\varepsilon_i'^2}{(1+\xi)^2}$$

$$\varepsilon_i' = 2\,\mathrm{Stk}\sqrt{\xi} + 2\,\mathrm{Stk}^2\xi \exp\left[-\frac{1}{\mathrm{Stk}\sqrt{\xi}}\right] - 2\,\mathrm{Stk}^2\xi$$

$$\varepsilon_D = 2.56\,N_D^{2/3} - 1.2\,N_D - 0.177\,N_D^{4/3}, \text{ when } N_D < 0.01$$

$$\varepsilon_D = 1 - 0.81904 \exp(-3.6568\,N_D) - 0.09752 \exp(-22.3045\,N_D) - 0.03248 \exp(-56.95\,N_D) - 0.0157 \exp(-107.6\,N_D) \text{ when } N_D > 0.01$$

$$\varepsilon_R = N_R\,(2 - N_R)$$

where

Stk = Stokes number (see Spurney)

N_D = coefficient of diffusive collection (see Spurney)

$$\xi = \frac{\sqrt{P}}{1 - \sqrt{P}}$$

P = porosity = 0.05

N_R = particle radius ÷ pore radius

δ = empirically derived structural parameter of a pore filter.

The calculation here applies to the pressurized state of the sample in the aircraft (850 mb, 280°K). Studies by Shaw (1980) and Twomey (1977) suggest 2 g per cm^3 as an appropriate particle density used in calculating the Stokes number.

Resulting transmission curves for the filter itself are given in Fig. 1-1 for the two pore sizes used in the program. These curves (except curve E) also account for the particle loss in the inlet tubing to the CN counters. According to Dennis (1976), this tubing loss can be expressed as:

$$\frac{n}{n_o} = 0.819 \exp(-14.627\Delta) + 0.096 \exp(-89.22\Delta) + 0.01896 \exp(-212\Delta)$$

where

Δ = aerodynamic coefficient (see Dennis, 1976)

The calculation indicates that diffusion losses in the 8 m length of inlet tubing alone amount to as much as 5 percent, 10 percent, and 50 percent of the particles present for diameters of 0.02 micron, 0.01 micron, and 0.002 micron, respectively. The particle loss in the inlet tube affects both the unfiltered and filtered CN measurements to the same degree.

Table 1-1. Key for Figure 1-1

Curve	Filter Pore Size Diameter (μm)	Assumed Particle Density, s (gcm^{-3})	ζ
A	1	2	0.15
B	1	2	1.00
C	8	2	0.15
D	8	2	1.00
E	8	2	1.00
F	8	21	0.15

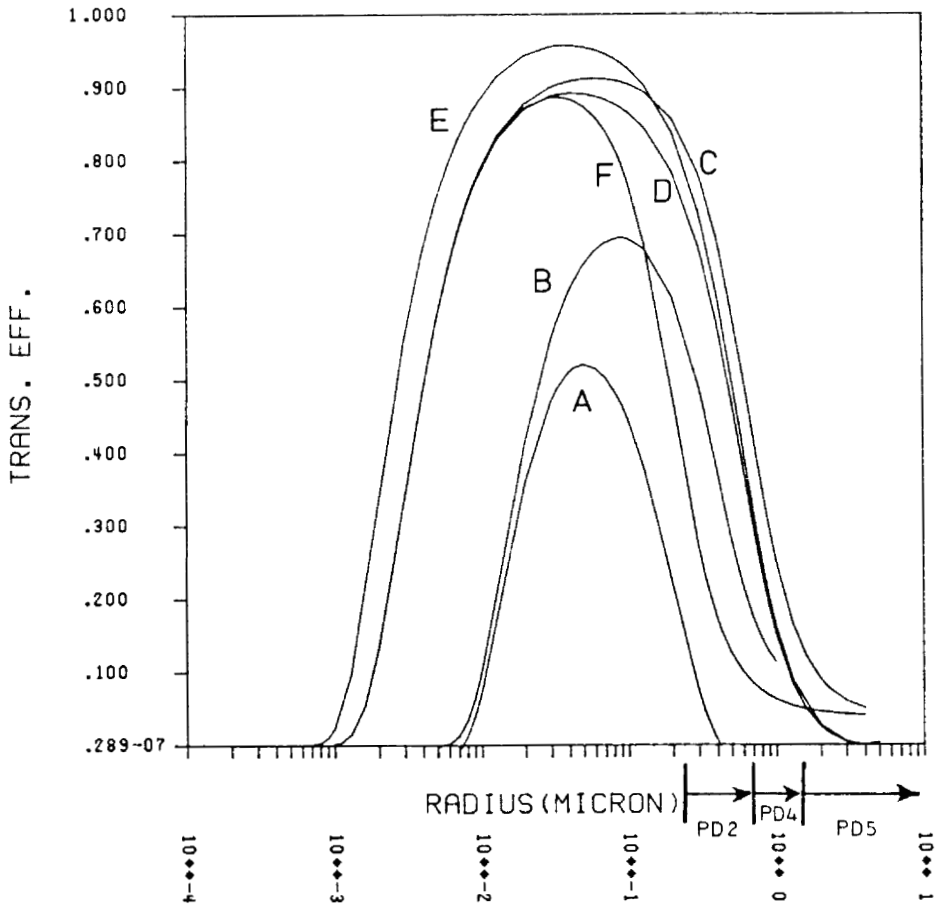

Fig. 1-1. Nuclepore filter transmission efficiency. Table 1-1 lists curve characteristics. All curves except E include inlet tube loss.

1.2.6 Meteorological Data

In addition to the trace constituent measurements, aircraft flight data are obtained to precisely describe meteorological and flight conditions. Aircraft position, heading, and the computed wind speed and direction are obtained from the inertial navigation system. Altitude, air speed, and static air temperature are collected from the central air data computer in the aircraft.

1.3 DATA

The data received from NASA Lewis Research Center is in 2 files as listed by flight and date in Table 1-2. The filter pore size for filtered CN data is 8 microns for file 1, and 1 micron for file 2. As a result of low transmission efficiency and narrow collecting range for the 1 micron filter (Fig. 1-1), most of the filtered CN data (hereafter FCN) in file 2 is very small and in the range of measurement error. Since the FCN data plays an important role in our interpretation, only the first file of data is used. For this study three derived variables were calculated for all file 1 flights: relative humidity with respect to water and relative humidity with respect to ice, and the ratio of total CN to FCN.

Computer plots of each flight served as the basis of the case studies described in Section 1.5. The legend in Table 1-3 applies to the plots presented in Section 1.5. Other details concerning the plots are as follows:

(1) The plot titles give flight departure data, departure-arrival airport pair, and flight number.
(2) The abscissa is Greenwich Mean Time (GMT).
(3) Some variables are not always recorded every 5 minutes, so the data spacing is irregular.
(4) Data not included in the range given in table 1-3 are not plotted.

For every flight, one or more National Meteorological Center (NMC) synoptic analysis maps were collected from the microfilm. For convenient reference, some of the flight routes were drawn on a polar stereographic projection of the Northern Hemisphere as shown in Fig. 1-2. Then the routes were mapped onto the synoptic analyses. After examining both the flight plots and synoptic maps, the flights were divided into categories of meterological interest which are described in Section 1.5.

TABLE 1-2 - GASP DATA USED IN CHAPTER 1 ANALYSES

A) FILE 1 (From VL0023, File 1)

	FLIGHT ROUTE	DEPARTURE DATE	DATA TIME INTVL(GMT)	NDATA
33	GP409 LAX-SFO	10/24/78	0203-0228	6
34	" SFO-NRT	10/24/78	2047-0633	114
35	" NRT-HNL	10/25/78	1232-1834	99
36	" HNL-PDX	10/25/78	2131-0146	51
37	" PDX-HNL	10/26/78	1856-2331	54
38	" HNL-PDX	10/27/78	0145-0552	48
39	" PDX-HNL	10/27/78	1716-2206	54
40	" HNL-OSA	10/28/78	0017-0755	106
41	" OSA-HNL	10/28/78	1041-1717	139
42	" HNL-NRT	10/29/78	0139-0638	75
43	" NRT-HKG	10/29/78	0929-1315	57
44	" HKG-DEL	10/29/78	1531-2019	59
45	" DEL-THR	10/29/78	2301-0205	37
46	" THR-FRA	10/30/78	0508-0914	47
47	" FRA-LHR	10/30/78	1114-1149	8
48	" LHR-JFK	10/30/78	1435-2055	77
49	" JFK-IAH	11/ 1/78	0252-0523	28
50	" IAH-JFK	11/ 1/78	1930-2140	27
51	" JFK-LHR	11/ 2/78	0049-0603	78
52	" LHR-FRA	11/ 2/78	0845-0910	6
53	" FRA-THR	11/ 2/78	1131-1534	96
54	" THR-BKK	11/ 2/78	1813-2333	65
55	" BKK-HKG	11/ 3/78	0131-0316	22
56	" HKG-NRT	11/ 3/78	0533-0813	33
57	" NRT-LAX	11/ 3/78	1125-1925	166
58	" LAX-HNL	11/ 4/78	0110-0537	54
59	" HNL-PPG	11/ 4/78	0755-1220	51
60	" PPG-PPT	11/ 4/78	1418-1613	22
61	" PPT-LAX	11/ 5/78	0720-1418	83
62	" LAX-SFO	11/ 5/78	1702-1727	6
63	" SFO-NRT	11/ 5/78	2143-0743	116
64	" NRT-HNL	11/ 6/78	1245-1826	161
65	" HNL-OSA	11/ 6/78	2345-0727	97
66	" OSA-HNL	11/ 7/78	1043-1718	79
67	" HNL-LAX	11/ 7/78	2135-0149	68
68	" LAX-JFK	11/ 9/78	0227-0632	48
69	" JFK-ATH	11/ 9/78	0852-1716	99
70	" ATH-BGR	11/ 9/78	2054-0521	100
71	" BGR-LAX	11/10/78	0830-1345	62
72	" LAX-PIK	11/10/78	2247-0652	96
73	" PIK-LHR	11/11/78	0839-0909	7
74	" LAX-HNL	11/12/78	0625-1045	51

A) FILE 1 (From VL0023, File 1)

	FLIGHT ROUTE	DEPARTURE DATE	DATA TIME INTVL(GMT)	NDATA
75	" HNL-LAX	11/12/78	2059-0114	51
76	" LAX-HNL	11/13/78	0602-1027	49
77	" HNL-AKL	11/13/78	1326-2103	108

TABLE 1-2 - CONTINUED

B) FILE 2 (From VL0024, File 1)

	FLIGHT ROUTE		DEPARTURE DATE	DATA TIME INTVL(GMT)	NDATA
117	GP425	JFK-LHR	2/ 9/79	1537-2114	120
118	"	LHR-LAX	2/10/79	1246-2235	127
119	"	LAX-HNL	2/11/79	0542-1042	75
120	"	HNL-OSA	2/11/79	2336-0750	95
121	"	OSA-HNL	2/12/79	1037-1634	83
122	"	HNL-NRT	2/12/79	2152-0512	87
123	"	NRT-HKG	2/13/79	0822-1232	50
124	"	HKG-DEL	2/13/79	1438-2001	60
125	"	DEL-FRA	2/13/79	2157-0637	99
126	"	FRA-LHR	2/14/79	0815-0850	8
127	"	LHR-JFK	2/14/79	1138-1742	71
128	"	JFK-IAH	2/15/79	0001-0226	29
129	"	IAH-MEX	2/15/79	0420-0539	17
130	"	MEX-IAH	2/15/79	1647-1749	30
131	"	IAH-JFK	2/15/79	2049-2249	24
132	"	JFK-LHR	2/16/79	0210-0735	61
133	"	LHR-FRA	2/16/79	1024-1054	7
134	"	FRA-DEL	2/16/79	1316-2041	81
135	"	DEL-HKG	2/16/79	2222-0253	67
136	"	HKG-NRT	2/17/79	0527-0803	32
137	"	NRT-LAX	2/17/79	1053-1903	99
138	"	LAX-SFO	2/17/79	2152-2217	6
139	"	SFO-SEA	2/18/79	0109-0204	12
140	"	SEA-LHR	2/18/79	0400-1230	101
141	"	LHR-SEA	2/18/79	1525-2347	154
142	"	SEA-SFO	2/19/79	0237-0337	13
143	"	SFO-NRT	2/20/79	0022-0952	115
144	"	NRT-HNL	2/20/79	1245-1815	3733

Table 1-3. Plot Legend for Figures 1-4; 1-6;1-10; and 1-13.

Variable	Symbol	Position	Label	Unit	Range
Wind Speed	W	Lower	MPS	M/S	0 to 100
Wind Direction	D	Lower	WINDR	deg	0 to 360
Temperature	T	Lower	TEMP	deg C	-68 to -35
Dew/frost Point Temperature	F	Lower	DFPT	deg C	-68 to -35
Cloud Seconds	S	Lower	CLSEC	seconds	0 to 256
Ozone Mixing Ratio	O	Lower	OZONE	ppbv	0 to 300
Water Vapor Mixing Ratio	H	Lower	H20	ppmw	0 to 800
Aerosol Concentration ($d \geq 0.45\,\mu m$)	2	Upper	PD2	$no./m^3$	10^5 to 10^7
Aerosol Concentration ($d \geq 1.4\,\mu m$)	4	Upper	PD4	$no./m^3$	10^3 to 10^6
Aerosol Concentration ($d \geq 3\,\mu m$)	5	Upper	PD5	$no./m^3$	10^1 to 10^6
Filter Ratio	/	Upper	CN/FCN	--	0 to 10
Condensation Nuclei	C	Upper	CN	$no./cm^3$	0 to 1000
Filted Condensation Nuclei	F	Upper	FCN	$no./cm^3$	0 to 1000
Altitude	P	Upper	PAMB	mb	180 to 300

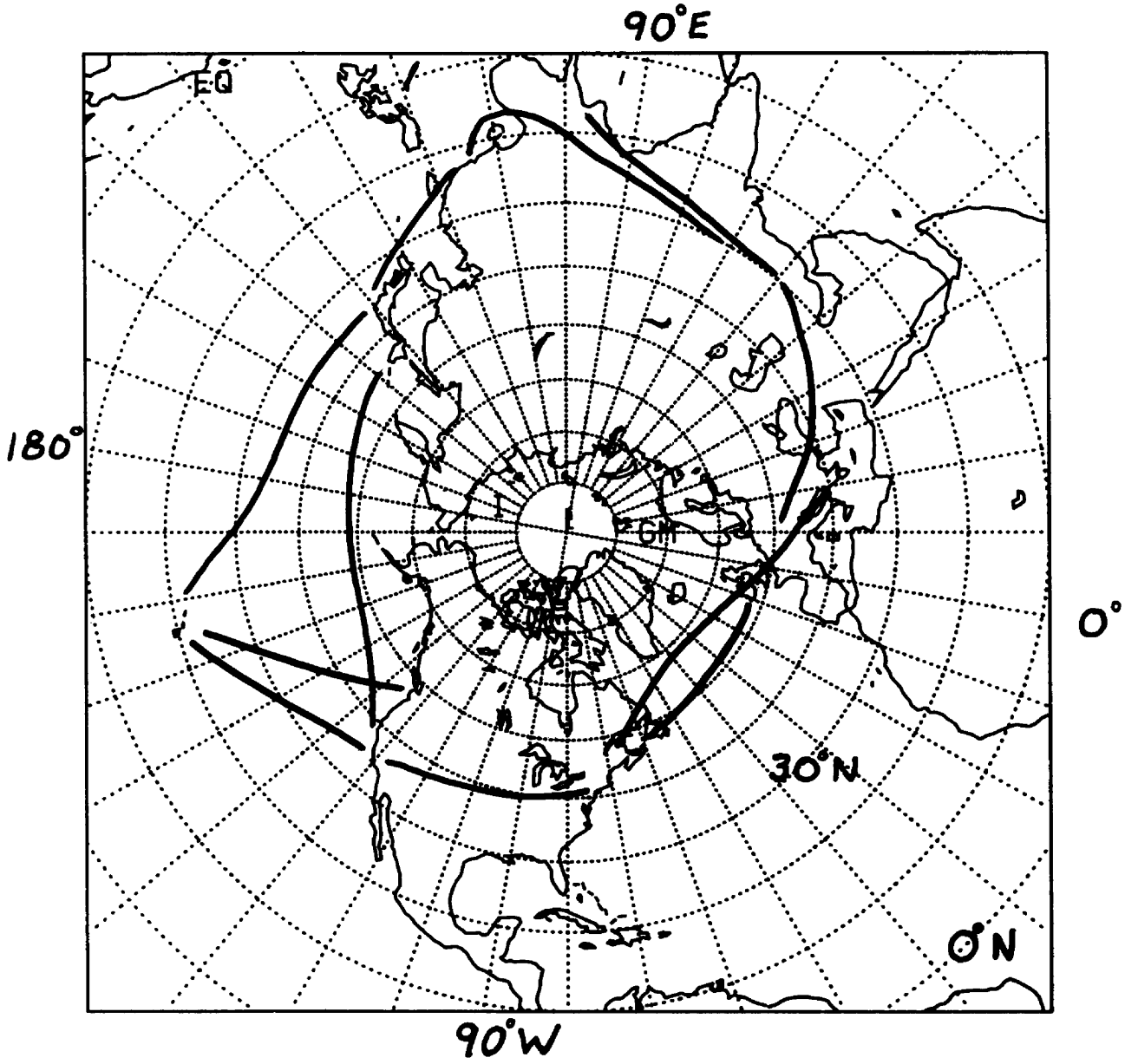

Fig. 1-2. Some major flight routes in the GASP

1.4 INTERPRETATION OF PARTICLE DATA IN TERMS OF THE SIZE SPECTRUM

In the discussion, the filter ratio will be used as an important variable in interpreting the size spectrum of atmospheric particles. The filter, or "tranmission", ratio is defined as the local CN/FCN. Particles counted as CN may range in size from 0.001 to about 10 microns (paticles smaller than 0.001 micron are removed by the inlet tubing), and apparently have a tropospheric source, especially near the earth's surface (e.g. Junge, 1961; Hoppel, 1973). Fresh particle populations usually are characterized by decreasing number concentration with increasing radius (see unfiltered curve in Fig. 1-3). At GASP flight level, for instance, CN have a typical value of roughly 180 particles per cm^3 in the troposphere, and only 40 particles per cm^3 in the stratosphere.

The 8 micron filter response curves in Fig. 1-1 show a maximum transmission at about 0.05 micron in radius. This was deliberately chosen to be close to the size of particles which are most long-lived in the atmosphere, because they are the size least affected by removal processes (Twomey, 1977). Removal processes tend to modify the ambient size distribution toward one resembling the transmission curves in Fig. 1-1 in shape (also see filtered curve in Fig. 1-3). Thus, a population of particles with a size spectrum peaking roughly in the range of 0.01-0.05 micron radius may be considered an aged spectrum. Here, "removal" means removal of a particle from its original size range, rather than physical removal from the local area. In the GASP data region, particles are removed mainly by coagulation, a process whereby particles join through collision. This process is particularly effective in reducing the concentration of small particles when large particles are present. Furthermore, when relative humidity with respect to water is greater than about 30 percent, particles start to grow by water vapor deposition (Pruppacher and Klett, 1978). Thus the growth of water or ice cloud particles broadens the size spectrum and will enhance the coagulation efficiency greatly (Twomey, 1977). Besides coagulation, sedimentation tends to remove the largest particles, but this effect is usually dominated by air motions at GASP altitudes.

In a well-fed aerosol population, the filter ratio (CN/FCN) decreases toward unity with time. Hereafter, the filter ratio will be used as an indicator of air with aged particle populations, with a rough inverse proportionality to the magnitude of filter ratio. In most situations, stratospheric air tends to have a small filter ratio (aged particles), as well as low absolute CN and FCN concentrations, while tropospheric air tends to have a larger filter ratio (fresh particles), mostly due to its large and fresh CN populations.

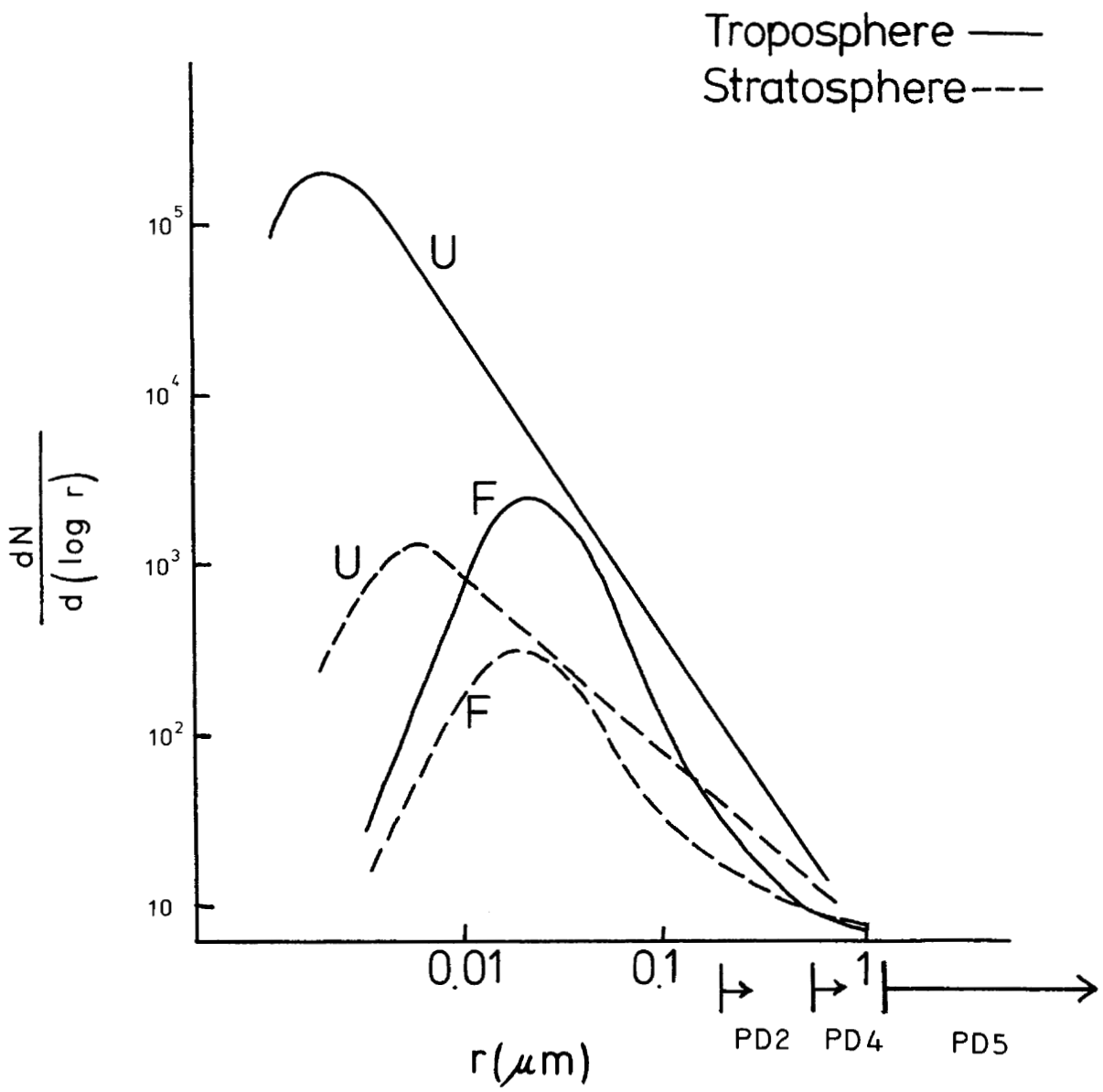

Fig. 1-3. Schematic comparison of unfiltered (U) and filtered (F) size distributions for stratosphere and troposphere.

1.5 CASE STUDIES

Four meteorologically defined categories were used to group the flights for further study.

(1) Trough crossings, where the tropopause was penetrated away from the presence of high wind.

(2) Jet crossings, in which strong winds and wind shear were observed as the aircraft flew across an upper level jet core nearly orthogonally.

(3) Along jets, for flights nearly parallel to an upper level jet such that the aircraft experienced much lower gradients than in (2) and sampled extensively on one side of the jet or the other.

(4) Tropical flights as distinct from the above mid-latitude cases. This category is easily subject to deep convection and always in tropospheric air.

1.5.1 Trough Crossings

Flight 41 (Table 1-2) shown in Figure 1-4 provides an example of constituent behavior during transitions between tropospheric and stratospheric air. The closest 200 mb upper air analysis available is 1200 GMT on 28 October 1978 (Fig. 1-5). This and subsequent analyses show a deepening trough tilted southwest-northeast over the mid Pacific, which the aircraft penetrated at about 1500 GMT.

Referring to Figure 1-4, penetration of stratospheric air is first recognized by the backing of the wind direction from north into the west, accompanied by a progressive increase in the ozone mixing ratio, beginning at approximately 1500 GMT. Concurrently, the water vapor mixing ratio decreases. The sharpest ozone gradients (1530 and 1605 GMT) are coincident with sharp temperature gradients, which can be interpreted as resulting from the plane's penetration of the thermally stable layer which constitutes the local tropopause. Lack of sounding information in the area rules out any investigation of the details of the tropopause region. The asymmetry of the temperature trace about the trough axis reflects the asymmetric height pattern of the trough evident on the 200 mb analysis.

A drop in CN and FCN particle concentrations corresponds clearly to the stratospheric portion of the flight as defined by ozone and the thermal structure. Since the two values are nearly equal in the stratosphere, the filter ratio (CN/FCN) is approximately one, reflecting the well-aged nature of the air. Presumably, most of the small particles (diameters less than 0.01 micron), which contribute to high CN levels in the troposphere, have been removed by coagulation in the stratosphere, leaving mostly particles which are also large enough to be passed by the Nuclepore filter.

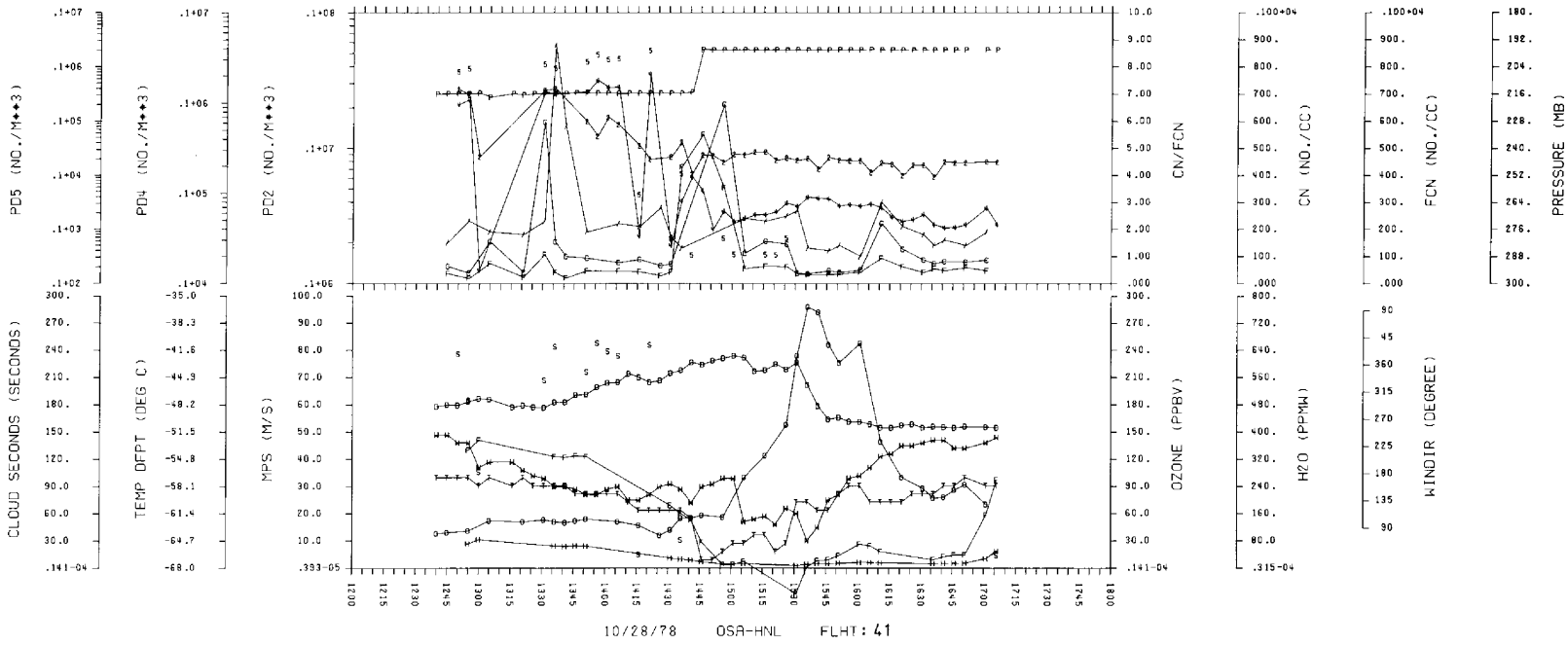

Fig. 1-4. Trough crossing flight plot. Osaka (OSA) to Honolulu (HNL) on October 28, 1978.

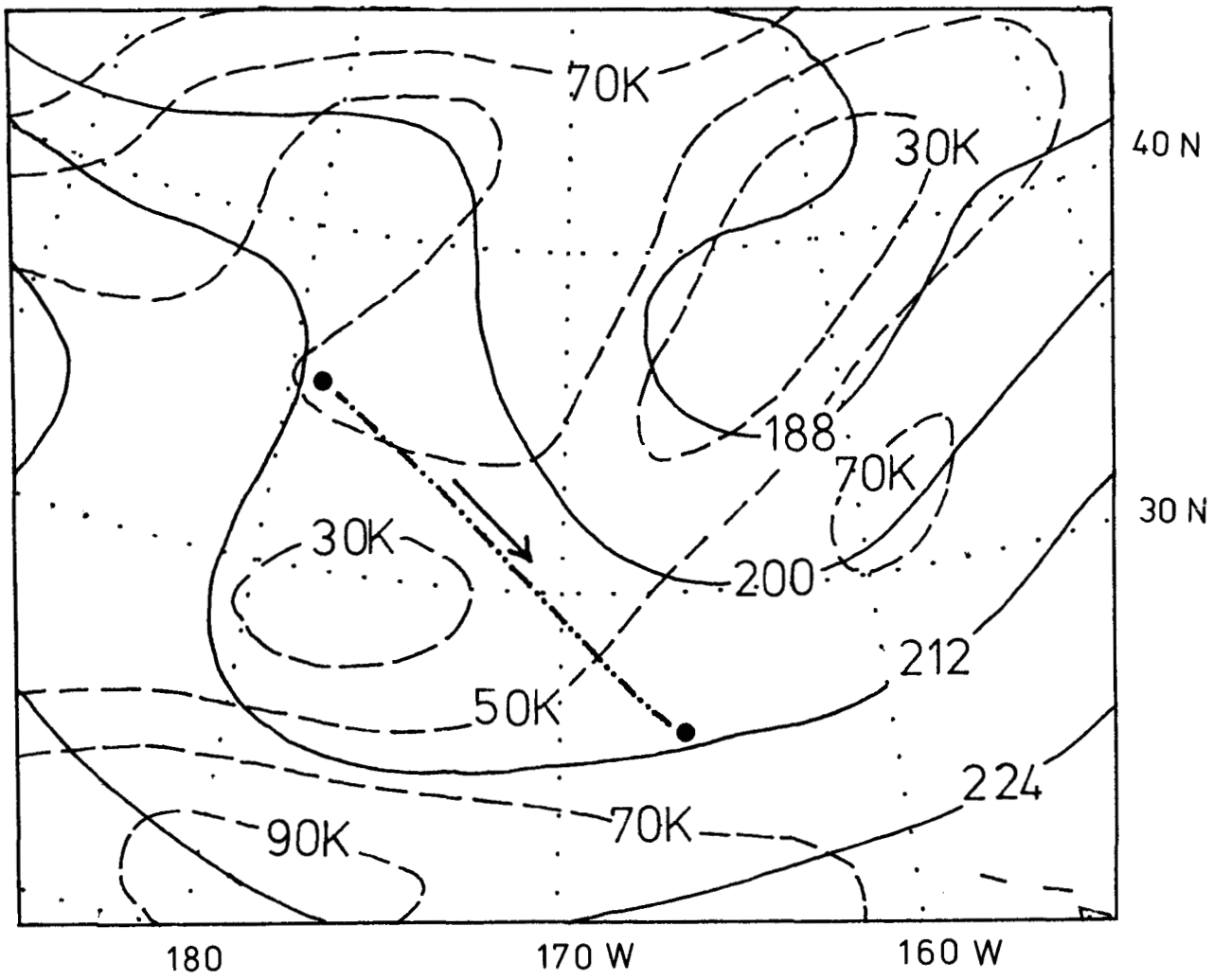

Fig. 1-5. Simplified NMC 200 mb analysis, 1200 GMT 28 October 1978. Flight segment discussed in the text is indicated by the dashed-dotted line. Solid lines represent geopotential height contours, in meters (e.g. 212 = 12,120 gpm). Dashed lines are isopleths of windspeed, in knots.

Another particle characteristic typical of the stratosphere is the maintenance of PD4 at a steady value of about 10^4 particles per m^3. This behavior is evident in Fig. 1-4, and is discussed further in Section 1.6 Finally, the absence of any PD5 observation reflects the lack of large particles (and cloud) in the stratosphere. This is in contrast to the abundant and variable large particle counts and cloud second observations in the tropospheric part of the flight prior to 1500 GMT.

1.5.2 Jet Crossings

Flight 48 (Table 1-2), shown in Figure 1-6, is chosen here as representative of flights across the core of the jet stream. On 30 October 1978, the 250 mb synoptic analysis (Fig. 1-7) shows a jet stream over the east coast of Canada. The airplane transected the jet between 1910 and 2045 GMT at a flight level of 238 mb. Flight wind speed data are in good agreement with a sounding made close to the jet maximum, which reports a maximum wind of 77 m/s at 235 mb.

The aircraft (Fig. 1-6) measured a peak wind of 73 m/s at 1940 GMT which is very close to the jet maximum from the sounding. Before reaching the maximum wind, the temperature dropped 5 deg C at constant flight level. This is equivalent to a 12 deg C change in potential temperature within 260 km, and represents an unusually intense temperature gradient for these altitudes.

The schematic jet structure shown in Fig. 1-8, suggested by Shapiro (1978) is useful in understanding this jet crossing. Because Shapiro's cross sections are based on several levels of meso-scale flight data as well as sounding data, it was possible for him to calculate potential vorticity distributions around jet streams for a few cases. In his paper, high concentrations of ozone typical of the stratosphere and high values of potential vorticity were observed to coincide near jet streams where stratospheric air was extruded into the upper troposphere. Calculations made in the course of this study indicated that detailed potential vorticity distributions could not be defined with GASP data, even when sounding data was available.

A cross section of the jet (parallel to flight 48) was constructed from the limited sounding data available at 1200 GMT, 30 October 1978, approximately 8 hours prior to the plane's passage (Fig. 1-9). The aircraft temperature data was used to influence some details of the vertical cross section analysis of potential temperature. However, from the synoptic analysis before and after this time, the 250 mb pattern is seen to be rapidly changing in time; the trough line shifted eastward 10 degrees of longitude in 12 hours. Therefore, this cross section may not well represent that at the flight time, and the

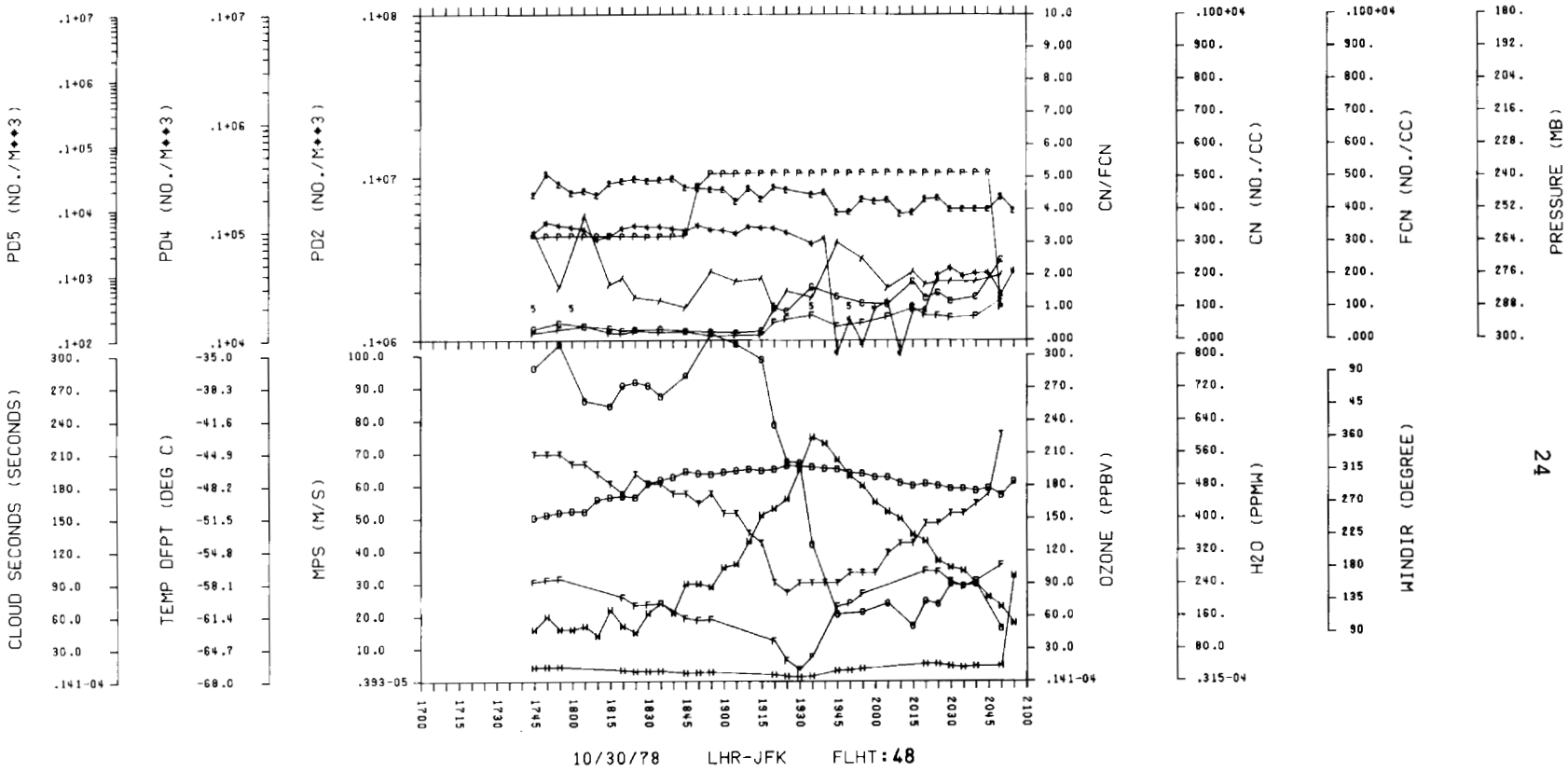

Fig. 1-6. Cross jet flight plot. London (LHR) to New York City (JFK) on October 30, 1978.

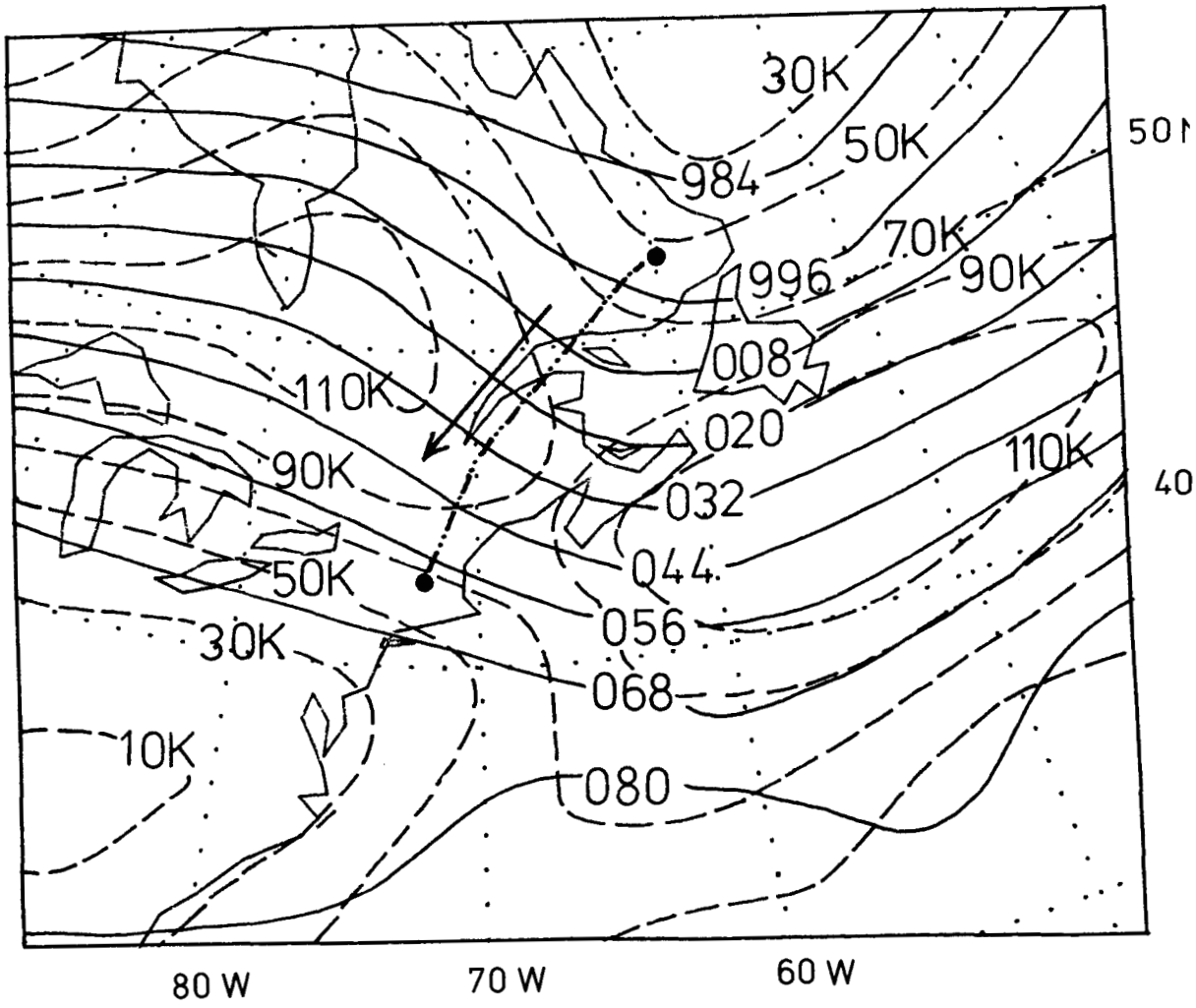

Fig. 1-7. Simplified NMC 250 mb analysis, 1200 GMT 30 October 1978. Flight segment discussed in the text is indicated by the dashed-dotted line. Solid lines represent geopotential height contours, in meters (e.g. 008 = 10,080 gpm). Dashed lines are isopleths of windspeed, in knots.

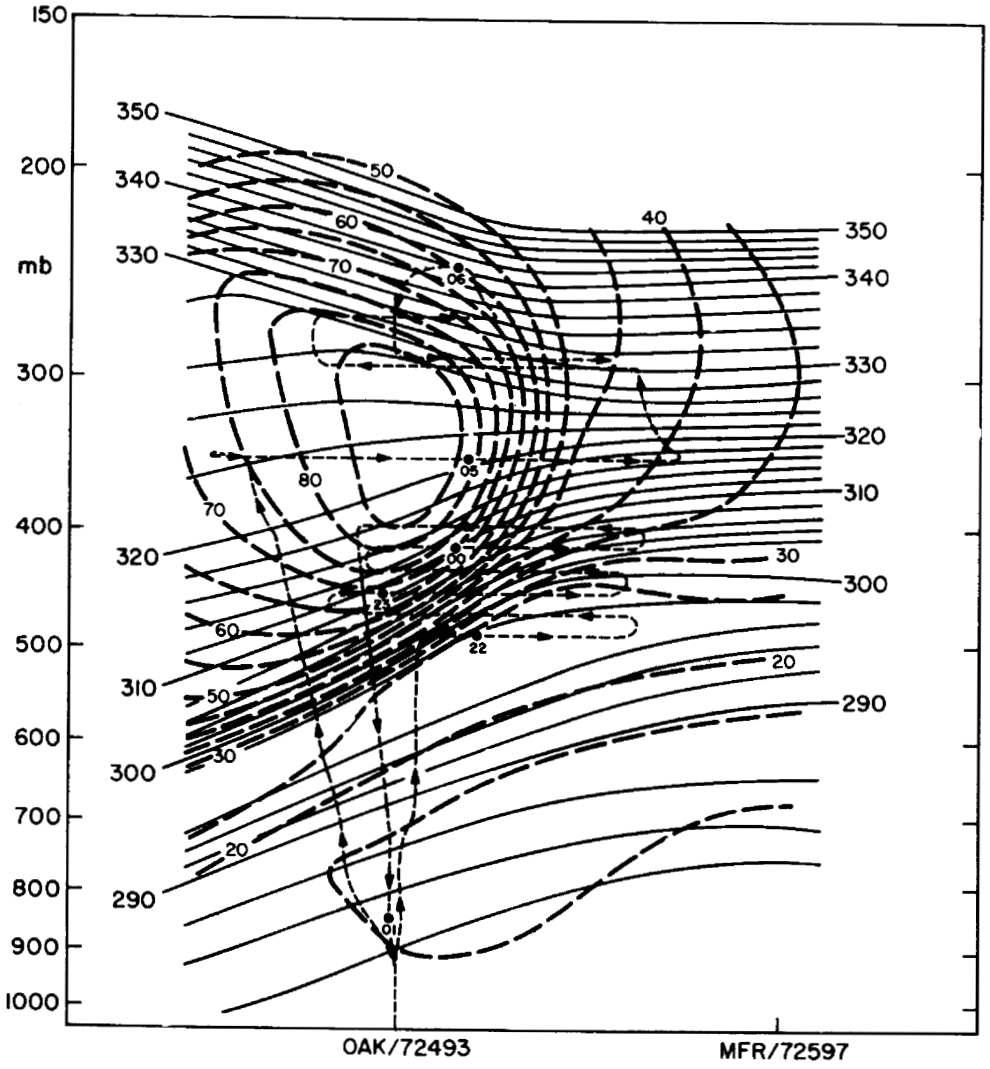

Fig. 1-8. Cross section analysis for 0000 GMT 16 April 1976, reproduced from Shapiro (1978). Windspeed (m/s), heavy dashed lines; potential temperature (^{o}K), solid lines. Flight path, light dashed lines with GMT hours, solid circles.

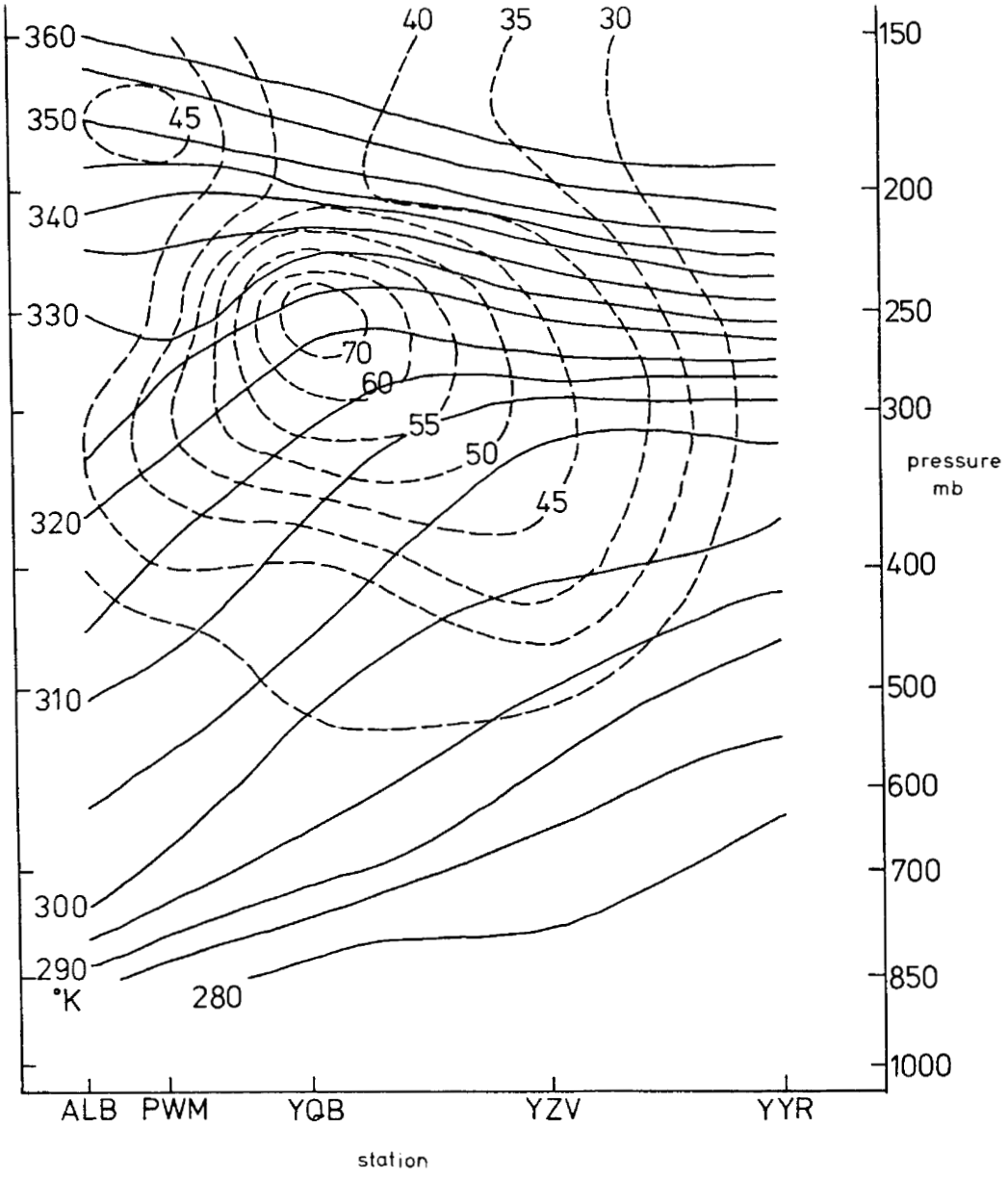

Fig. 1-9. Cross section of flight 48: 1200 GMT 30 October 1978. Wind speed (m/s), dashed line; potential temperature (°K), solid lines.

flight data should not be expected to coincide exactly with the cross section. The aircraft measured a wind increase from 43 m/s to 75 m/s in about 325 km, equivalent to a wind shear of about $10^{-4}s^{-1}$, and therefore, comparable to that in Shapiro's example. The temperature trace in Fig. 1-6 is asymmetrical with respect to the jet maximum, with a nearly discontinuous temperature change on the poleward side of the jet, at 1915 GMT. Although it would be interesting to construct the 3-dimensional structure of this feature, which has no obvious counterpart in Shapiro's cases, this is not possible with the data available. The boundary between stratospheric and tropospheric ozone levels in Fig. 1-6 is located in the same position with respect to the jet core as in Shapiro's case. Shapiro's calculations indicate that the ozone gradient corresponds to a strong potential vorticity gradient on the poleward side of the jet, which is manifested in Fig. 1-6 by the strong wind shear from 1900 to 1930 GMT. In general, this cross section analysis is consistent with Shapiro's. However, we cannot resolve the meso-scale potential vorticity distribution, which may be present due to the wind shear (Fig. 1-6). This underscores one recurring dilemma associated with the GASP data, namely that the spatial resolution in our data analysis is restricted to non-continuous observations along a particular path and to twice-daily, synoptic scale radiosounding profile data.

The comparison with Shapiro's case is useful for interpreting the particle distributions shown in Fig. 1-6. One might expect strong particle gradients in the vicinity of the jet core and coincident with the ozone gradient. However, while CN, water vapor and the filter ratio are low in the stratosphere, as expected, the change in these variables near the jet is not as dramatic as the ozone change. The gradients across the tropopause in other situations are generally sharper (category 1), but wind speed is generally much lower as well. Therefore, the lack of strong gradient may be a result of mixing near the jet core, which could be accomplished by turbulent motions (Shapiro, 1978). As in category 1, PD4 is seen to have a high, rather constant level in the stratosphere. It is interesting that the constituents which are abundant in the stratosphere (PD4 and ozone) show a sharp gradient across the jet, while those which originate in the troposphere (CN and water) show a much weaken gradient. This may be a result of a general asymmetry in the mixing processes across the interface of tropospheric and stratospheric air, near jet streams.

1.5.3 Along Jets

The GASP airliner flights were frequently oriented parallel to jet streams to reduce fuel consumption on eastward flights.

Flight 57 (Fig. 1-10) has a route parallel to the jet stream axis over the Northern Pacific Ocean. This jet stream (Fig. 1-11) is strong not only in its wind speed (90 m/s), but also in longitudinal scale, and in vertical scale, since it extended from 300 mb to 200 mb with similar strength.

In the flight data, wind speeds greater than 70 m/s prevailed from 1300 GMT to 1515 GMT. This 2 1/4 hour interval will be referred to as the along-jet region. Frost point temperature is about the same as ambient temperature through the region, and water vapor mixing ratio is double its value outside the region. The presence of large particles is indicated by cloud second readings, and high particle concentrations in the PD4 and PD5 size ranges, which correspond to small ice crystal size at this altitude. All the features above suggest the presence of cloud, which at this altitude would be of the cirrus variety such as is frequently found on the equatorial (ascending) side of jet streams (Mahlman, 1973). Not surprisingly, cloud cover is reported by surface stations below this region; however, these were primarly low and middle level cloud decks associated with an occluding low pressure disturbance ahead of the upper jet stream core (Fig. 1-12).

The high moisture and particle levels, and low ozone, indicate this segment of the flight was in the troposphere. But the filter ratio averages 1.3, which is a typical value for stratospheric air. The filter ratio is usually higher in tropospheric cases, especially with cloudiness, and in this respect this flight is atypical. Section 1.4 described the coagulation process which is effective in removing particles, especially in wet and persistent situations like this case. Judging from the flight data, the aircraft must have experienced nearly or completely ice saturated air over the 1600 km interval of particle encounter. Thus the moisture and vertical motion around the intense jet in this case may have produced unusually effective coagulation conditions, which would rapidly remove the smallest particles, while not affecting the larger particles appreciably. Thus the meteorological conditions may have enhanced the aging process, leading to a filter ratio lower than usually observed in the troposphere. In other similar tropospheric cases, the filter ratio is probably higher either because it is not as wet, and the coagulation efficiency is lower, or the cloud system is not as uniform, such that fresh populations of CN are continually injected (such as in deep, cellular convection in the tropics).

1.5.4 Tropical Comparison

Fig. 1-13 (Flight 61 in Table 1-2) serves as an example of the tropical flights in the data set, most of which occur over open ocean and are therefore lacking upper air analyses. All such

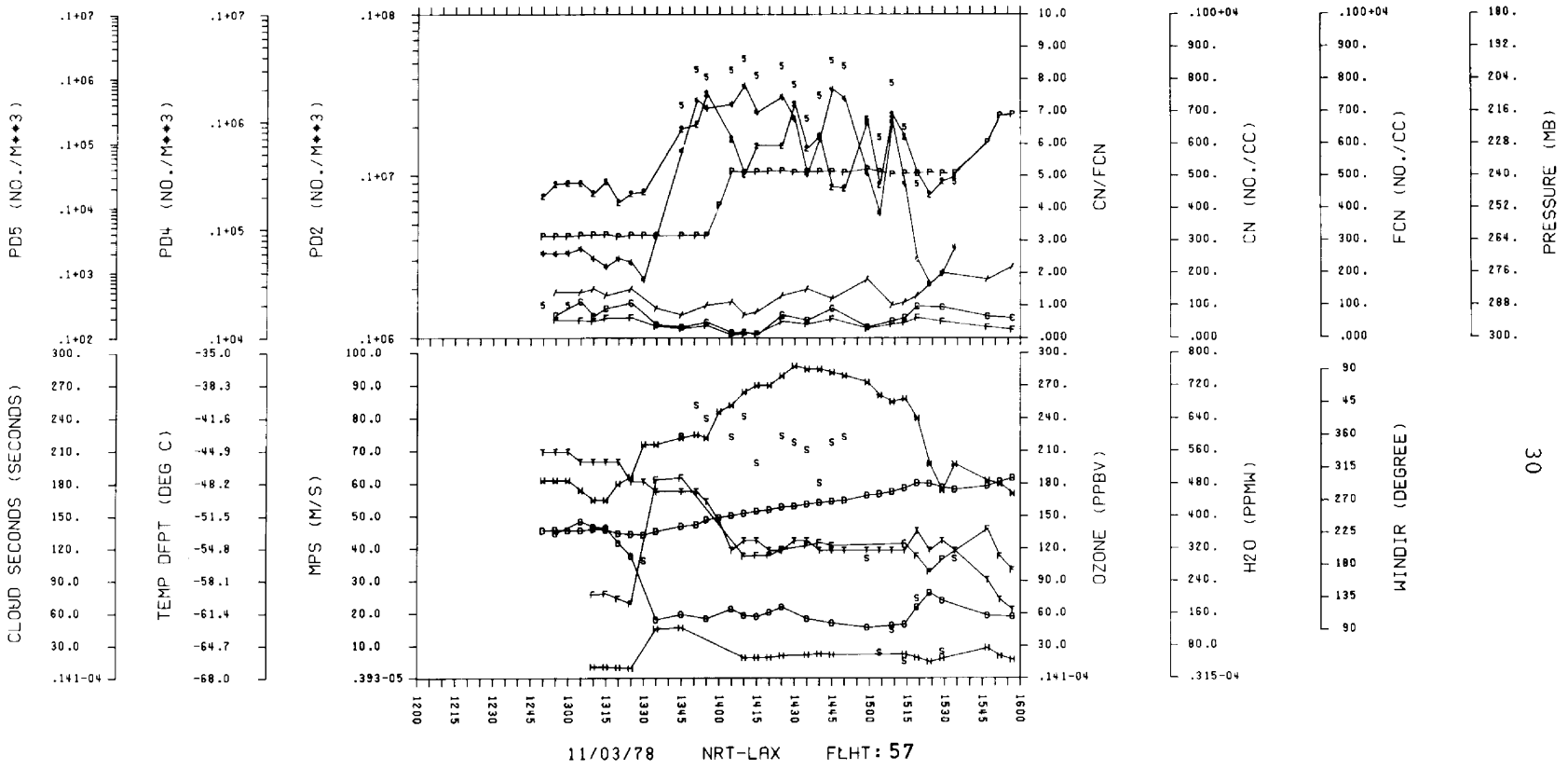

Fig. 1-10. Along jet flight plot. Tokyo (NRT) to Los Angeles (LAX) on November 3, 1978.

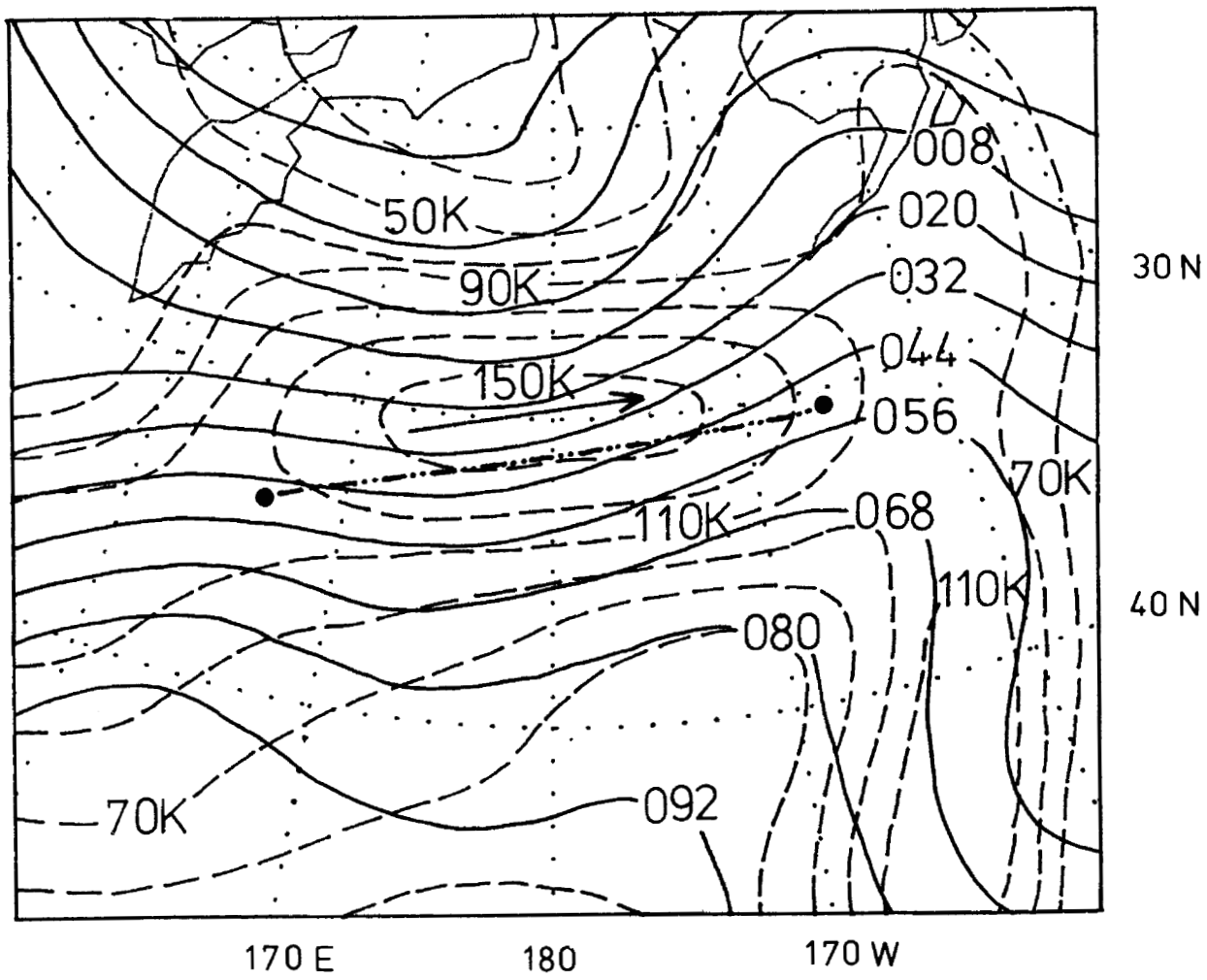

Fig. 1-11. Simplified NMC 250 mb analysis, 1200 GMT 3 November 1978. Flight segment discussed in the text is indicated by the dashed-dotted line. Solid lines represent the geopotential height contours, in meters (e.g. 008 = 10,080 gpm). Dashed lines are isopleths of windspeed, in knots.

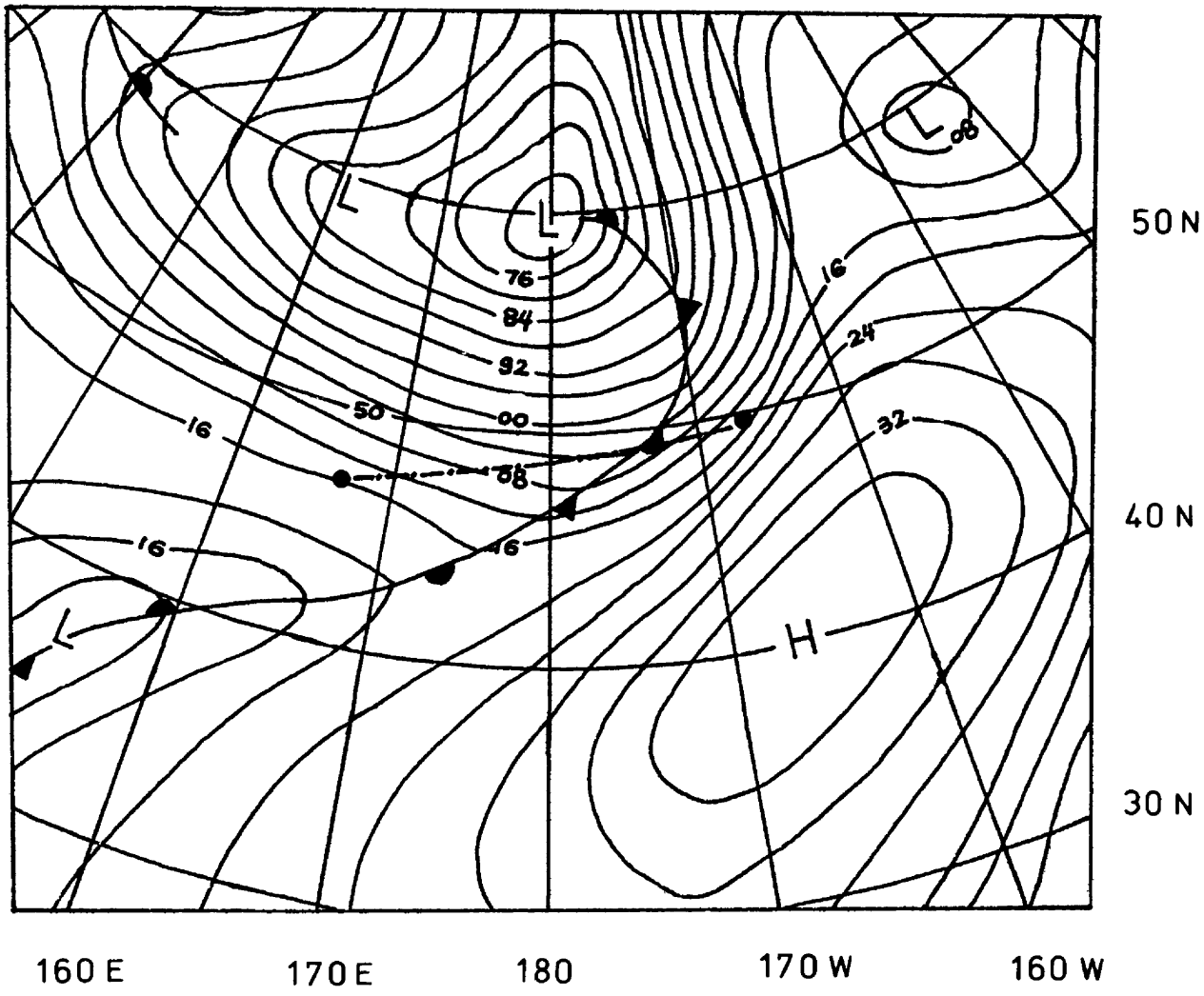

Fig. 1-12. Simplified NMC surface analysis, 1200 GMT, 3 November 1978. Flight segment discussed in the text is indicated by the dashed-dotted line. Solid lines represent the surface isobars, in millibars (e.g. 92 = 992 mb).

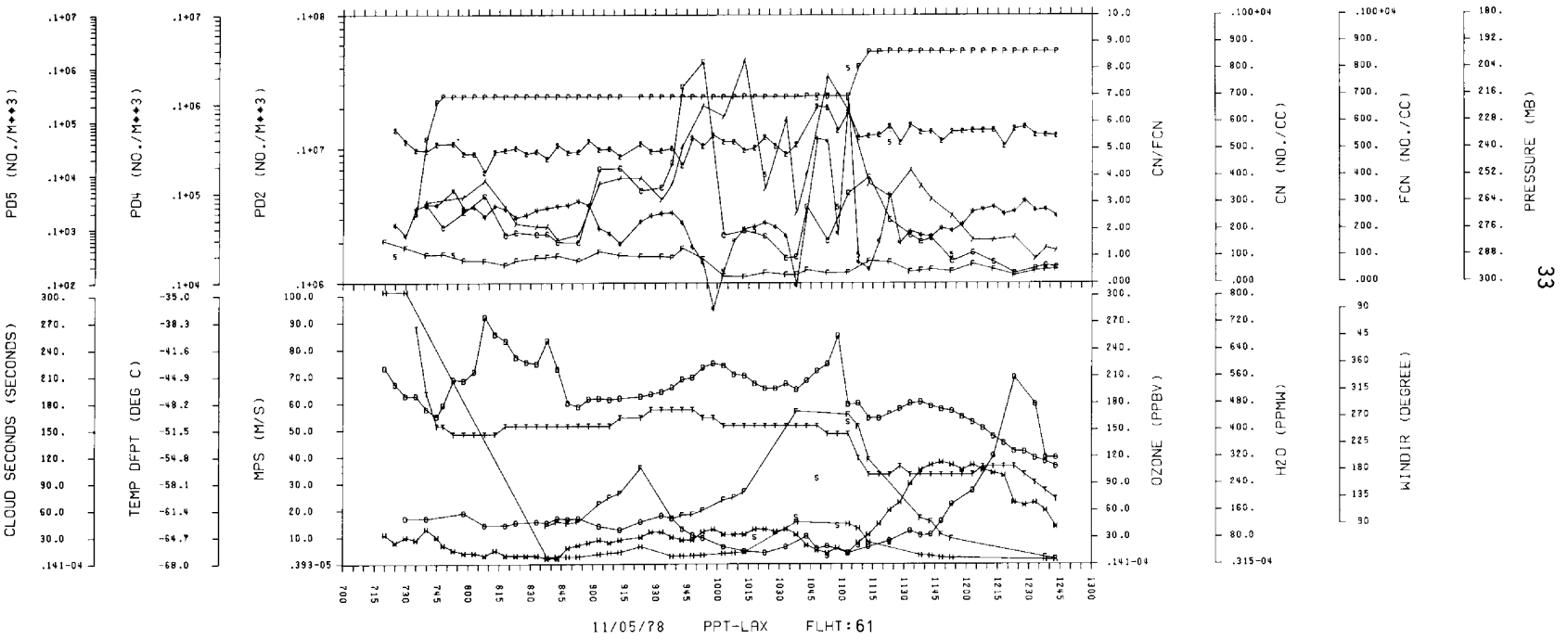

Fig. 1-13. Tropical flight plot. Tahiti (PPT) to Los Angeles (LAX) on November 5, 1978.

flights were located well below the high tropical tropopause, and recorded nearly constant temperature across the equatorial zone, as well as low ozone concentrations (averaging 34 ppbv in Fig. 1-13). The water vapor mixing ratio is higher in the cloudy region (from 1015 to 1115 GMT) than is usually seen in mid-latitude cases. The filter ratio tends to be more variable, and also reaches higher values, than in the mid-latitudes.

1.6 DATA BASE PROPERTIES

This section describes average properties based on the entire data set, or subsets of it, rather than individual flights.

1.6.1 Size Range Averages

Table 1-4 provides a summary of tropical and mid-latitude flights in the troposphere and in the stratosphere. Category averages were formed from the number of flights and data points listed in the table, after inspection and subjective selection from the flights in file 1. The wet categories are defined as data times with non-zero cloud second measurements, while dry means those without. Ozone is clearly lower and water vapor higher in the tropics, as expected, even in the high troposphere. CN are more abundant in the tropics, especially in dry situations. However, FCN are approximately the same, within wet or dry categories, so that the filter ratio is higher in the tropics than in the mid-latitude. Such higher levels of CN and filter ratio in the tropics are consistent with the idea that the upper tropical troposphere is subject to more direct and frequent supply of particles from below, resulting in a fresher population with a large percentage of small particles. The tropical cloudiness and large particles encountered by the GASP aircraft is more likely to be deep convection which provides rather direct transport of low level air to flight level. This process was documented more completely with synoptic and satellite data for one of the GASP flights over equatorial Africa (Pratt and Falconer, 1979). Cloud areas in the mid-latitudes are generally of the cirrus variety and more likely to consist of air which has spent a large time in the upper troposphere. The occasional low values of filter ratio which lead to the variability seen in Fig. 1-13 are likely a result of areas of dense cloud particles in which coagulation has proceeded rapidly, which alternate with areas of fresh particle injection from below.

To complete the comparison, stratospheric averages are also shown in Table 1-4. As expected, ozone is high and water vapor low. The low value of CN is consistent with the role of the troposphere as the source of small particles. Since the FCN is not much different from the other categories, the filter ratio is low indicating well-aged air. Fig. 1-3 shows schematically the difference between the total particle population and the filtered population in the stratosphere and troposphere. The absolute difference between total CN (areas beneath the nearly straight lines) in the two regions occurs mainly in the small particle sizes. The areas under the curved lines in Fig. 1-3 correspond to the number of particles counted as FCN, after the original particle populations pass through the filter.

Table 1-4. Date Base Averages

	TROPOSPHERE						STRATOSPHERE
	Tropical			Mid-Latitude			
	Net	Dry	All	Net	Dry	All	
Number of flights used in average	3	3	3	3	8	8	9
Range of data points used in average	16 to 44	28 to 78	49 to 115	12 to 134	88 to 157	154 to 291	120 to 213
CN ($no./cm^3$)	134.3	277.5	232.5	113.6	184.3	149.1	40.1
FCN ($no./cm^3$)	40.3	72.0	60.8	42.7	83.1	63.2	31.1
Ozone (ppbv)	21.7	31.2	28.7	47.5	61.2	84.9	251.4
Mixing ratio (ppmw)	208.8	100.0	129.9	86.2	44.3	62.7	22.8
Filter ratio	3.7	3.7	3.6	2.7	2.2	2.4	1.4
PD2 ($no./m^3 x 10^5$)	6.4	7.0	7.2	7.4	9.0	8.8	8.6
PD4 ($no./m^3 x 10^4$)	4.3	0.4	1.6	7.7	0.4	3.8	0.95

CN has an overall data average of 177 particles per cm^3 which is close to most observations at this level (Cadle and Langer, 1975; Kaselau, 1974). The stratosphere averages 40 particles per cm^3. This corresponds closely to, for instance, Junge's (1963) measurement of 35 particles per cm^3 at 1 km above the tropopause. The higher concentration of CN in the troposphere vs. the stratosphere is consistent with the presumed tropospheric source of CN, while the opposite situation exists for ozone. The tabulated values of CN and PD2 indicate that in the stratosphere, 2 percent of the particle population is greater than 0.45 micron in diameter, while for mid-latitudes and the tropics, the fraction is only 0.6 percent and 0.3 percent, respectively. (Recall that PD2 is the cumulative total of all particles greater than 0.45 micron diameter. The schematic sketch in Fig. 1-3 will be helpful for the following discussion.) Thus, the stratospheric air has a higher proportion of larger particles than the troposphere. Furthermore, of the stratosphere particles greater than 0.45 micron in diameter, 10 percent are larger than 1.4 micron. This compares with 40 percent and 26 percent in the mid-latitude and tropical troposphere, respectively. That means, in the stratosphere, 90 percent of PD2 fall between 0.45 and 1.4 micron diameter, and extremely large particles are rare compared to the troposphere.

1.6.2 Scatter Plots

In order to investigate the overall behavior of particle data, scatter plots were developed among the constituents PD4, CN and ozone. PD4 was chosen as representative of the larger particles because the PD2 range has been found to have an excessive noise level, while PD5 size particles are not as frequently observed.

Fig. 1-14 is a scattergram from the entire data set between ozone concentration and filter ratio, which summarizes very effectively the nature of the particle size distribution in the stratosphere and troposphere. The "L" shape indicates that when ozone concentration is high (in the stratosphere) the filter ratio usually does not exceed 2.0, while high values of the filter rato are only found with low (tropospheric) values of ozone. The scattergram between ozone and CN (Fig. 1-15) also has an "L" shape, suggesting that CN has a tropospheric source while ozone has a stratospheric source. These scattergrams summarize relationships which are normally observed in the individual flight plots.

The scattergram between PD4 and ozone (Fig. 1-16) show that PD4 has a typical stratospheric value around 10^4 particles per m^3, while PD4 concentrations vary widely at tropospheric levels of ozone. Fig. 1-6 is shown as an example of this behavior.

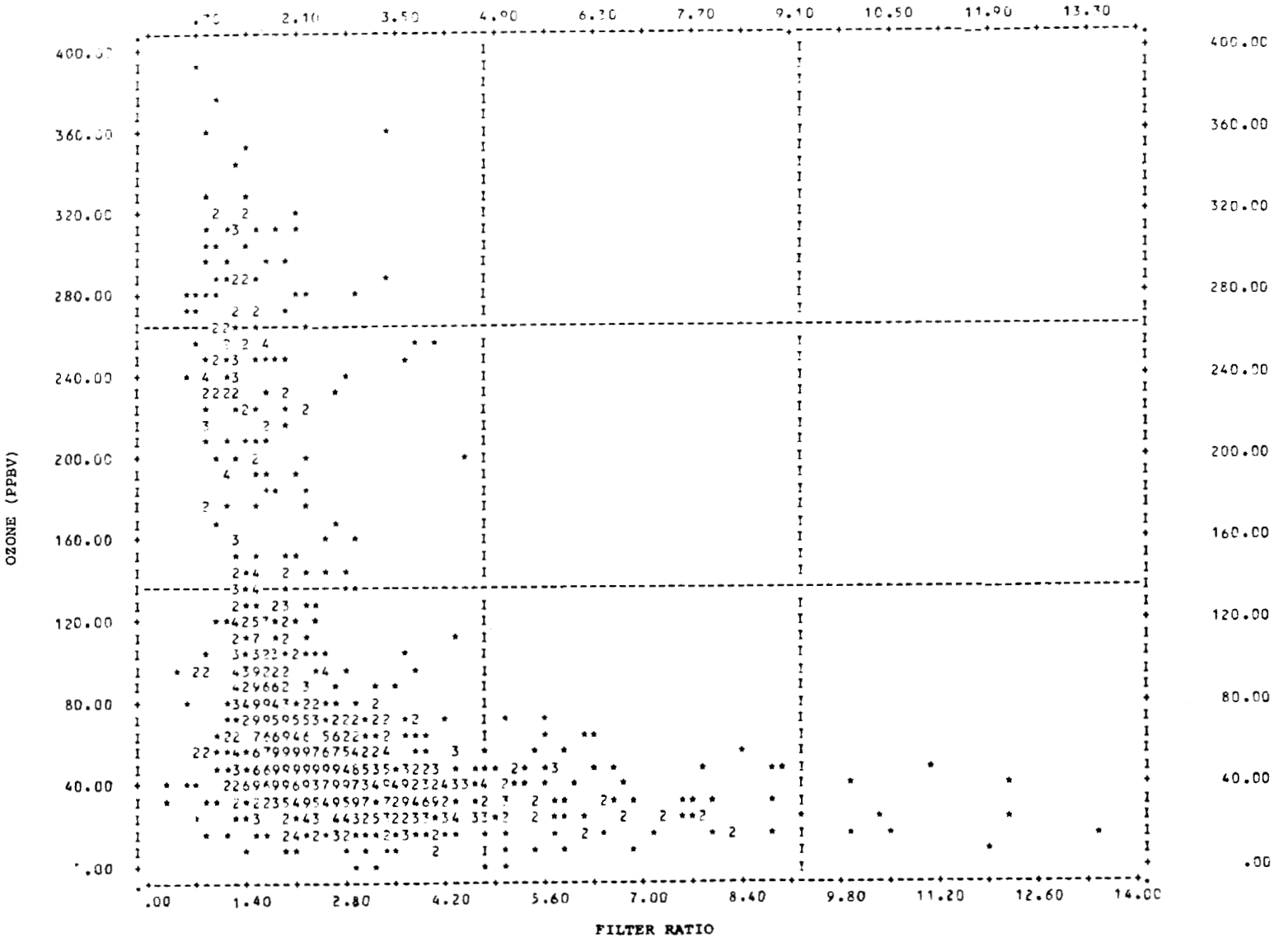

Fig. 1-14. Scattergram between ozone and filter ratio, all data. Numbers refer to number of observations (e.g. 9 = nine or more data points).

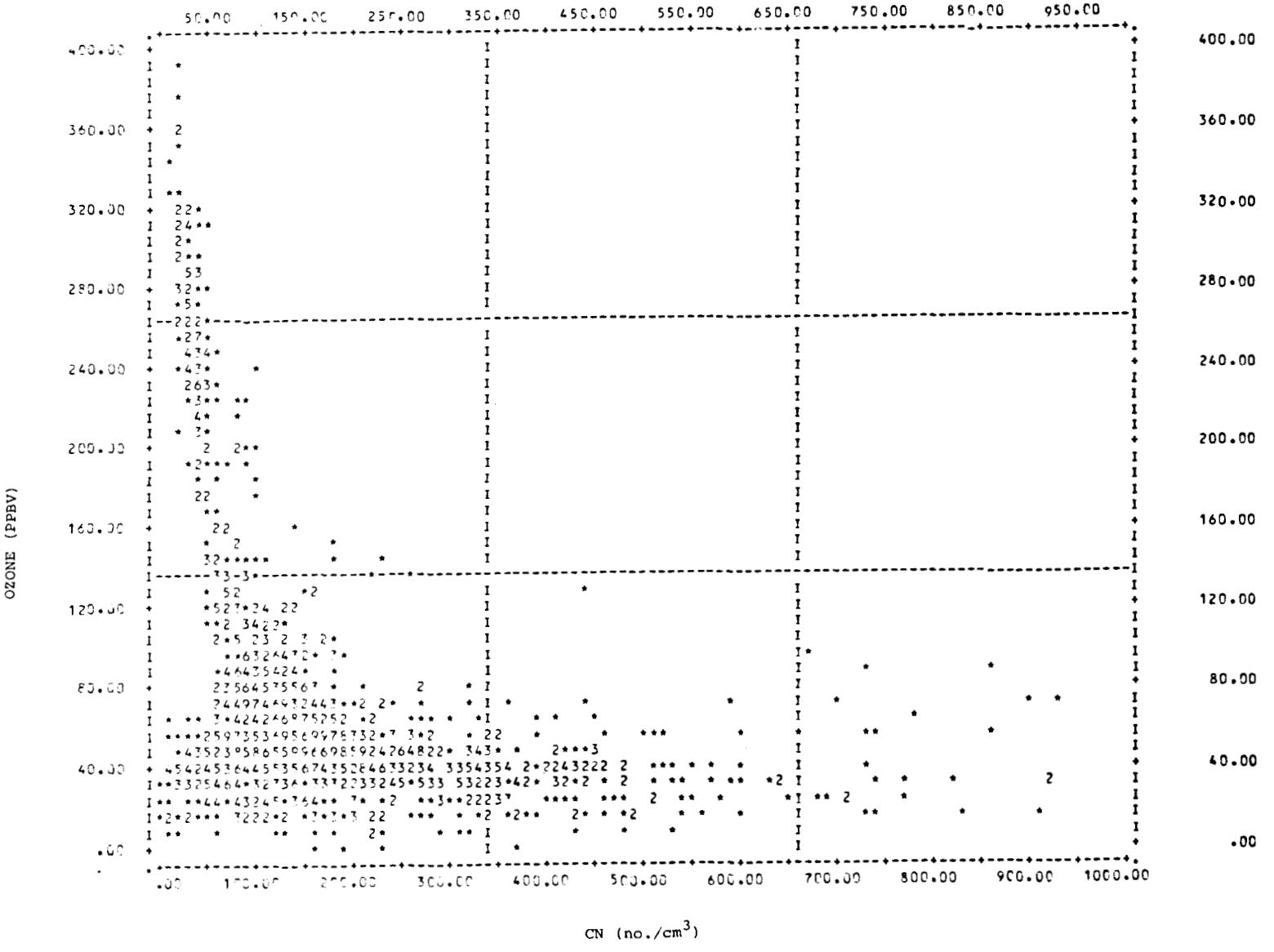

Fig. 1-15. Scattergram between ozone and CN, all data.

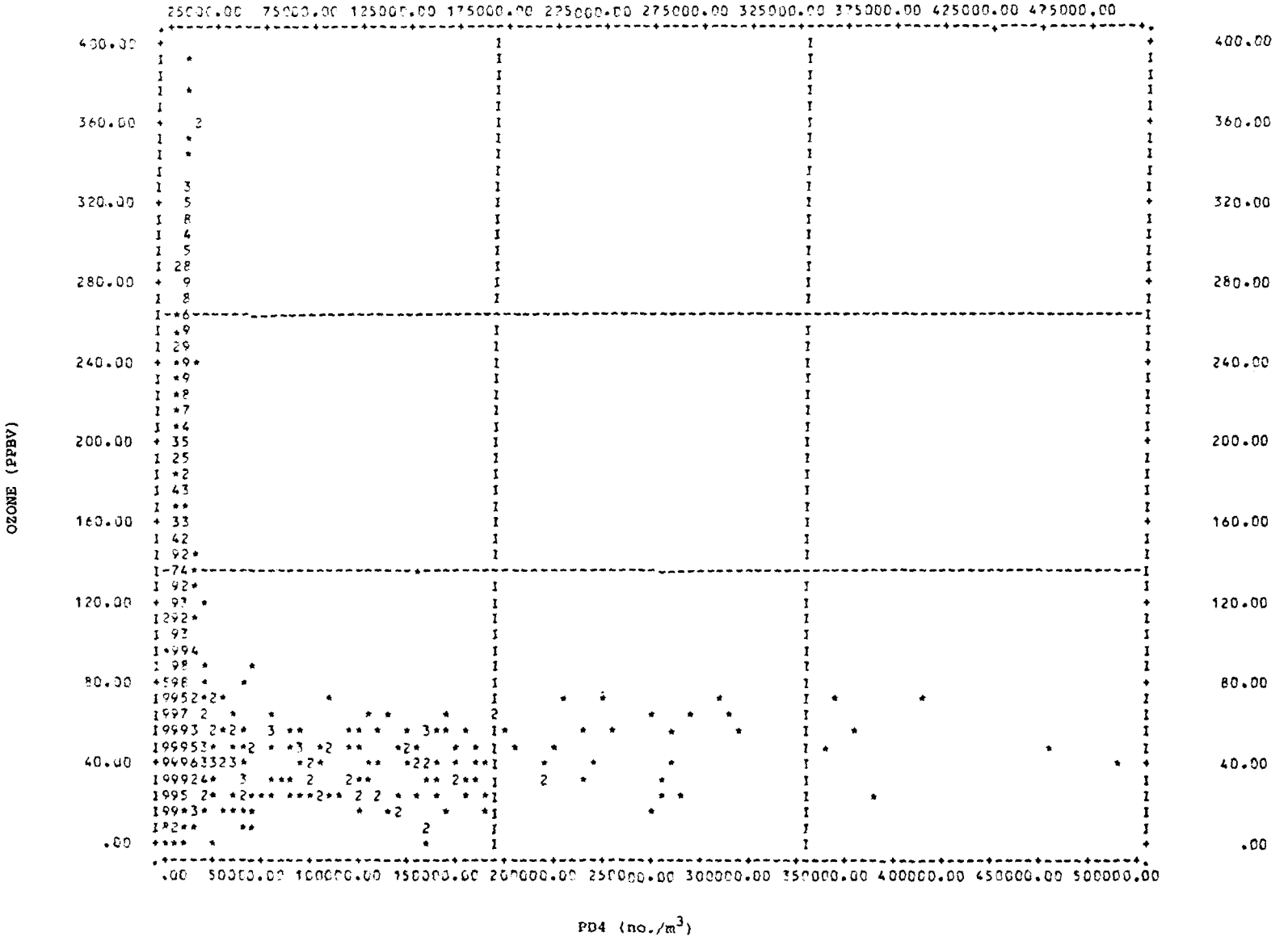

Fig. 1-16. Scattergram between ozone and PD4, all data.

1.6.3 Stratospheric Value of PD4

The typical stratospheric level in the PD4 size range was investigated further by excluding tropospheric data from a scattergram between PD4 and ozone. This is shown in figure 1-17. The correlation obvious in Fig. 1-17 (equal to 0.65 at the 99.95 percent significance level, assuming the data are independent) raises a suspicion that a PD4 gradient exists in lower stratosphere, and that PD4 size particles may be transported downward toward the tropopause, as is known to occur for ozone. (The units of both ozone and PD4 in Fig. 1-17 are mixing ratio.) This is plausible since Junge et al. (1961) have shown the existence of an aerosol layer in the middle stratosphere which might serve as a particle source. Also, the soundings by Hofmann et al. (1975) suggest a downward flux from particle data, although the vertical mixing ratio gradient is small in magnitude. However, this possiblity of a vertical gradient with a source region above GASP altitudes is contrary to the observations made on the GASP file 2 flights which occur in mid winter. In these flights, PD4 concentrations seldom exceed 10^4 particles per m^3, even when ozone reaches extreme levels (over 1000 ppbv). Therefore, the correlation between ozone and PD4 particles in Fig. 1-17 is probably a result of the dilution of lower stratospheric air by tropospheric air with low ozone and low concentrations of PD4 particles. The scattergram between CN and ozone for the stratosphere (Fig. 1-18) is consistent with this idea, keeping in mind that CN have a tropospheric source, and ozone a stratospheric source.

This explanation of the ozone-PD4 correlation in terms of dilution by tropospheric air with lower PD4, may seem inconsistent with the existence of tropospheric concentrations of PD4 which are higher than the typcial stratospheric value (as in Fig. 1-16). Fig. 1-19 is a scattergram of relative humidity with respect to water vs. PD4 concentrations. This figure suggests strongly that the higher concentrations of tropospheric PD4 size particles are water droplets (or ice particles) growing in a moist environment. This is confirmed by Fig. 1-20 which uses the same data but excludes any observation of PD4 when PD5 size particles are present. PD5 size particles are usually ice crystals (Twomey, 1977), and Fig. 1-20 confirms that PD4 and PD5 particles are usually found together and are probably growing ice particles. Therefore, any tropospheric air which may be mixed into the stratosphere would probably lose most of its (ice) PD4 particles by sublimation, as it mixes with dry stratospheric air.

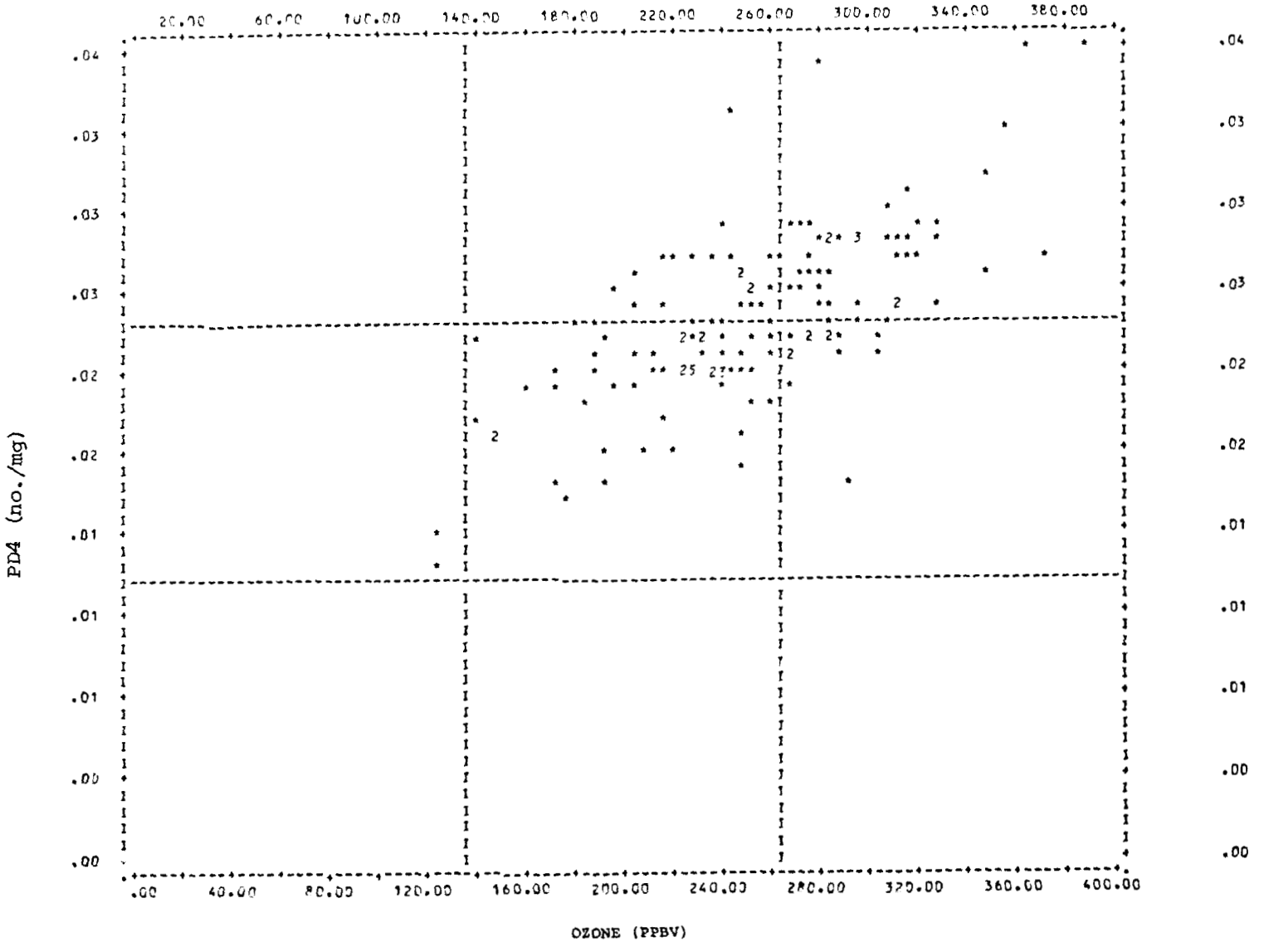

Fig. 1-17. Scattergram between ozone and PD4, stratospheric air. (Note reversal of axes compared to Fig. 1-16, and mixing ratio units for PD4.)

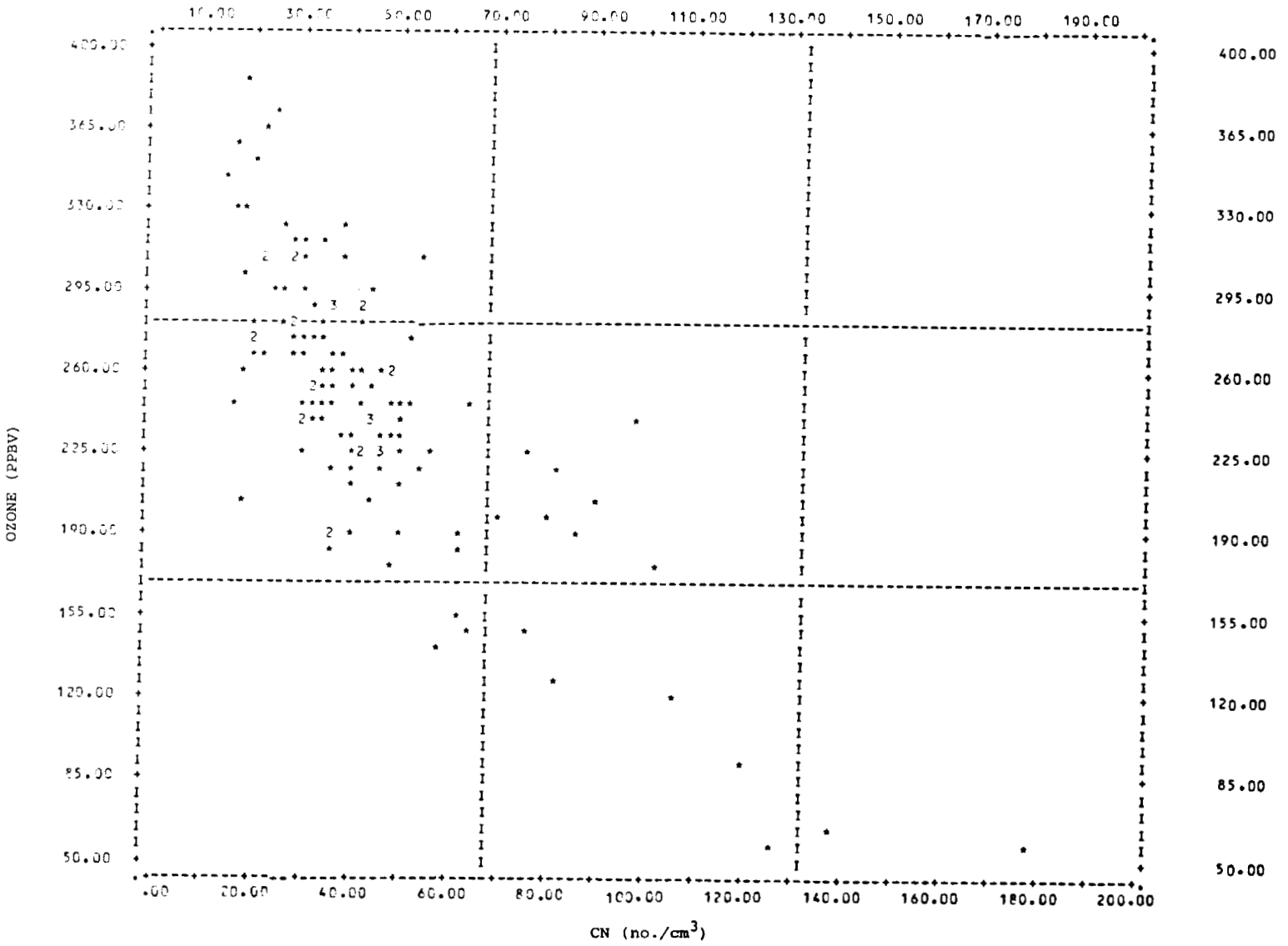

Fig. 1-18. Scattergram between ozone and CN, stratospheric air.

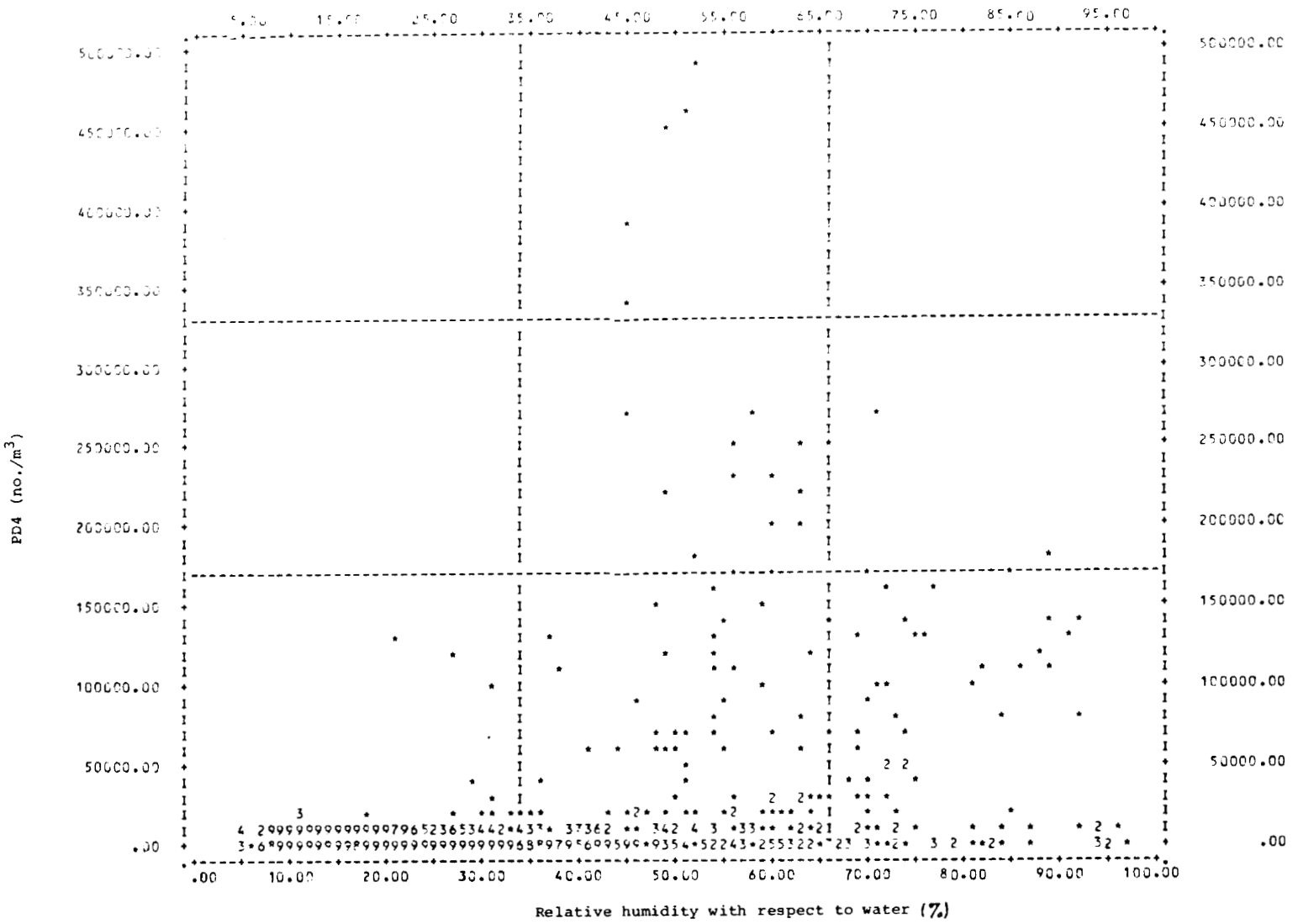

Fig. 1-19. Scattergram between PD4 and relative humidity with respect to water. All data.

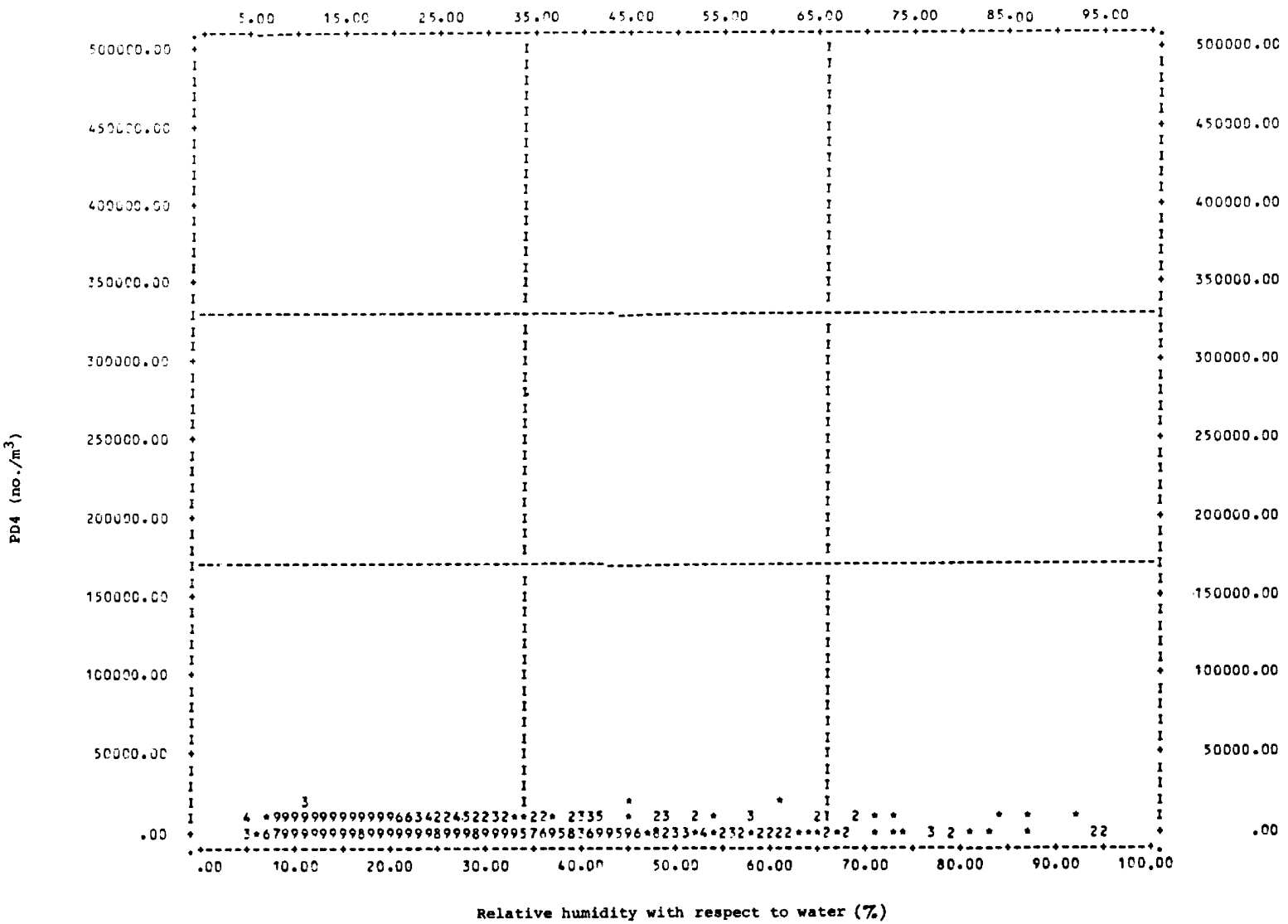

Fig. 1-20. Scattergram between PD4 and relative humidity with respect to water, exclusive of any observation of PD4 when PD5 size particles are present. All data.

If the interpretation presented here is correct, Figs. 1-17 and 1-18 indicate that the lower stratosphere is diluted by tropospheric air, based on observations of ozone, PD4, and CN. While these data show no evidence of a flux of PD4 size particles downward through the stratosphere, the question of how the stratosphere maintains what appears to be a uniform concentration of particles of this size is intriguing and remains unanswered.

1.7 SUMMARY

The GASP data set from fall of 1978 consists of measurements of ozone, particles and meteorological variables from a wide variety of meteorological situations near the mid-latitude and tropical tropopause. The ratio of CN concentration in the free air to those in which the ambient airstream was passed through a Nuclepore membrane filter provided a measure of the amount of particle aging by the coagulation process. Ozone and water vapor have served largely as reference constitutents in this study, against which the measurements of large (light-scattering) and small particles have been evaluated.

The data characterize the stratosphere as a region of low total particle populations which have been well aged, compared to the tropospheric air with fresher and higher particle populations. This is consistent with the accepted understanding of the surface of the earth as the source of small particles. The largest size particles (diameters greater than 3.0 micron) are found only in the moist regions of the troposphere, and probably consist of ice particles. In the troposphere, the tropics seem to have younger and fresher, although more variable populations than the mid-latitudes, probably because this region contains deep convective motions which are more effective than mid-latitude motions in transferring air from the surface to flight level. One of the most "aged" populations in the mid-latitude troposphere was found in the extremely saturated cloud region on the ascending side of an intense jet. This was probably due to the rapid coagulation effected by plentiful ice crystals, as well as the poor sources of small particles for upper tropospheric air in the mid-latitudes.

Case studies of mid-latitude jet penetrations yielded distributions consistent with Shapiro's (1978) more detailed analyses of such structures. However, of the constituents measured through the jet, two which have a tropospheric source, had a very weak gradient across the jet core, while the two which have a stratospheric source showed a sharp gradient similar to that seen in potential vorticity in Shapiro's analyses. This suggests an asymmetry in the mixing mechanisms for tropospheric and for stratospheric constituents crossing the tropopause near jets, and demonstrates the usefulness of

particle measurements in the type of detailed, dedicated aircraft investigation carried out by Shapiro. Such an asymmetry would be crucial to the proper simulation of cross-tropopause transport by numerical models. In contrast, GASP flights through the tropopause in the absence of high winds frequently showed a distinct boundary between stratospheric and tropospheric characteristics, suggesting that cross-tropopause mixing is small over wide areas of the mid-latitude tropopause.

In clearly stratospheric air, particles of diameter greater than 1.4 micron (PD4) were found to remain nearly uniform in concentration at about 10^4 particles per m^3 while concentrations in this size range varied erratically above and below that level in the troposphere. However, PD4 concentrations fell below this level and were correlated with ozone, for concentrations of ozone less than several hundred ppbv. This situation implies that some as yet undetermined mechanism maintains the PD4 size range at a constant level in the lower stratosphere, except for a rather distinct region at the bottom of the stratosphere which is subject to the effects of dilution of PD4 particles, as well as ozone, by tropospheric air.

REFERENCES FOR CHAPTER 1

Briehl, D., T. J. Dudzinski, and D. C. Lui, 1980: NASA Global Atmospheric Sampling Program (GASP) Data Report for Tape VL0014. NASA TM-81579, 59 pp.

Cadle, R. D., and G. Langer, 1975: Stratospheric aitken particles near the tropopause. Geophys. Res. Lett., 2, 329-332.

Davis, D. D., 1980: Project GAMETAG: An overview. J. Geophys. Res, 85, 7285-7292.

Dennis, R., 1976: Handbook on Aerosols. National Technical Information Services. Springfield, 142 pp.

Ehhalt, D. H., L. E. Heidt, R. H. Lueb, and W. Pollock, 1975: The vertical distribution of trace gases in the stratosphere. Pure Appl. Geophys., 113, 389-402.

Englund, D. R., and T. J. Dudzinski, 1981. The Water Vapor Measurement System in the NASA Global Atmospheric Sampling Program. NASA Technical Paper (in press).

Friedlander, S. K., 1977: Smoke, Dust and Haze. John Wiley & Sons, Inc. New York City, 317 pp.

Green, H. L., and W. R. Lane, 1964: Particulate Cloud: Dust, Smokes and Mists. University Press, Belfast, Ireland, 471 pp.

Hofmann, D. J., J. M. Rosen, T. J. Pepin, and R. G. Pinnick, 1975: Stratospheric aerosol measurements I: Time variations at northern mid-latitudes, J. Atmos. Sci., 32, 1446-1456.

Hoppel, W. A., J. E. Dinger, and R. E. Ruskin, 1973: Vertical profiles of CCN at various geographical locations. J. Atmos. Sci., 30, 1410-1420.

Junge, C. E., 1963: Air Chemistry and Radioactivity. Academic Press, New York City, 382 pp.

Junge, C. E., C. W. Chagnon, and J. E. Manson, 1961: Stratospheric aerosols. J. Meteor., 18, 81-108.

Kaselau, K. H., 1974: Measurements of aerosol concentrations up to a height of 27 km. Pure Appl. Geophys., 112, 877-885.

Mahlman, J. D., 1973: On the maintenance of the polar jet stream. J. Atmos. Sci., 30, 544-557.

Nyland, T. W., 1979: Condensation Nuclei (Aitken Particle) Measurement System used on the NASA Global Atmospheric Sampling Program. NASA TP-1415, 25 pp.

Pratt, R., and P. Falconer, 1979: Circumpolar measurements of ozone, particles, and carbon monoxide from a commercial airliner. J. Geophys. Res., 84, 7876-7882.

Pruppacher, H. R., and J. D. Klett, 1978: Microphysics of Clouds and Precipitation. D. Reidel Pub. Co., Inc., Boston, 714 pp.

Reck, G. M., D. Briehl, and T. W. Nyland, 1977: In situ measurements of arctic atmosphere trace constituents from an aircraft. NASA TN D-8491, 61 pp.

Rosen, J. M., and D. J. Hofmann, 1976: Balloonborne measurements of condensation nuclei. J. Appl. Meteor., 16, 56-62.

Shapiro, M. A., 1978: Further evidence of the mescoscale and turbulent structure of upper level jet stream-frontal zone systems. Mon. Wea. Rev., 106, 1100-1111.

Shaw, G. E., 1980: Optical, chemical and physical properties of aerosols over the antarctic ice sheet. Atmospheric Environment., 14, 911-921.

Spurny, K. R., J. P. Lodge, Jr., E. R. Frank, and D. C. Sheesley, 1969: Aerosol filtration by means of nuclepore filters, structural and filtration properties. Environmental Sci. & Tech., 3, 453-464.

Tiefermann, M. W., 1979: Ozone Measurements System for NASA Global Air Sampling Program. NASA TP 1451.

Twomey, S., 1977: Atmospheric Aerosols. John Wiley & Sons, Inc., New York City, 302 pp.

CHAPTER 2

GASP CLOUDS

Andrew Detwiler *

2.1 INTRODUCTION

Atmospheric state parameters and trace constituents in the upper troposphere and lower stratosphere were measured from March 1975, until June 1979, during the NASA Global Atmospheric Sampling Program (GASP) using automated measuring and sampling systems aboard several Boeing 747 commercial airliners as well as the NASA Convair 990. Windspeed and wind direction, static air temperature, dew/frostpoint temperature, condensation nuclei, light scattering particles, ozone, carbon monoxide, sulfate, nitrate, chloride, fluoride, and ^{7}beryllium were monitored. The measurements were obtained whenever the aircraft were above six km. No attempts were made to alter the flight paths specifically for the purpose of making measurements, and so the GASP data set consists of a series of strings of measurements typical of conditions encountered by en-route high altitude jet aircraft, with each string being a random sample of typical atmospheric circulations on the various scales from the mesoscale to the synoptic scale.

Normally data are recorded every five minutes. At typical cruising speeds this amounts to a spatial separation of about 70 km. Within a string of measurements along a flight, however, there will likely be a high degree of autocorrelation between adjacent measurements, since atmospheric circulations are typically organized on scales of this dimension or much larger.

Sometimes sequential flights by the same aircraft back and forth along the same commercial route cross the same synoptic-scale circulation features 6 to 12 hours apart. Since

---

* (Post-doctoral Research Associate, Department of Atmospheric Science, State University of New York at Albany. NSF support is acknowledged.)

synoptic-scale features typically have lifetimes much longer than this, one cannot consider every flight a completely independent string of measurements for some statistical applications. However, for many purposes it is possible to derive quite useful statistics on atmospheric characteristics and behavior for the extensive GASP data set.

From December 1975, through January 1978, nearly 300,000 sets of measurements were recorded over almost the entire globe (Briehl et. al., 1980). Between January 1978, and June 1979, when the GASP program terminated, more than 300,000 additional observations were accumulated. Final processing of the data is just being completed. Data archived on magnetic tapes will be available from the National Climatic Center for the entire collection of GASP flights.

Some aspects of the global distribution of clouds above six kilometers in the atmosphere have recently been explored using the GASP data set (Nastrom et al., 1981). In addition to locations where clouds were detected, the temperature, humidity, trace gas constitutents and particle concentrations in the clouds, also available at each measurement point, were studied for "in cloud" records.

In this report we will begin with a discussion of some general aspects of the global distribution of high altitude clouds and their microphysical characteristics, including the recent work of Nastrom et al. We will then explore how the GASP data set might be further used to gain additional information about upper tropospheric clouds. Our approach will be to take a small subset of the GASP data set, containing only 45 flights, and analyze it in some detail. This type of analysis will compliment the much broader analysis of Nastrom et al.

Although data are reported at altitudes above, nominally, six kilometers, the GASP aircraft spend most of their time at cruise altitudes well-above the 6 km level. Nearly all data were recorded at altitudes between 9 and 11 kilometers (between the 300 and 200 hectopascal (mb) pressure "levels." At these altitudes almost all of the clouds encountered will be ice particle, or cirrus, clouds. We will restrict the following discussion to cirrus clouds, and assume that almost all clouds encountered above 6 kilometers were cirrus.

2.2 CIRRUS CLOUD OCCURRENCE

Cirrus clouds generally form when rising tropospheric air cools and the relative humidity increases sufficiently to produce ice particles on a small fraction of the ambient aerosol.

With respect to mid-latitude synoptic disturbances, these conditions are most frequently encountered below the tropopause on the equatorward side of mid-latitude jet streams, downstream of upper level troughs and in the warm air gliding upward over the warm-frontal zone associated with advancing wave cyclones. A schematic diagram of flow about such a disturbance is shown in Figure 2-1.

In addition to the broad patterns of synoptic-scale upward motion in this type of situation, sub-synoptic scale circulations transverse to the jet stream tend to wrap tropospheric air upward on the equatorward (anticyclonic shear) side of the jet and stratospheric air downward on the poleward (cyclonic shear) side of the jet. (See Figure 2-2). These sub-synoptic scale circulations are forced, in part, by curvature of the flow (Scorer, 1978) and also by momentum imbalances in the entrance and exit regions of jet streaks (small packets of very high wind speeds that propagate along the mid-latitude jets), as noted by Riehl et al. (1954), and Reiter (1963). In addition, inertial instabilities in the strong, anticyclonic shear zones on the equatorward sides of jets can result in a variety of wave disturbances and turbulence in this zone. This often leads to the varied and intriguing patterns in the cirrus clouds that form in the updrafts associated with these turbulent zones (Viezee et al., 1967; Scorer, 1972).

Ice particle growth and sublimation are typically quite slow in the upper troposphere. That means that millimeter-size ice crystals may fall several kilometers through relatively dry air before they have completely sublimated away. This gives jet stream cirrus clouds their characteristic filamentary appearance. Thus small numbers of ice crystals may be encountered even in quite dry air well below and some distance away from the visible cirrus clouds in which they originally nucleated and grew (Barnes, 1980; Braham and Spyers-Duran, 1967). Radiative equilibrium calculations show that the surface temperature of a millimeter-size ice particle may be a degree (Celcius) or more lower than the air temperature, and so growth may even occur in air that is apparently undersaturated with respect to ice (Hall and Pruppather, 1976; Heymsfield, 1975b).

Cirrus are also observed to "blow off" of the tops of towering cumulonimbus convective clouds. The ice particles are nucleated in, or at the tops of, the updrafts of the clouds and carried nearly to or even above the tropopause. There they are

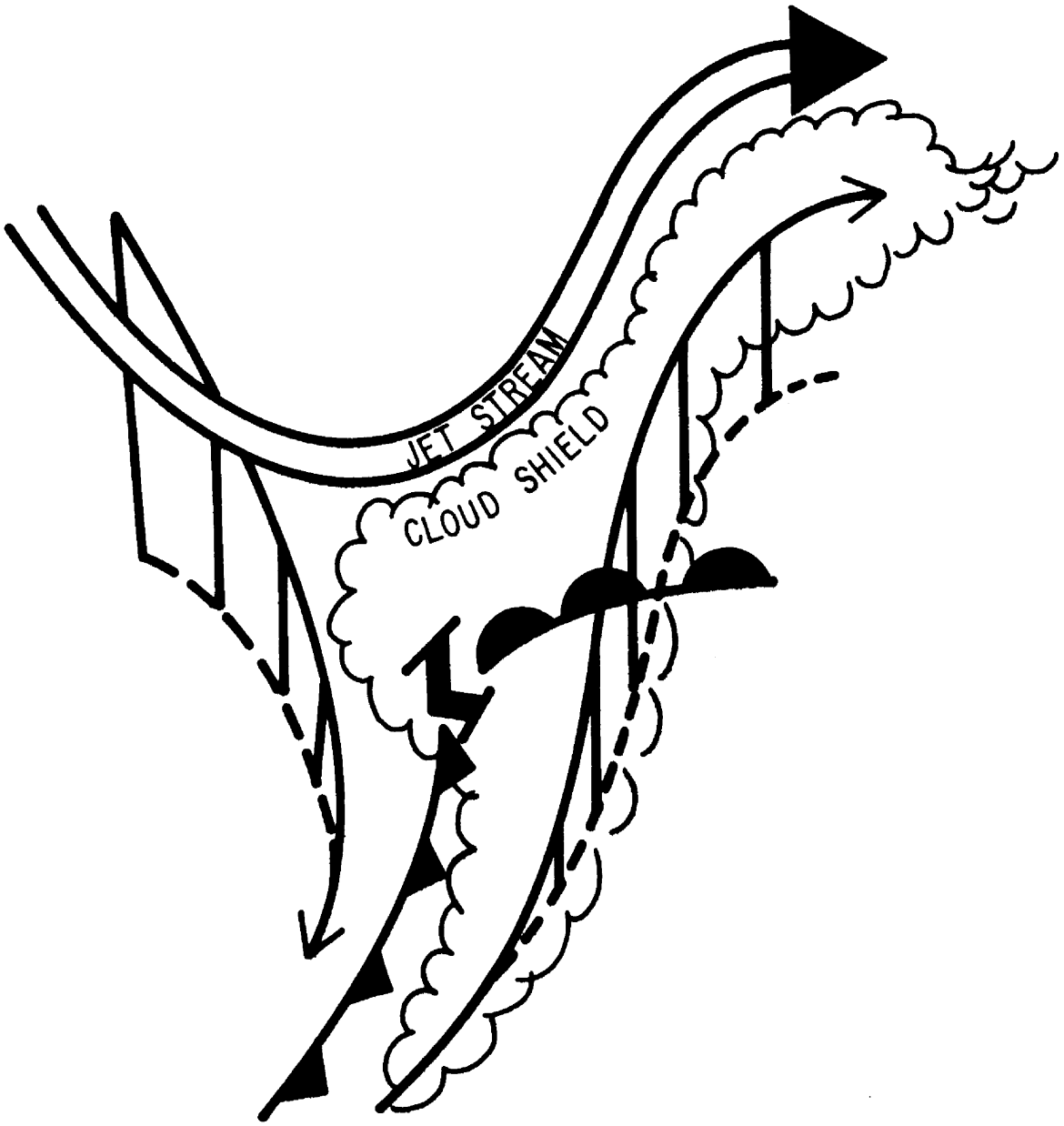

Fig. 2-1. A schematic of air flow about a mid-latitude wave cyclone, based on Palmen and Newton (1969). The air in which cirrus clouds form typically rises from the sub-tropical surface boundary layer through several cloud formation episodes ahead of the cold front and over the warm front before cirrus formation occurs. Cirrus formation occurs in the upgliding regions (possible turbulent) near the tropopause and equatorward of the jet stream.

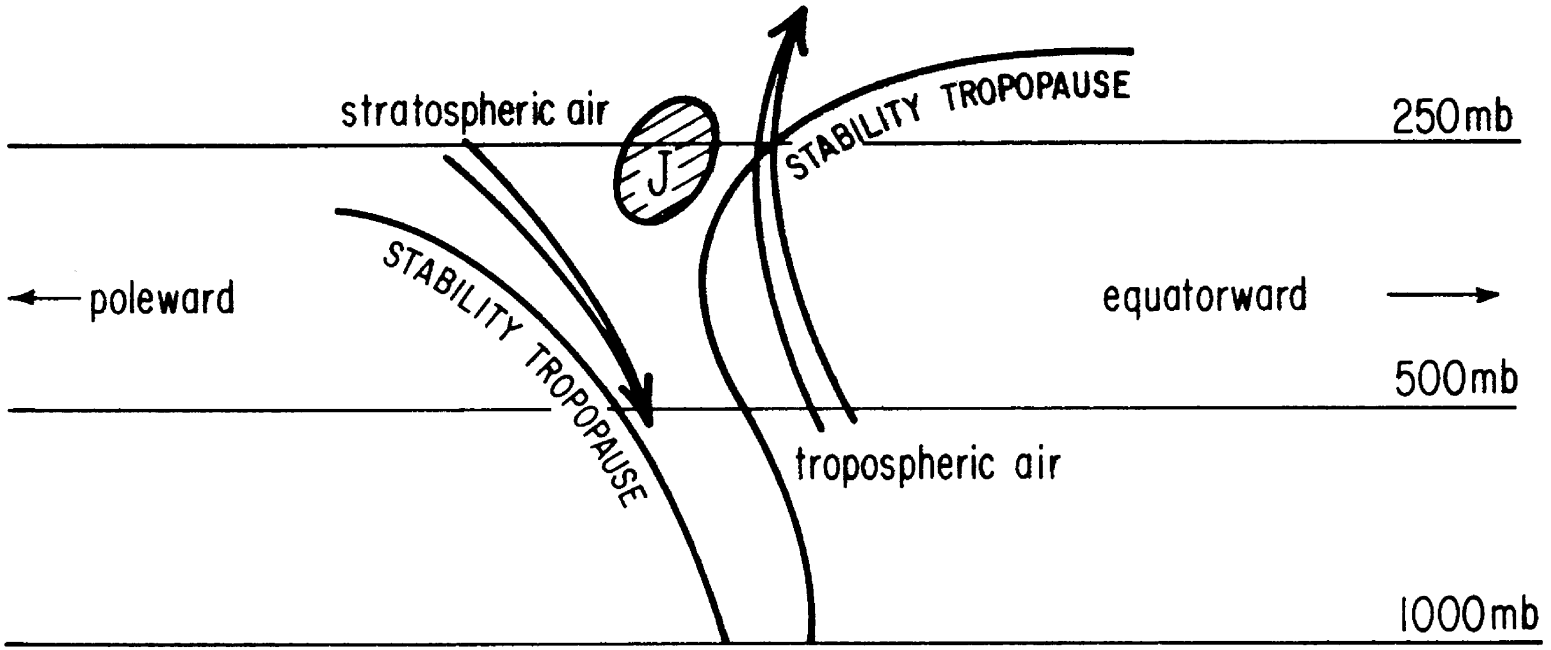

Fig. 2-2. A schematic of the transverse flow about jet streams. This figure is adapted from Shapiro et al. (1980).

entrained in the circulation about the top of the cloud and carried downwind. These "anvil" cirrus may be quite extensive, extending hundreds of kilometers downwind from the cloud. Cumulonimbus cirrus anvils have been observed by satellite to drift overnight hundreds of kilometers downwind of the cloud over which they formed and affect the development of convective clouds on the following day (E. Holroyd, personal communication).

Cirrus also form in atmospheric wave motions that are frequently generated to the lee of mountains. Under conditions favorable for mountain wave formation, these wave cirrus may be quite extensive.

2.3 CIRRUS CLOUD MICROPHYSICS

Cirrus clouds typically form in relatively gentle updrafts (approximately 10 cm/sec) in clear air at temperatures below -35°C. As mentioned above, this formation typically takes place in the upper troposphere either ahead of mid-latitude wave cyclones, in orographically-induced wave motions, or in somewhat more vigorous updrafts associated with towering cumulonimbus clouds.

The air in which cirrus clouds form is primarily of tropospheric origin. As in the formation of liquid water clouds at higher temperatures, some type of nucleus is required in order for ice particles to form from the vapor at observed tropospheric ice supersaturations. These nuclei will be tropospheric aerosol particles.

Ice particles may form in basically three ways, depending on the relative humidity and type of nucleus involved. A first way is the condensation-freezing process. A relative humidity with respect to liquid water (RHW) of greater than 100% is required. A liquid water droplet nucleates on a suitable aerosol particle and begins to grow. At some point it freezes and growth of the ice phase continues thereafter.

A second process of ice formation can take place at RHW close to, but less than, 100%. This is called the sorption-freezing process. For RHW close to, but less than, 100% many types of aerosol particles will adsorb or absorb significant quantities of water. If the temperature is less than -35°C or so, only a relatively small amount of water need be adsorbed in a liquid, or semi-liquid, state before freezing occurs in many cases. On the other hand, if the particle absorbs the water into solution (say, for instance, an ammonium sulphate solution), then, again, at temperatures less than -35°C or so that solution droplet need not get very large, i.e. dilute, before its probability of freezing, homogeneously or otherwise, gets very large. So ice particles may form by freezing of haze droplets at RHW less than 100% and temperatures near -35°C and below. At higher temperatures freezing of adsorbed or absorbed water proceeds somewhat less readily unless the nucleating particle has characteristics that stimulate the freezing of water. Once freezing occurs, growth of the ice phase continues as long as ice supersaturation persists.

Finally, ice may form directly from the vapor onto suitable ice nuclei at some relative humidity with respect to ice (RHI) greater than 100%. Typical ice nuclei require a threshold RHI somewhat greater than 100% before they can nucleate ice directly from the vapor. But note that at all temperatures

less than 0°C, and for a given water vapor pressure, RHI is greater than RHW. RHI may be significantly above 100% while RHW is still quite a bit less than 100%. At -50°C, for instance, RHI equal to 137% corresponds to RHW equal to 85%. So ice nuclei active at relatively small ice super-saturations will probably nucleate ice in conditions too dry for the sorption-freezing mechanism to work.

Because tropospheric aerosol loading generally decreases with increasing altitude and with increasing distance from exposed ocean surfaces (i.e. out over the polar ice caps), it is inferred that the exposed ocean surfaces, and also their flora and fauna, are the main sources of the natural tropospheric aerosol or its precursor gases.

It is thought (Ludlam, 1980, pp. 96-99) that in the troposphere effective ice nuclei derive naturally almost solely from solid mineral and organic material at the earth's surface. A very small fraction may derive from meteoric material settling downward from the stratosphere or deposited in the troposphere directly by incoming meteors. Because ice-nucleating particles derived from surface material are typically 0.1 micrometer or more in diameter, and because they are very likely to be nucleated in supercooled liquid water clouds as they work their way into the upper troposphere from the surface, there are typically very few ice nuclei present in th upper troposphere capable of nucleating ice directly from the vapor at ice supersaturations corresponding to RHW less than 100%.

So it is likely that most cirrus cloud ice particles form by a condensation-freezing or sorption-freezing process. Aerosol particles sampled in the upper troposphere tend to be hygroscopic sulphate particles, usually ammonium sulphate. There are a variety of ways such particles can form in air from water vapor, gaseous sulphur compounds, ammonia, and other trace gas constituents. Some may form near the earth's surface and mix upward, others may form in the upper troposphere in situ, and still others, or their precursors, may form in the stratosphere and mix downward. (Pruppacher and Klett, 1978 has a detailed discussion of the atmospheric aerosol).

Given the presence of this hygroscopic aerosol, the most likely means by which ice particles form in cirrus clouds is the sorption freezing process. Detailed calculations of the nucleation and growth of cirrus cloud particles in an updraft from precursor ammonium sulphate aerosol have been performed by Heymsfield (1973, 1975b). He shows that for such an aerosol the RHW required to initiate the ice phase is typically somewhat greater than 85% at temperatures near -50°C. Such an

RHW corresponds to RHI equal to 137% at this temperature. The threshold RHW is higher at warmer temperatures. Once the ice particles form, their growth will continue until an RHI near 100% is reached. But until RHW exceeds 85% or so, no ice cloud will form in air containing only this sulphate aerosol, according to Heymsfield's calculations. Thus it is possible in the upper troposphere to measure frostpoint temperatures several degrees Celcius warmer than the ambient air temperature in clear air.

The balance between the rate of cooling in an updraft and the total rate of ice deposition on the particles of ice growing in the updraft determines the maximum supersaturation reached, and therefore, the fraction of the ambient aerosol that nucleates to ice. The higher the maximum supersaturation, the larger the number of ice particles nucleated, in general. Higher maximum supersaturations are favored by higher updraft speeds. Unlike liquid water clouds, which typically have a rather narrow spectrum of droplet sizes present (in the absence of coalescence), cirrus clouds tend to have a very wide spectrum of particle sizes present with the largest fraction of the total number in the smallest size ranges, near a few micrometers maximum dimension. (Refer to the results of Varley (1978a, 1978b) Varley and Brooks (1978), Varley and Barnes (1979), and Cohen (1979), hereafter noted as AFGL 1978/79). At the temperatures characteristic of liquid water clouds, droplets rapidly reach equilibrium with ambient humidity changes in their environment. At cirrus cloud temperatures, however, growth and sublimation are much slower. So in water clouds the water vapor made available in the updraft by adiabatic cooling is distributed about equally among the liquid droplets present, and the droplets are all nearly the same size, at least until coalescence begins to occur. But in cirrus clouds a wide spectrum of sizes appears to coexist in the airstream sampled by aircraft. (The sample volume is collected over a path of at least several hundred meters of flight. It is conceivable that cirrus cloud ice particle sizes might be found to be more monodisperse, had a small volume of air been sampled).

Figure 2-3 shows a sample droplet spectra in a water cloud at the earth's surface and of ice particles in an upper tropospheric cirrus cloud. The volume of water cloud sampled is derived from a flight path only a few tens of meters in extent, while the volume of cirrus sampled in Figure 2-3 was along an aircraft track several kilometers long.

Disagreement among different investigations as to the total number concentration of ice particles typically found in a cirrus cloud (see Heymsfield, 1975a) probably depends more on the minimum particle size measured with the equipment employed in a given investigation than on variations between clouds.

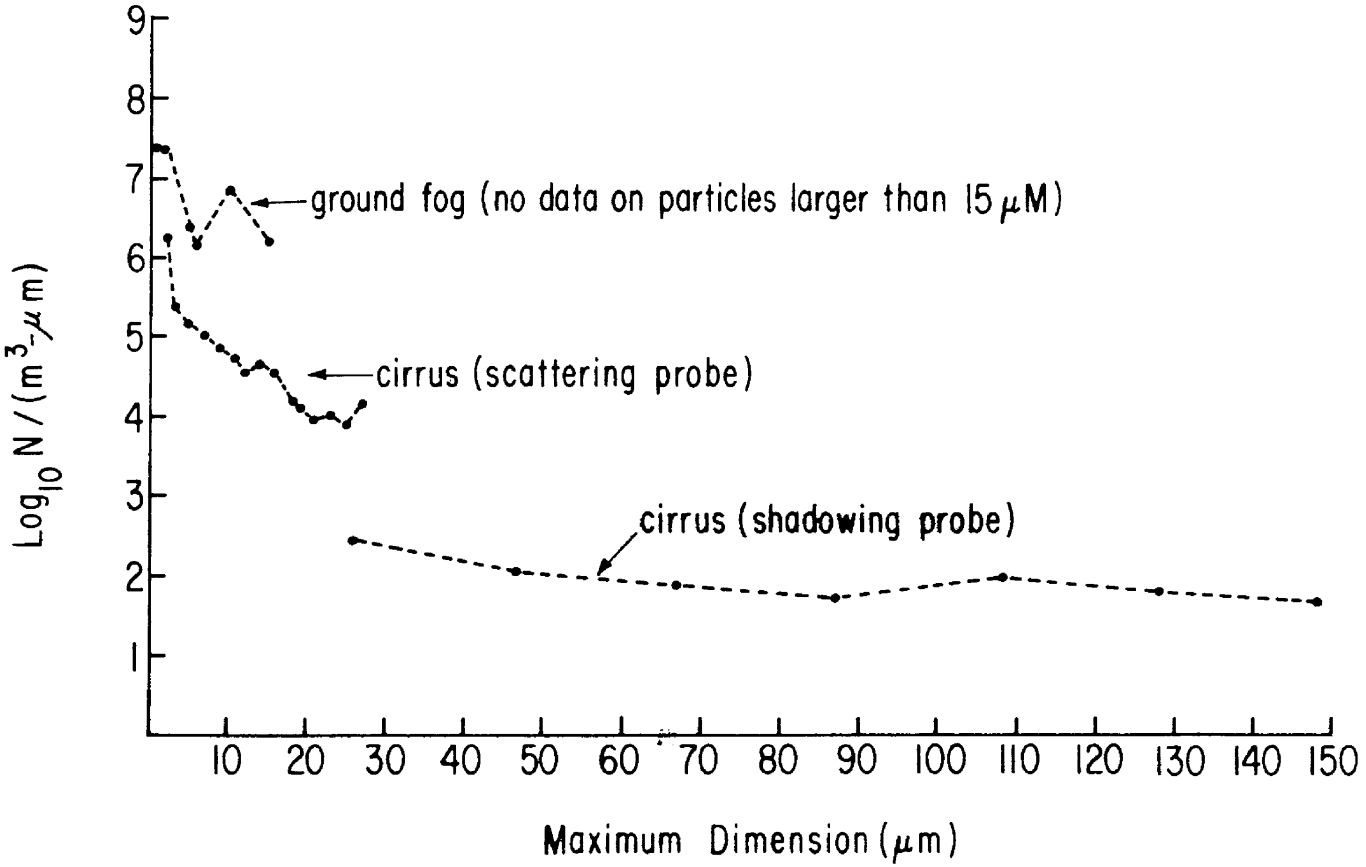

Fig. 2-3. The size spectrum of water droplets in a ground fog (Meyer et al., 1980) is compared to a typical size spectrum of cirrus ice particles (AFGL, 1978 and 1979). Note the two order of magnitude disagreement in cirrus particle number concentration between the two different AFGL probes for sizes near 25 μm. These data points were acquired simultaneously.

The slope of the size spectrum for cirrus particles, as seen in Figure 2-3, is typically quite steep. Small variations in the minimum size measurable will lead to large variations in the total number deduced.

The shape of the larger ice particles formed during the sorption-freezing and subsequent growth processes appears to be typically bullet-shaped hexagonal columns or clusters of such columns (bullet rosettes) (Heymsfield, 1975a). Smaller numbers of hexagonal, and non-hexagonal, plates and columns are also observed (Heymsfield, 1975a; Ohtake and Inoue, 1980; Smiley et al., 1980). Available aircraft instrumentation is unable to clearly resolve the shapes of particles much smaller than about 100 μm maximum dimension.

2.4 IMPORTANCE OF CIRRUS CLOUD STUDIES

Information on the number concentration of cirrus ice particles, their size spectrum and shapes, and the global distribution of cirrus clouds, is important for calculating the effects of cirrus clouds on the transmission of solar and terrestrial radiation through the atmosphere. In addition, interference by cirrus clouds may degrade the performance of various remote-sensing and communications systems employed by aircraft and by earth-orbitting satellites. Information on the extent, and microphysical properties, of cirrus clouds is important in the design and operation of these systems, too.

The study of cirrus clouds also has applications to the problem of erosion of high speed objects passing through clouds of tiny ice particles, the static charge build-up on such objects, and the increase of drag on laminar-flow-control winged aircraft when passing through such clouds. Thus basic knowledge of the global distribution, and microphysical properties, of cirrus clouds can be applied to several important problems. For this reason, we have undertaken to explore the GASP data set for information that might be available concerning these aspects of cirrus clouds, in addition to the work already performed by Nastrom et al. (1981) on the problem of cirrus cloud occurrence at aircraft cruising levels.

2.5 GASP DATA USEFUL FOR CIRRUS CLOUD STUDIES

Let us look at the GASP data set and examine the types of measurements available that might be used in studying (1) the microphysical aspects of cirrus clouds, and (2) the distribution of cirrus clouds with respect to atmospheric circulation systems on various scales. For details on GASP instrumentation and data acquisition beyond those presented here, see Briehl et al. (1980) and Perkins and Gustafson (1975).

Normally GASP data is recorded for a 16 second period following 255 seconds of sampling. This leads to an interval between data recordings of, nominally, five minutes. Due to the nature of the various types of measurements made, some of the data represents a nearly instantaneous value characteristic of a very small region near the aircraft at the time of the recording, while other data represent some portion of the preceding 255 seconds (70 km) of flight. Sometimes the constituent averages are formed over even longer periods (distances).

2.5.1. Optical Particle Counter

The presence of cirrus clouds in the GASP data can be indicated by the optical particle counter. The GASP automatic optical particle counter is a modified version of a commercially available ROYCO (Menlo Park, CA) unit. The light scattered in the near-forward direction by a particle passing through the focused image of a light bulb filament is collected. Based on a calibration with transparent latex spheres, particles are sorted into three categories; those greater than .45 μm diameter; those greater than 1.4 μm diameter; and those greater than 3.0 μm diameter. These size categories are better described as "equivalent" size categories, meaning that a particle's assigned size is equal to the size of a latex sphere that scatters the same amount of light in the near-forward direction.

No tests were done with particles similar in shape and refractive index to cirrus ice particles in order to calibrate the optical particle counters specifically for this type of particle. Deviations from spherical shape probably led to sizing errors for particles larger than 1.4 μm diameter (i.e. for those particles with a circumference several times or more larger than the wavelength of the scattered light (Pollack and Cuzzi, 1980).

Variations in response of the various ROYCO instruments flown on the different GASP aircraft probably introduce a relative uncertainty of a factor of three or so in the reported concentrations for a given channel, comparing the counts of one instrument to those of another. The instrument is programmed to accumulate counts for 60 seconds, and this translates into an averaging over roughly 15 km of flight path at typical cruising airspeeds. The minimum detectable concentration is 30 particles/ambient cubic meter. The numbers of particles recorded every five minutes are the numbers accumulated in the first 60 seconds of the 255 second sampling period.

An observation of the light-scattering particle count during a flight through a cirrus cloud with the visibility reduction of a light haze, early in the GASP program, led to the somewhat arbitrary definition that the GASP aircraft was considered to be "in cloud" whenever the concentration of particles whose diameter was greater than 3 μm exceeded 66,000/ambient cubic meter. During the 255 sec interval between recordings, a monitor was kept on the rate at which particles greater thn 3 μm were being counted. If, over one second, this rate corresponded to a local concentration greater than 66,000/ ambient cubic meter, then that second was accumulated in a "cloud second" register. So every five minutes, along with the optical particle data, the number of cloud seconds out of the last 255 seconds was also recorded, and also, the number of times the counting rate in the largest size channel went above 66,000 and then below 8,000 ambient cubic meter threshold values was recorded. This last variable was termed "cloud layers", and may be regarded as a measure of the patchiness of cloud cover at a given altitude.

It is likely that particles much larger than 10 to 20 μm diameter were not included in the optical particle counts. This upper size limit, which is not precisely known, is the result of limitations of the internal electronics and also of the transmission efficiency of the sampling tubing for larger particles. (G. Lala, personal communication· D. Briehl, personal communication). The air containing the particles was brought into the ROYCO counter from outside of the aircraft through approximately 1.24 meters of tubing. The air was decelerated in a small chamber and the ROYCO sample was drawn from that chamber. Some unknown amounts of sample heating, and particle evaporation, break-up and loss may have occurred before the sample passed through the ROYCO. A temperature sensor on the ROYCO particle-counting head indicated temperatures typically between 0^{o} C and 20^{o} C in-flight (J. D. Holdeman, personal communication).

2.5.2 Condensation Nuclei

Something of the past history of an air parcel can be indicated by its total aerosol content, and the aerosol size spectrum. A measure of the total aerosol content was given by a modified Environment/One automatic condensation nucleus counter (Nyland, 1979). This counter can detect the presence of most aerosol particles in the diameter range 0.01 μm to several micrometers. Ambient air brought into the aircraft was mixed with clean air and brought to cabin pressure, whereupon it was fed into the condensation nucleus counter where an adiabatic expansion led to condensation and the growth of a small cloud in the expansion chamber. From the optical density of the cloud, an aerosol particle concentration is inferred. The counters were calibrated against a standard Pollock counter for given sizes and types of aerosols; the reported accuracy is $\pm$ 6.6%. The primary variation is due to variation in the physicochemical properties of the sampled particles, and also in small part to variations in the optical extinction measured for different clouds formed on the same number of particles. Additional information is given in Nyland (1979).

2.5.3 Humidity

Humidity is a valuable measurement in examining cloud microphysical processes. During the 45 flights considered here, the water vapor concentration was detected with a custom-designed, cooled-mirror dew/frostpoint instrument manufactured by EG&G, Waltham, Mass. (Englund and Dudzinski, 1981). Three stages of thermoelectric cooling were used to cool the mirror accurately to stratospheric frostpoint temperatures. Laboratory calibration showed the instruments to have an essentially first-order response to humidity changes. Dew/frostpoint changes as fast as 1.5^{o} C/sec could be accurately tracked at temperatures from +17^{o}C to -40^{o}C. For dew/frostpoint depressions of more than about 5^{o} C below ambient, and also for all measurements at ambient temperaures below -40^{o} C, the instrument responded somewhat more slowly. Cold chamber calibrations typically showed a standard deviation of about 1.2^{o} C around the nominally correct values for temperatures between +17^{o} C and -68^{o}C.

Air was brought into the dew/frostpoint instrument through a de-iced air scoop and then through a constricted flow tube in such a way that sample pressure remained close to the ambient pressure. Frostpoint - ambient air temperature differences amounting to more than 10% of the air temperature itself (in^{o}C) were occasionally reported, particularly during and following cloud

encounters. This was probably due to some combination of internal electronics problems in the mirror temperature balancing circuit and water/ice contamination in the sampling system (E. Lezberg and T. Dudzinski, personal communication). These anomalously high readings were deleted during processing of the raw data (see also Section 1.2.2).

2.5.4 Ozone and Carbon Monoxide

Ozone and carbon monoxide can be used, respectively, as tracers of stratospheric and tropospheric air. Ozone was monitored using an ultraviolet absorption zone photometer which had a range from 3 to 20,000 ppbv with a stated sensitivitiy of 3 ppbv. For this instrument each measuring cycle takes 20 sec, so a data record contains the value determined in the most recently completed cycle. Instruments were periodically recalibrated and in general their relative performance was quite stable (Tiefermann, 1979). There is some uncertainty about their absolute calibration, however, and the reported values may be consistently 9% too high (Briehl et al, 1980). "Instantaneous" values, as well as values averaged over 128 seconds and the standard deviation over 128 seconds, are recorded every 256 seconds.

Carbon monoxide was measured by an infrared absorption technique Dudzinski (1979). The measurements are judged too noisy to be used in this investigation, and carbon monoxide will not be considered further here.

2.5.5 Aerosol Composition

Aerosol particle composition was monitored in the GASP program by exposing filters for two-hour intervals at altitudes above 9.6 km and then analyzing the filters in the laboratory for sulfate, chloride, fluoride, nitrate, and ^{7}beryllium. Although such measurements might be of some interest in the study of cirrus cloud microphysics, the two-hour sampling period corresponds to a spatial averaging over distances well in excess of 1000 km. This will mean averaging over several circulation systems, various amounts of cloudy and clear air, and over upper tropospheric and lower stratospheric air, typically.

The size range of particles collected on filters is, apparently, unknown. Typically, sulfates and nitrates form the largest fraction of the particle mass collected in most GASP

flights. Some flights in tropical areas show significant amounts of chloride, which may be material of marine origin carried upward in deep convective clouds to the upper troposphere. Flights through the stratosphere typically show a greater concentration of ^{7}Beryllium than do those through the troposphere because ^{7}Be is thought to be produced above the tropopause by cosmic rays.

2.5.6 Other Parameters

In addition to the above parameters, static air temperature, pressure (altitude) and airspeed are recorded from the central aircraft data computer. Aircraft position and vertical acceleration are derived from the inertial navigation system. Date and time are recorded from a special GASP unit.

Finally, in addition to the data recorded during the GASP flights, the archived GASP data (available from the National Climatic Center) also contain auxiliary data derived subsequent to the flight. These include solar elevation angle and the National Meteorolgical Center (NMC) tropopause height. These data were not yet available for the 45 flight data set considered in this work.

2.6 INVESTIGATIONS TO BE PERFORMED WITH THE GASP DATA

Data from GASP flights which include all or almost all of the types of measurements described in the preceding section could be used to investigate the following aspects of cirrus clouds.

(1) The global distribution of cirrus cloud occurrence between approximately 200 and 300 hPa (mb) pressure levels could easily be investigated. Comparison of individual records of cloud episodes to corresponding standard meteorological synoptic analyses would provide a means of correlating occurrence of these clouds with atmospheric circulation features.

(2) In addition to the occurrence of cirrus clouds, the occurrence of nearly clear, but ice-supersaturated, air can also be studied using the GASP data. Clear, ice-supersaturated regions are commonly indicated by the formation and persistence of aircraft contrails in apparently clear air. In these regions, RHI exceeds 100% but RHW has yet to become large enough to initiate natural cloud formation by the sorption-freezing process. Casual observations from the ground as well as a survey of satellite images to the earth show that contrails usually persist in regions near where natural cirrus clouds are found (Detwiler, 1980). Such cloudless regions might be seeded with ice-nucleating agents in order to form clouds artifically and to modify the radiative heating and cooling of the earth and lower atmosphere. It is of interest to determine whether clear, ice-supersaturated regions can be found in situations where artificial cloud formation would be beneficial.

(3) It is important to determine the number of small ice particles present in typical cirrus clouds in order to allow more accurate calculation of radiative transfer through such clouds. Previous results show that the largest number of particles usually have a size close to the detection limit of the instruments employed to measure ice particle size spectra from aircraft. Since the GASP optical particle detector can sample particles somewhat smaller than detected by instrument packages used in previous investigations, the GASP data set may be able to give some useful information about the presence of ice particles in cirrus clouds less than a few micrometers in diameter.

(4) By looking at the measured humidities and particle size spectra in cirrus clouds, some verification of the theoretical ice particle growth simulations of Heymsfield can be made. In addition, a humidity criterion might be developed for use by numerical modelers to parameterize the presence or absence of cirrus clouds in a model atmosphere.

For this study the data records collected during 45 commercial flights late in 1978 were analyzed in detail. These flights are from file 1 of GASP archive tape VL0023, and are identified by route and date in Table 2-1. Detailed time profiles of the variation of temperature, frostpoint temperature, condensation nuclei, light-scattering particles, wind speed and direction, flight pressure level and ozone concentration for each flight were examined. Synoptic analyses of meteorological fields for times nearly coincident with each data record were examined and compared to the flight profiles. Finally, scatter diagrams were prepared to explore the co-variation of several pairs of parameters. Several additional statistical calculations were performed, using the entire 45 flight data set. Results relating to the four topics described in this section are presented below.

TABLE 2-1 - FLIGHTS FROM GASP TAPE VL0023, FILE 1 (N655PA)

	FLIGHT	ROUTE	DEPARTURE DATE	DATA TIME INTVL(GMT)	NDATA
33	GP409	LAX-SFO	10/24/78	0203-0228	6
34	"	SFO-NRT	10/24/78	2047-0633	114
35	"	NRT-HNL	10/25/78	1232-1834	99
36	"	HNL-PDX	10/25/78	2131-0146	51
37	"	PDX-HNL	10/26/78	1856-2331	54
38	"	HNL-PDX	10/27/78	0145-0552	48
39	"	PDX-HNL	10/27/78	1716-2206	54
40	"	HNL-OSA	10/28/78	0017-0755	106
41	"	OSA-HNL	10/28/78	1041-1717	139
42	"	HNL-NRT	10/29/78	0139-0638	75
43	"	NRT-HKG	10/29/78	0929-1315	57
44	"	HKG-DEL	10/29/78	1531-2019	59
45	"	DEL-THR	10/29/78	2301-0205	37
46	"	THR-FRA	10/30/78	0508-0914	47
47	"	FRA-LHR	10/30/78	1114-1149	8
48	"	LHR-JFK	10/30/78	1435-2055	77
49	"	JFK-IAH	11/ 1/78	0252-0523	28
50	"	IAH-JFK	11/ 1/78	1930-2140	27
51	"	JFK-LHR	11/ 2/78	0049-0603	78
52	"	LHR-FRA	11/ 2/78	0845-0910	6
53	"	FRA-THR	11/ 2/78	1131-1534	96
54	"	THR-BKK	11/ 2/78	1813-2333	65
55	"	BKK-HKG	11/ 3/78	0131-0316	22
56	"	HKG-NRT	11/ 3/78	0533-0813	33
57	"	NRT-LAX	11/ 3/78	1125-1925	166
58	"	LAX-HNL	11/ 4/78	0110-0537	54
59	"	HNL-PPG	11/ 4/78	0755-1220	51
60	"	PPG-PPT	11/ 4/78	1418-1613	22
61	"	PPT-LAX	11/ 5/78	0720-1418	83
62	"	LAX-SFO	11/ 5/78	1702-1727	6
63	"	SFO-NRT	11/ 5/78	2143-0743	116
64	"	NRT-HNL	11/ 6/78	1245-1826	161
65	"	HNL-OSA	11/ 6/78	2345-0727	97
66	"	OSA-HNL	11/ 7/78	1043-1718	79
67	"	HNL-LAX	11/ 7/78	2135-0149	68
68	"	LAX-JFK	11/ 9/78	0227-0632	48
69	"	JFK-ATH	11/ 9/78	0852-1716	99
70	"	ATH-BGR	11/ 9/78	2054-0521	100
71	"	BGR-LAX	11/10/78	0830-1345	62
72	"	LAX-PIK	11/10/78	2247-0652	96
73	"	PIK-LHR	11/11/78	0839-0909	7
74	"	LAX-HNL	11/12/78	0625-1045	51

		FLIGHT ROUTE	DEPARTURE DATE	DATA TIME INTVL(GMT)	NDATA
75	"	HNL-LAX	11/12/78	2059-0114	51
76	"	LAX-HNL	11/13/78	0602-1027	49
77	"	HNL-AKL	11/13/78	1326-2103	108

2.7 RESULTS

2.7.1 Global Distribution of Cirrus Cloud Encounters

The global distribution of cirrus cloud encounters in the GASP data set has already been examined using a larger subset of the total set than is considered here, covering the period from late 1975 through 1977 (Nastrom et al., 1981). The distribution of clouds between, nominally, 200 and 300 hPa (mb), with respect to latitude and longitude, height above and below the NMC tropopause, and frequency of occurrence along selected commercial air routes were presented in that study. It was shown that cirrus clouds are encountered most frequently over the intertropical convergence zone (ITCZ) and over the mid-latitude baroclinic zones, where the mid-latitude jet streams and wave cyclones are most often found. The seasonal and spatial variation of cirrus clouds in the GASP data set was consistent with the seasonal migration of the ITCZ and the mid-latitude baroclinic zones. The results of this study are consistent with the work of London (1957) and Appleman (1961), who used surface observations and a small sample of aircraft observations, respectively, to develop their cirrus climatologies.

From these results, it appears that weather and climate modelers who wish to parameterize the presence of cirrus cloud in their models might do so with some expression relating the presence and extent of cirrus clouds to the location and strength of the ITCZ, and the mid-latitude baroclinic zones and their associated cyclones.

Nastrom et al. computed local relative vorticity from NMC upper level wind analyses at the location of each GASP data record in their study. They found, basically, that cirrus clouds tended to occur more frequently, and at higher altitudes, in areas of negative relative vorticity than in areas of positive relative vorticity. This is quite consistent with the discussion above in which the tendency for cirrus clouds to form on the anticyclonic side of jet streams (negative relative vorticity due to anticyclonic wind shear) and downstream of mid-latitude wave cyclones (negative relative vorticity due to anticyclonic flow curvature in this region).

The criterion for cloud seconds used in defining the presence of clouds during GASP flights (66,000 counts per ambient cubic meter for particles of diameter greater than 3 μm) appears to be reasonable. From Figure 2-4, we see that most of the cloud second reports appear with the reports of RHI greater than 80% or so. Comparison with the more comprehensive cirrus particle

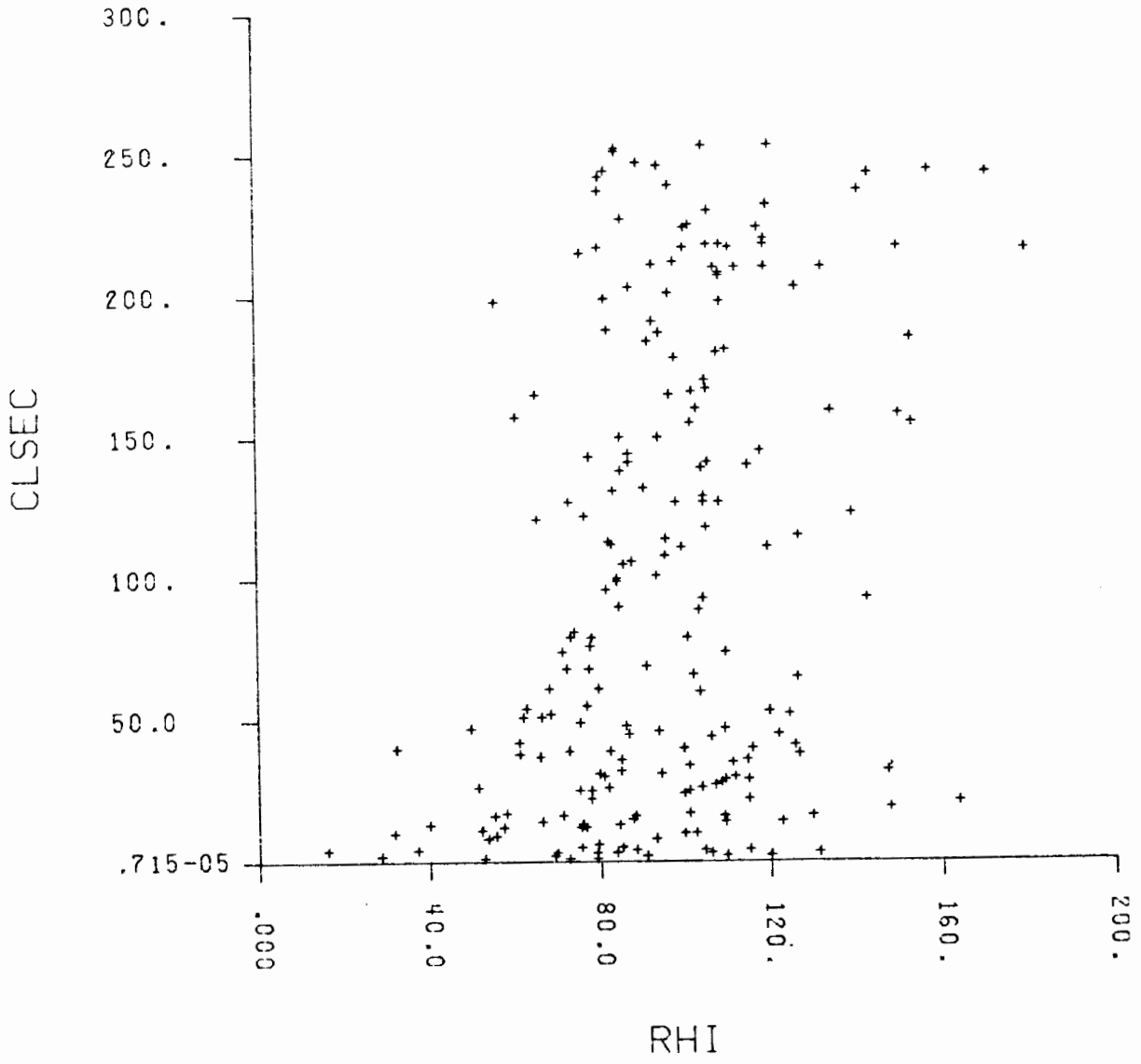

Fig. 2-4. A scattergram showing the relation between cloud seconds and RHI (%) observed in the 45-flight subset of GASP data.

size spectra observed using the AFGL cirrus studies (AFGL, 1978/79) shows that cirrus particles a few micrometers or less in equivalent scattering diameter are almost always present when a visible cirrus cloud is penetrated.

A comparison of the 45 flight data series used in this study with corresponding meteorological synoptic analyses confirmed that the distribution of flight-level cirrus clouds followed the distribution of cirrus with respect to wave cyclones, jet streams, and the ITCZ discussed previously.

A small fraction of the clouds observed in the studies of Appleman (1961) and Nastrom et al. (1981) were noted to be above the analyzed NMC tropopause. However, if ozone is used as an indicator of stratospheric air, then the GASP data suggest that cirrus clouds always occur in ozone-depleted tropospheric air. The source of the disagreement seems to be either that the NMC tropopause is analyzed on too coarse a scale to pick up small scale variations in tropopause height, or that the lapse rate criterion used to define the NMC tropopause is not completely comparable to the tropopause defined by gaseous tracer discontinuities.

A second interesting relation observed in this study was the extremely sharp boundary between cloudy, moist and clear, dry air observed when a GASP aircraft crossed a jet stream axis at a constant pressure level. These boundary zones would be typically narrower than the distance covered by the GASP aircraft between observations (i.e., less than 70 km).

Most of the GASP data are concentrated in the heavily-travelled, mid-latitude Northern Hemisphere air routes. In the limited volume of data available from the 45-flight data set pertaining to sub-tropical areas it was intriguing to note that when cirrus clouds were observed, they tended to occur in short-wave ridges downstream from short-wave troughs in the upper level wind flow. Even though the sub-tropics are not characterized by the same type of frontal wave-cyclone as mid-latitudes, the synoptic-scale waves and convective cloud complexes that occur in the sub-tropics seem to produce a pattern of cirrus cloudiness that is related to that sub-tropical upper level flow in the same way as the pattern of cirrus cloudiness associated with mid-latitude disturbances is related to mid-latitude upper level flow. (See Ch. 14, Palmen and Newton, 1969.)

It should be noted that the GASP data set suffers from fairly serious biases. Most of its data is collected along constant-pressure-level flights between 300 and 200 hPa. If cirrus cloudiness tends to occur at flight level in ridges, say, and beneath flight level in troughs, then the GASP data

indication that cirrus are rarely observed in troughs and often observed in ridges does not imply that cirrus are not observed at any level in troughs. It is only when the cirrus cloudiness distribution observed in the GASP data is compared to the distribution derived by other means of observation that definite conclusions can be drawn about the overall tropospheric distribution of cirrus clouds.

To summarize this section, it appears that the distribution of flight-level cirrus clouds, related to synoptic circulations and to latitude and longitude, observed in the GASP program is reasonably consistent with the distribution derived by other means of observation. The unique feature of the GASP set is that the simultaneous measurement of presence of cloud and ozone allows one to conclude that cirrus clouds always occur in air of tropospheric character, based on ozone content. Previous indications that cirrus clouds could sometimes be observed above the tropopause were probably in error due to inadequate definition of the tropopause in the cloud region.

2.7.2 Cloudless Ice-Supersaturated regions

Before examining the GASP data set for the occurrence of cloudless ice-supersaturated regions, some limitations on the accuracy of the humidity measurements in the data set must first be considered. Determination of RHI is made by dividing the equilibrium vapor pressure of water over ice at the frost point temperature by the equilibrium vapor pressure over ice at the static air temperature. So the accuracy with which RHI can be determined is limited by the accuracy with which the static air temperature and frostpoint are measured.

The accuracy with which the static air temperature is measured is not stated in the GASP literature. However, since dynamic air temperatures sensed by objects moving at typical GASP cruising speeds can be 20^{o} C or more higher than static air temperatures, determination of static air temperatures is not a trivial problem. An accuracy for the reported static air temperature of plus or minus 1^{o} C is reasonable.

The frost point instrument has a nominal accuracy of about plus or minus 1.2^{o}C in the laboratory. Now, if one optimistically takes a typical error range for both the static air temperature and the frostpoint of plus or minus 1^{o} C, then the error in the determination of RHI can be on the order of plus or minus 15% at temperatures in the neighborhood of -50^{o}C. The error will be somewhat less at higher temperatures and somewhat greater at lower temperatures, assuming the same precision of temperature and frostpoint measurements.

In regions where temperature and humidity are fluctuating, there will be additional errors due to mismatched response times of the static air temperature sensor and the frost point sensor, and due also to humidity fluctuations on time scales much shorter than the response times of either of the instruments.

Finally, for purposes of determining clear air, it must be remembered that the reported optical particle counts are accumulated over a 60 second period 3 to 4 minutes preceding the time that the humidity and particle counts are recorded. Even though the air may be clear at the location where the temperature and frostpoint are recorded, if any clouds were encountered over the previous 70 km then the light-scattering particle count may be quite high.

In the following discussion, particle counts will be expressed in three cumulative size ranges. PD2 is the number of particles per ambient cubic meter larger than 0.45 μm diameter; PD4 is the number larger than 1.4 μm; and PD5 is the

number larger than 3.0 μm. By definition, PD4 is less than PD2 while PD5 is less than PD4, for each recorded set of counts. Now taking the presence of PD5 as an indication of the presence of ice particles, we see from Figure 2-5 the range of RHI over which significant numbers of PD5 are observed in our 45 flight data set. Following this, in Figure 2-6 is shown the range of RHI over which at least some optical particle counts were observed (PD2), but none of the counted particles were large enough to fall into the PD5 range. It can be seen that in a few percent of all cases where both humidity and optical particle counts are both available there is apparently "cloudless" ice-supersaturated air (on a horizontal scale of 70 km or more).

The "cloud second" data recorded by the GASP instrument package can also be used to make some inference about the presence of clear ice-supersaturated regions. For cloud seconds close to 255 one can infer cloudiness uniormly denser than what visually looks like "a light haze" over distances of 70 km or so. For fewer cloud seconds one can infer a patchier, more variable cloudiness. In Figure 2-4 it can be seen that most cloud second observations are accompanied by RHI between 75% and 130%. It can also be seen that there are few cloud second reports near 255 seconds. This indicates variations in cirrus cloud structure on scales less than 70 km. (The cloud layer observations average around four per 255 seconds, with a standard deviation of about two. The counts of number of cloud layers per 255 sec interval are not truly normally distributed. The distribution is skewed somewhat towards higher counts.)

The frequency distribution of the cloud second counts observed in our 45 flight data series is shown in Figure 2-7. It can be seen that even though the average number of cloud seconds reported is in the neighborhood of 50 or so, the frequency distribution is skewed towards the low end.

Casual inspection of satellite imagery and observations of the sky from the ground also show that cirrus cloudiness in indeed typically quite patchy and variable, often on a scale of a few kilometers.

Looking through the 45 flights, one finds that about 7% of the data records available with both humidity and optical particle data present have (1) RHI greater than 70%, and (2) less than 10 cloud seconds accumulated over the previous 255 seconds. There is some tendency for these records to appear sequentially (see Figure 2-8). The combination of relatively higher RHI accompanied by little cloudiness might be taken as a crude

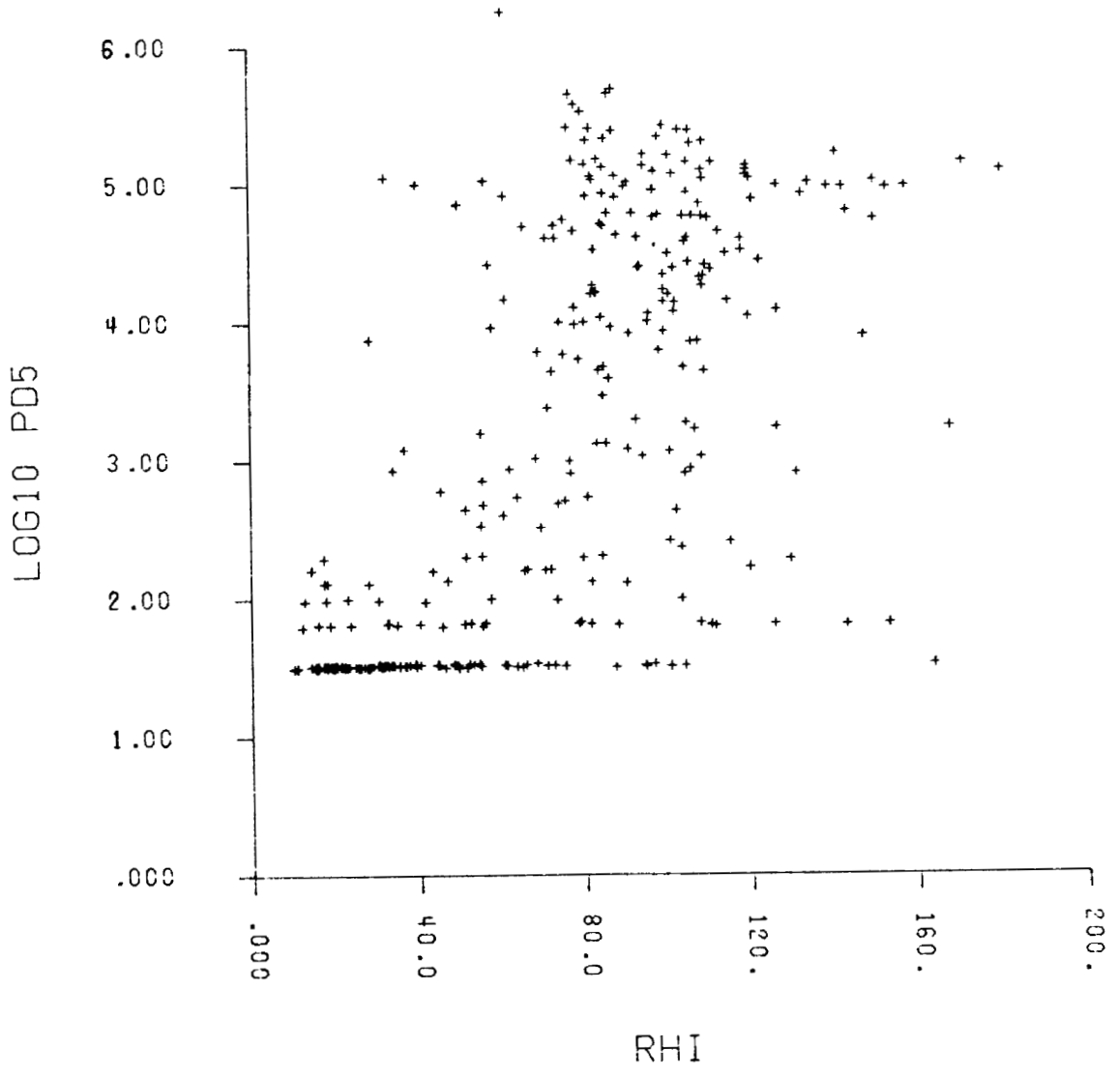

Fig. 2-5. A scattergram of log PD5 (number per ambient cubic meter) versus RHI (%). Note the large number of observations at the lower threshold of instrument sensitivity, corresponding to one particle counted in 60 sec. Well-defined lines of points above this lowest one correspond to two, three, and four counts in 60 sec, respectively.

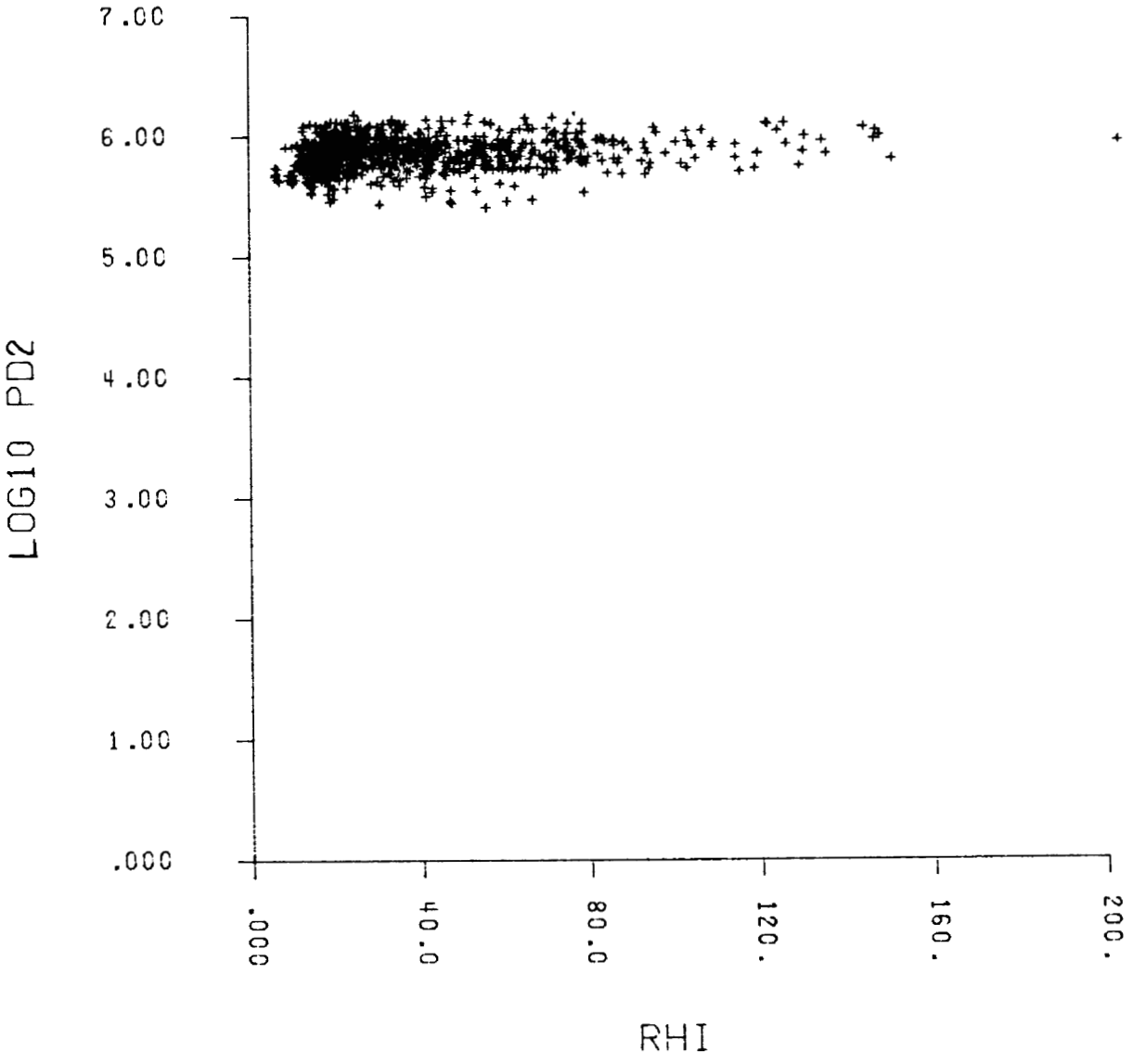

Fig. 2-6. A scattergram of log PD2 (number per ambient cubic meter) versus RHI (%), excluding those cases where PD5 are present. This figure essentially gives the frequency of occurrence of data records with both ROYCO and humidity data present, but no particles larger than three micrometers equivalent diameter, as a function of RHI.

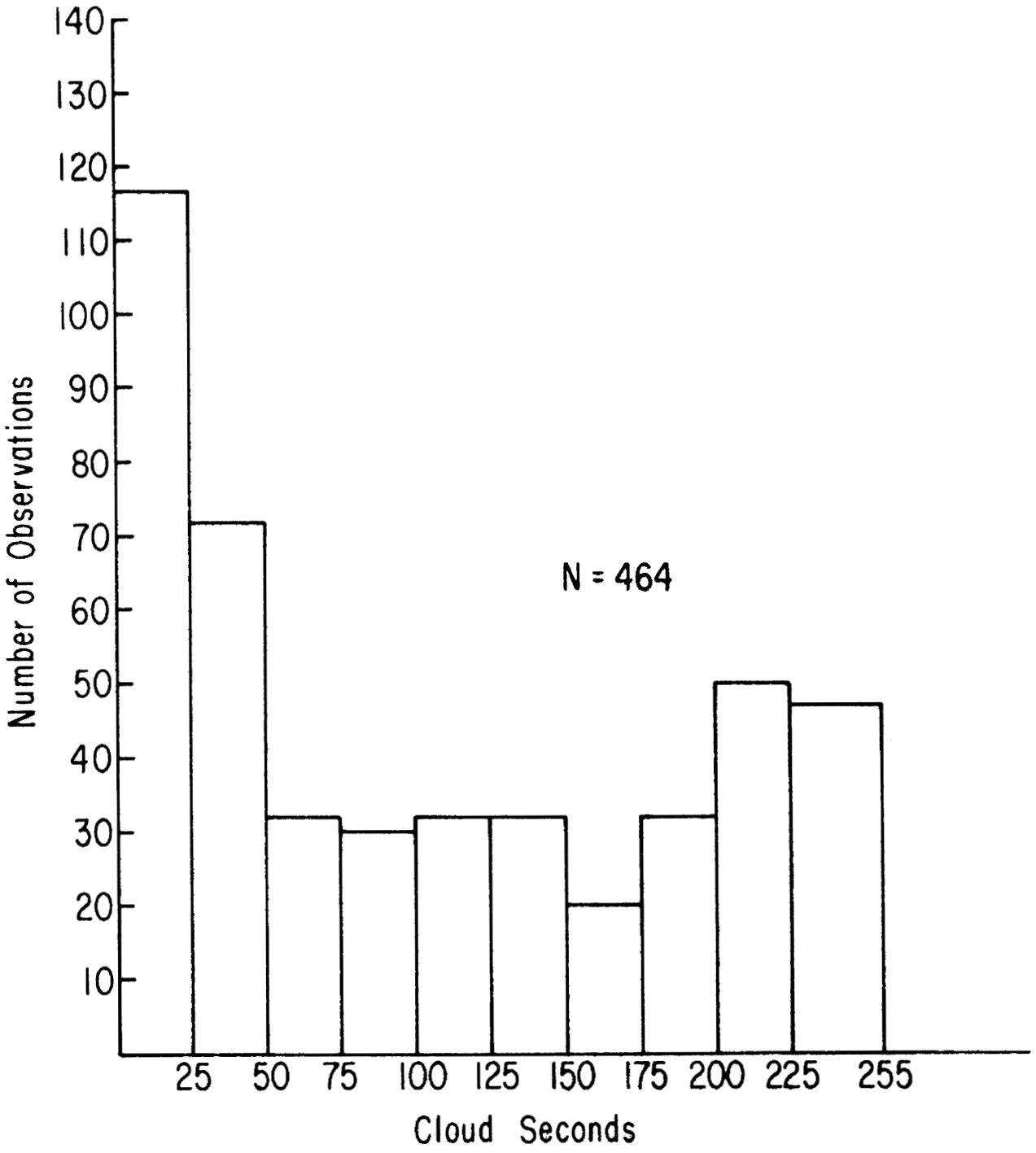

Fig. 2-7. A bar graph showing the frequency distribution of cloud second reports observed on the 45 flights.

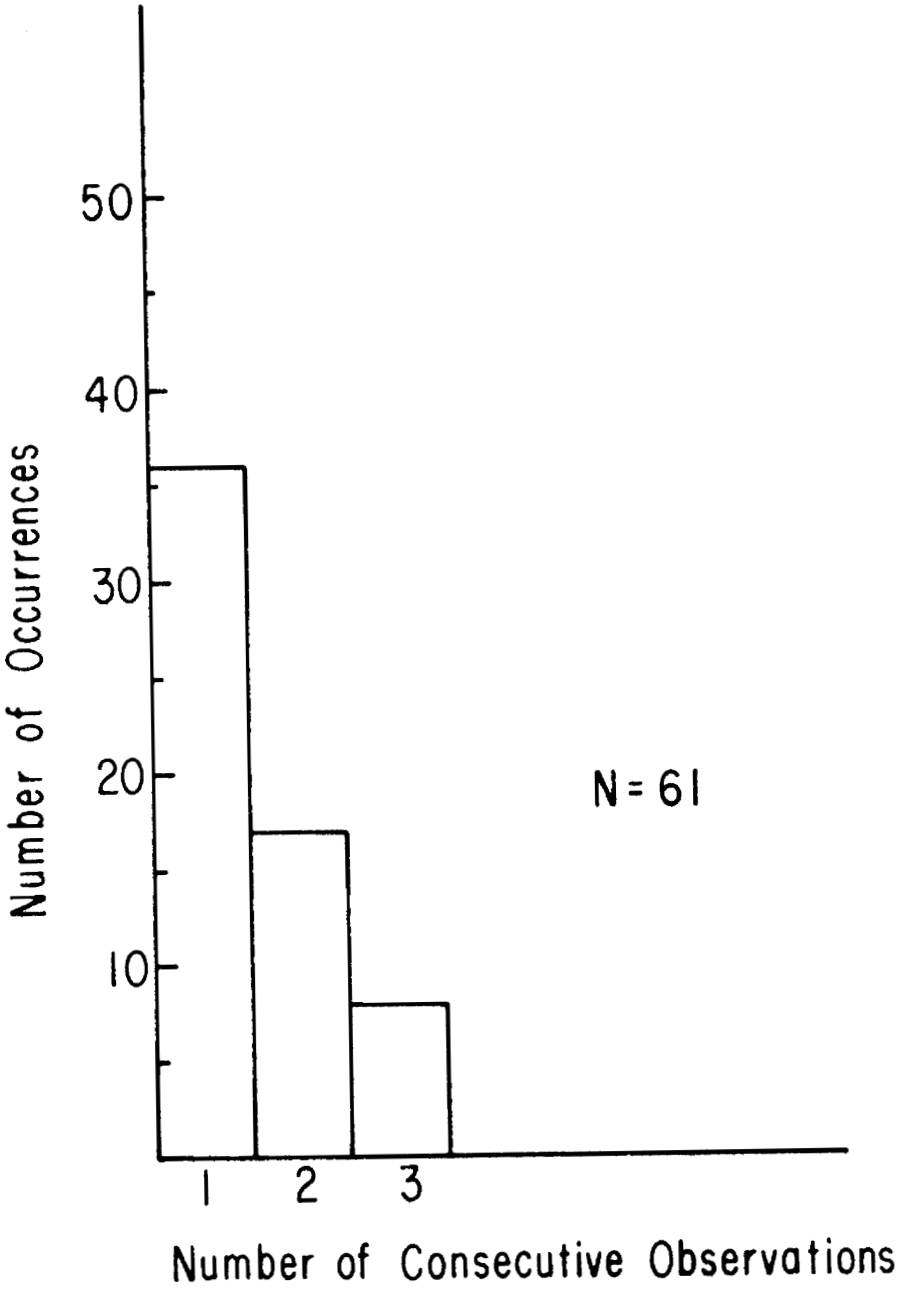

Fig. 2-8. A bar graph showing the frequency distribution of the number of occurrences of one, two, or more successive observations with (1) RHI greater than 80%, and (2) less than 10 cloud seconds. The horizontal distance between successive observations is about 70 km.

indication of an opportunity for seeding to increase the amount of cloudiness.

The result that 7% of the available records, by this criterion, show an opportunity for clear-air seeding is consistent with the personal observations of Beckwith (1972) who noted that persisting aircraft contrails in clear or scattered cloud conditions near flight level were observed in about 7% of the 395 observations which he made during nearly 300,000 km of flight on commercial airliners between 1964 and 1972. It should be noted that Beckwith's observations were made predominantly over the continental US and between California and Hawaii, while the 45-flight record considered here extended around the globe with some flights over subtropical and tropical areas.

The nearly clear, humid air along the GASP flight routes always had a low ozone concentration and was probably of predominantly tropospheric origin.

In summary, then, it appears that extensive regions of clear ice-supersaturated air (say, 100 km or more in extent along a flight path) are relatively rare, occurring during only a few percent of the total time during the 45 flights. Comparison with meteorological synoptic analyses shows that these kinds of regions typically occur in the same synoptic situations as do cirrus clouds. Beckwith also noted that such regions are typically much less than 50 km in extent (Beckwith, 1972). Evidence derived from satellite imagery, and not presented here, also shows that contrails persisting in lengths of 100 km or more in completely clear air are rarely observed. In almost all observations of contrails, what appeard as natural cirrus clouds were generally present within a few tens of kilometers of the contrails (Detwiler, 1980).

As in the case of the distribution of cirrus clouds just discussed above, the appplication of GASP data to the question of occurrence of clear ice-supersaturated regions required corroboration by other means of observation to answer many interesting questions. In particular, it is impossible to infer from the GASP data the presence of clouds above or below a particular length of clear ice-supersaturated flight path. The usefulness of making clouds artificially will probably be much greater in a column of clear air than in a column that already contains cirrus clouds above or below the artificially-produced ones.

2.7.3 Cirrus Cloud Small Particle Counts

The question of the number of small particles present in cirrus clouds can be directly answered using the GASP data set, as long as some of the unique characteristics of the GASP sampling system are kept in mind. Particle sizes are expressed in terms of the size of latex spheres required to produced an equivalent amount of near-forward scattering. Also, the particle counts are accumulated over roughly 70 km of flight path, which may encompass several smaller-scale regions of cloud growth or dissipation, or both, with distinctly different particle size spectra.

In Figure 2-5, the range of the observed PD5 counts versus RHI was shown. Typically, on the order of 100,000 particles per ambient cubic meter were present in clouds. Examination of the 45 flight set of records shows that whenever RHI is greater than about 80%, PD4 is typically within a factor of two of PD5. Also, PD4 greater than roughly 10,000 per ambient cubic meter is almost never observed unless PD5 are also present (see Figures 2-9 and 2-10). In regions of RHI less than 70%, the number of PD4 is typically less than 10,000, but much greater than PD5, indicating that the large ratios of PD4/PD5 observed in Figure 2-9 for RHW less than 80% are due to very small numbers of PD5 appearing in relatively dry air, accompanied by a few thousand PD4 per cubic meter.

If, averaged over 70 km or so in more or less continuous areas of cirrus cloudiness, there are roughly as many particles with a size between 1.4 and 3.0 μm as there are between 3.0 and about 20 μm, then an update to past computations of the radiative properties of cirrus clouds may be required (Roewe and Liou, 1978; Derr, 1980). These computations did not account for the presence of large numbers of such small particles.

The GASP data are in reasonable agreement with the AFGL data, showing similar concentrations of particles of few micrometers in diameter or less (AFGL, 1978/79). The AFGL group uses an instrument to count particles in this size range that operates on the same principles as the GASP ROYCO counters, but is a different design and manufacturer (PMS, Boulder, CO). Due to some of the uncertainties mentioned above concerning the accuracy of such optical particle counters' size assignment, it would be prudent to look for corroborating evidence derived from particle sizing instruments operating on different principles.

An additional problem is the fragile nature of many cirrus ice particles. A. Hogan (personal communication) has indicated the extreme difficulty of sampling ice crystals settling slowly in nearly calm air near the surface in polar regions. They

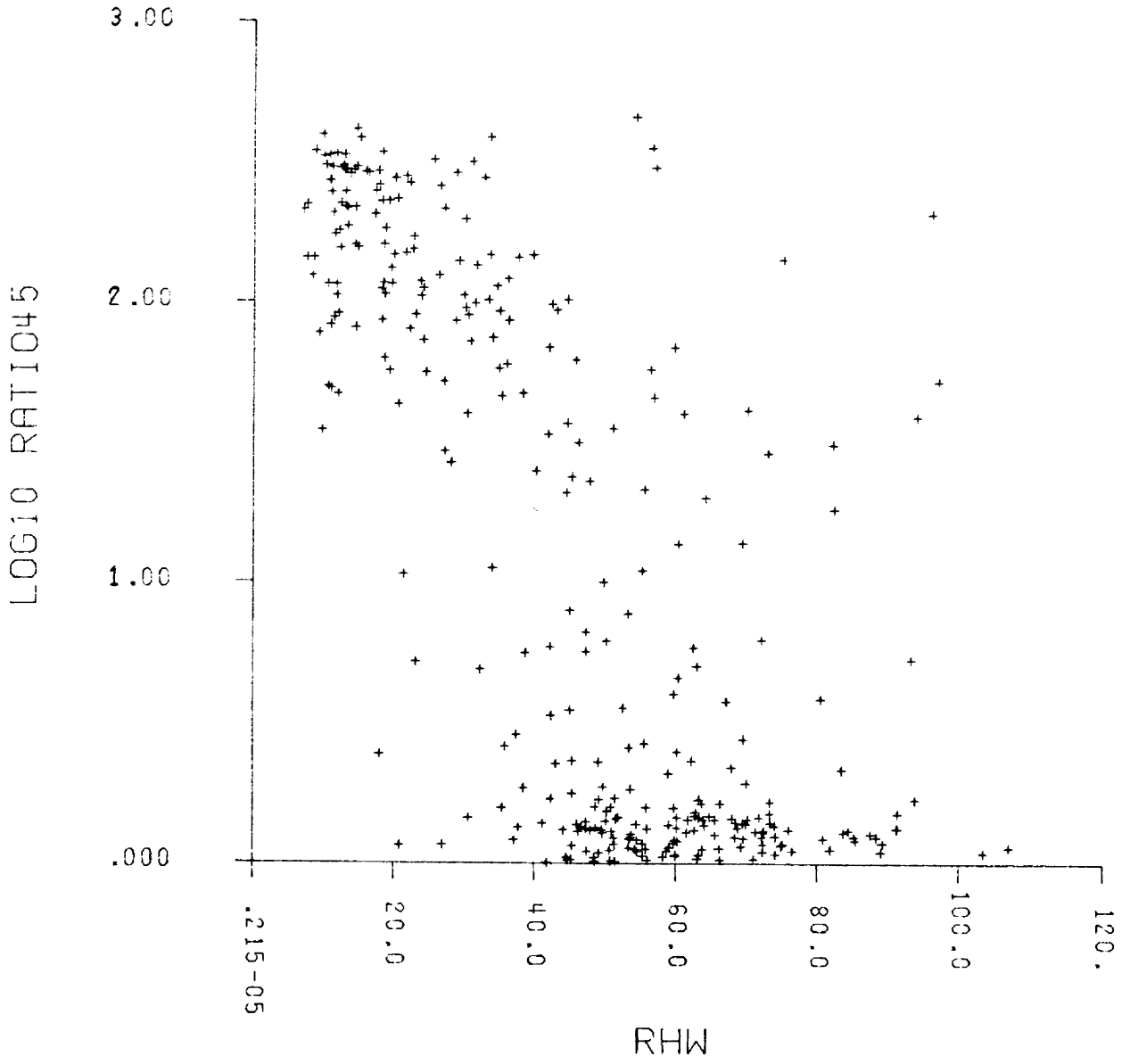

Fig. 2-9. A scattergram of the log of the ratio PD4/PD5 versus RHW (%).

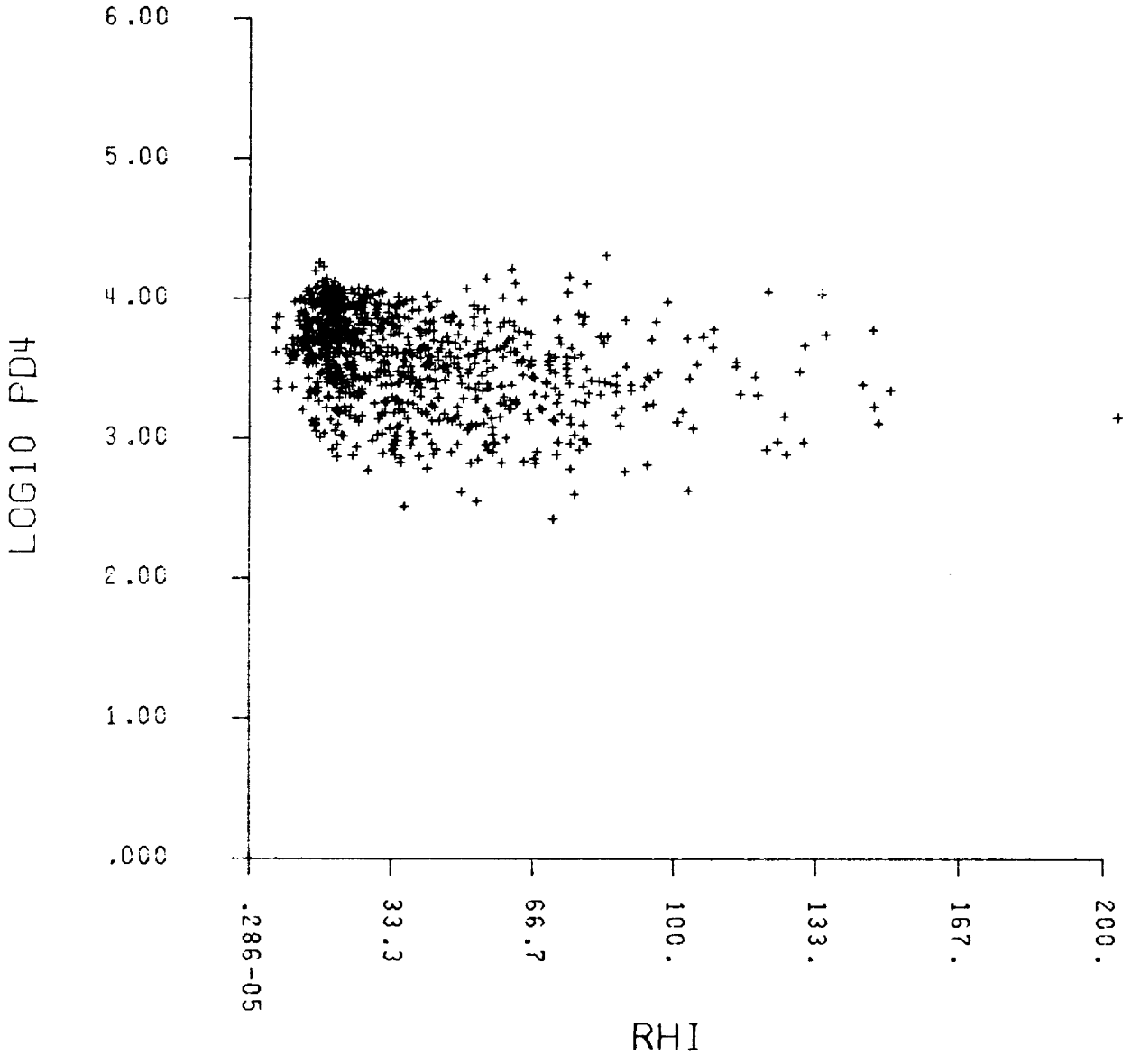

Fig. 2-10. A scattergram of log PD4 (number per ambient cubic meter) versus RHI (%) for cases where PD5 were not detected.

often break up when they fall onto glass slides coated with Formvar. One might expect some ice particle break-up in the ROYCO sampling tubing. It is intriguing to note though, that the AFGL instrument (Particle Measuring Systems (PMS) axially-scattering probe) that is sensitive to these small particles can sample them in the free air stream. It detects roughly the same numbers of small particles a few micrometers or less in equivalent scattering diameter in cirrus clouds as does the GASP ROYCO. It is possible, though, that the cirrus ice particles are so fragile that they are broken up in the turbulent flow field surrounding the aircraft, so that even when sampling in the free airstream several centimeters from the aircraft the sampled crystals ave been already broken somewhat during passage through the aircraft's bow wave.

Heymsfield's (1973) cirrus simulations would suggest that large numbers of small particles (a few micrometers or less in size) should be present in updrafts where cirrus clouds are forming and new ice particles nucleating continuously. The steep slope of the more complete AFGL cirrus particle size spectra, like that shown in Figure 2-3, shows that typically less than 10% of the ice particles present are 10 μm or greater in equivalent diameter. However, it should also be noted that most of the ice mass will usually be present in the size range from tens to hundreds of micrometers.

To summarize this section, the size spectra of cirrus cloud particles sampled over many tens of kilometers along constant pressure flight paths show that PD4 and PD5 counts are typically within a factor or two of each other in regions where the humidity is high enough to indicate presence of stable cloud. In these zones, typically on the order of 100,000 particles larger than 3.0 μm in size are present per ambient cubic meter. In drier air somewhat smaller counts of PD4 and much smaller counts of PD5 are observed. One might infer that in zones of RHI greater than 80% or so, the largest number of particles is usually in the size range from 1.4 μm to somewhat above 3 μm.

2.7.4 Cirrus Cloud Humidities

In a young cloud formation zone there will be predominantly micrometer-size haze particles and a few larger ice particles. In an older region of cloud there will be predominantly larger ice particles that are tens or hundreds of micrometers in equivalent scattering diameter. In terms of the GASP data, this means that in young formation zones PD4 will greatly exceed PD5. That is, there will be many particles between

1.4 μm and 3.0 μm. In an older region PD4 will be close to PD5. That is, many of the particles larger than 1.4 μm will also be larger than 3.0 μm.

Figures 2-9 and 2-11 show the observations where both humidity and particle data were present, and the relationship between the ratio PD4/PD5 and relative humidity. It can be seen that for RHW greater than about 45% and RHI greater than about 80% most observations show a relatively small ratio indicative of an aged aerosol population. For lower humidities mostly larger ratios were observed. At the same time, Figures 2-5 and 2-12 show that above these threshold relative humidities (RHI $\geq$ 80% and RHW $\geq$ 45%) larger PD5 counts were observed, indicating that clouds were usually present.

We may conclude from these observations that most of the cirrus penetrated by GASP aircraft were composed of relatively aged particle populations. This suggests that cloud formation zones must both be of relatively small scale and have short lifetimes compared to the entire scale and lifetime of the clouds. The small-scale variations in cirrus cloud structure discussed in the preceding section would, of course, lead one to expect this.

In terms of the discussion in Section 2.7.2 concerning regions in which artificial cloud formation might be stimulated, it is the small number of regions with relatively high humidity and relatively low large particle concentrations in which such cloud formation might be attempted. In such regions, dispersal of ice nucleating agents might lead to earlier and more extensive cloud formation than would have occurred naturally.

From these results, and the cloud-second verus RHI relationship shown in Figure 2-4, it appears that RHW greater than roughly 45% and RHI greater than roughly 80%, on scales of 70 km or so, usually indicates scattered to overcast cirrus cloudiness at temperatures lower than -40^{o} C.

Unfortunately, from Figure 2-4 it is seen that a point measurement of humidity exceeding these thresholds cannot be uniquely related to some specific amount of cloudiness. It is possible that a distribution function describing the extent of cirrus cloudiness might be derived from the GASP data for use by weather and climate modelers who wish to parameterize the amount of cloudiness in terms of a measure of relative humidity. Although a unique relationship between the spatial content of cirrus and relative humidity may not be available, the extent of cloudiness over a particular region might be specified in a stochastic sense by selecting a cloud amount at random from such a distribution function. The exact details of the parameterization would, of course, depend on the detailed workings of the model in which it is used.

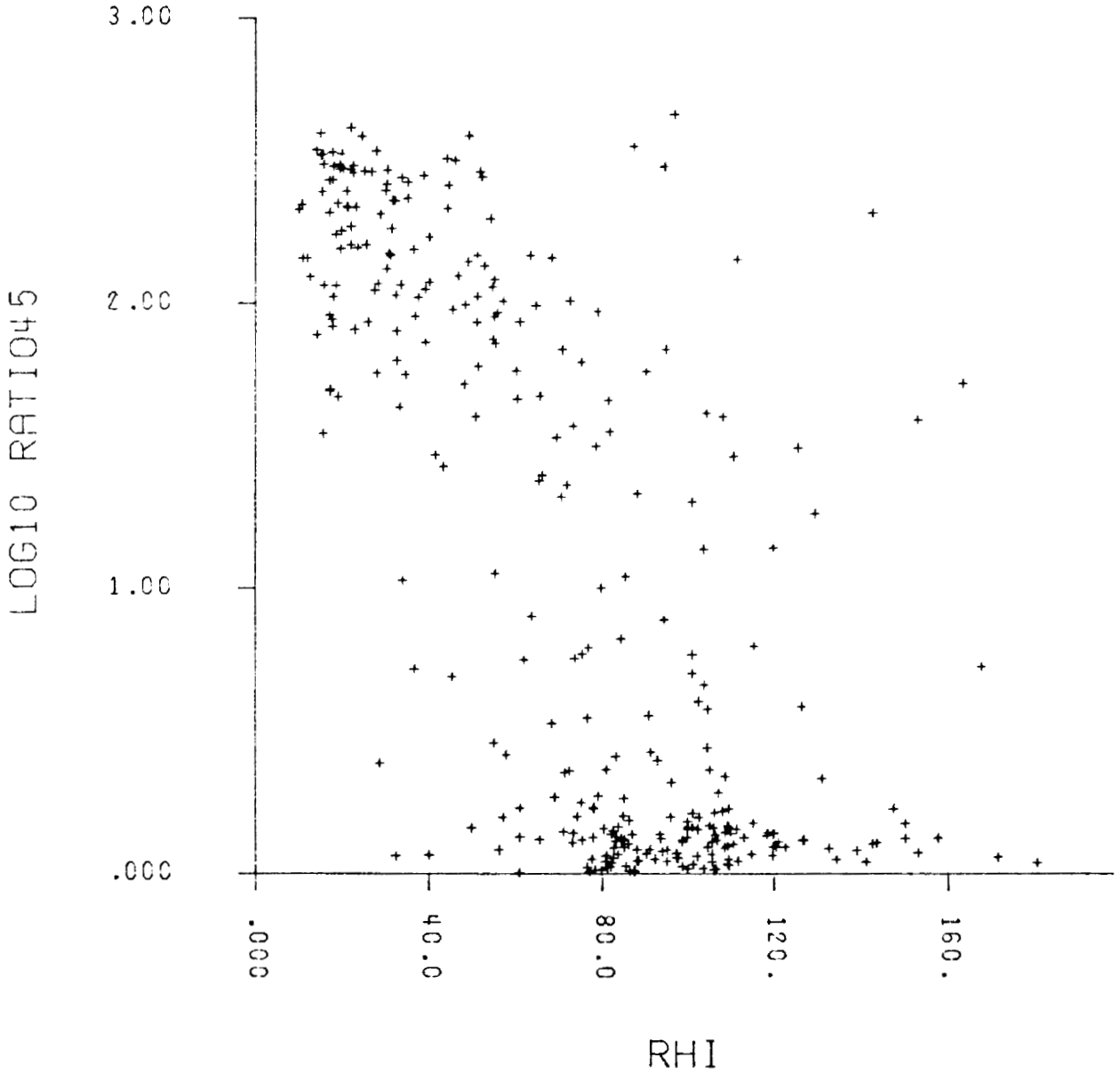

Fig. 2-11. A scattergram of the log of the ratio PD4/PD5 versus RHI (%).

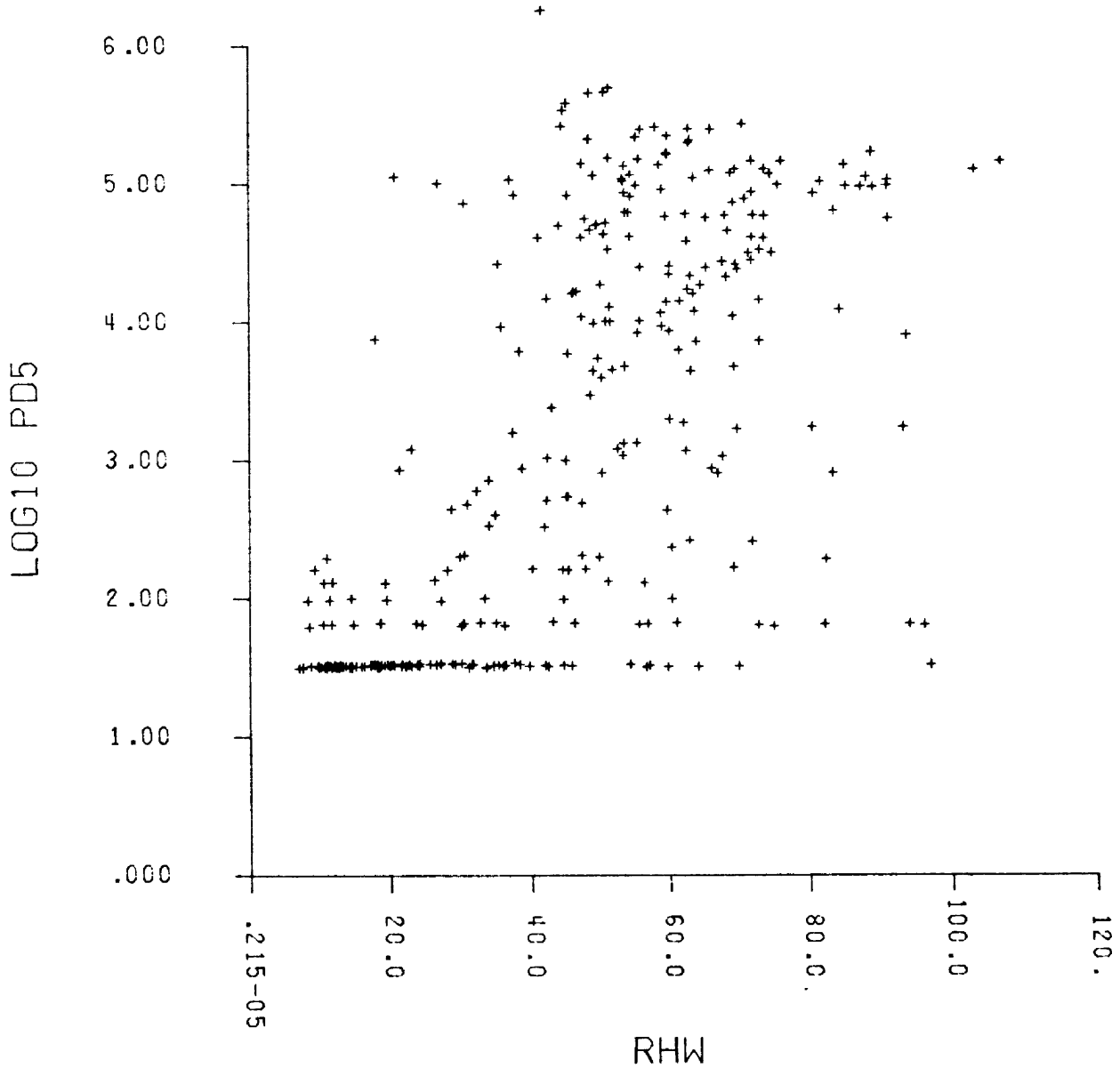

Fig. 2-12. A scattergram of log PD5 (number per ambient cubic meter) versus RHW (%).

2.8 SUMMARY AND CONCLUSIONS

In this report we have looked in detail at a relatively small part of the entire GASP data set. Our purpose has been to study several aspects of cloud formation and distribution at levels above 300 hPa in the troposphere, and to compare the results of this study to previous cirrus cloud studies.

The somewhat arbitrary criterion used in the GASP data reduction to indicate the presence of clouds along the flight path appears to be reasonable. The distribution of such "clouds" at GASP flight levels with respect to atmospheric circulation features is in good agreement with past studies based on ground observations and special aircraft flights. For the 45 flights studied here, which contained mainly Northern Hemisphere mid-latitude and sub-tropical data, cirrus clouds tended to occur ahead of mid-latitude wave cylones and equatorward of the jet streams, and also in small-scale upper-level ridges in the sub-tropics. The cirrus always appeared in ozone-poor air.

Nearly clear, ice-supersaturated regions about 70 km long were indicated in about seven percent of the observations taken during the 45 flights.

Based on th GASP and AFGL cirrus data, it appears that most visible cirrus clouds contain on the order of 10,000 to 100,000 particles per cubic meter a few micrometers or less in equivalent scattering diameter.

Finally, the GASP data indicate that on a scale of tens of kilometers, the threshold liquid water relative humidity accompanying cirrus cloud presence is only about 45%. this corresponds to an ice-phase relative humidity of 80% at upper tropospheric temperatures.

REFERENCES FOR CHAPTER 2

Appleman, Herbert S., 1961: Occurrence and Forecasting of Cirrostratus Clouds, WMO Technical note No. 40, World Meteorological Organization, Geneva, 22 pp.

Barnes, A. A., 1980: Ice particles in clear air. Communications a la VIIIeme Conference Internationale sur la Physique des Nuages, Clermont-Ferrand, 15-19 Juillet, 1980, pp. 189-190.

Beckwith, W. Boynton, 1972: Future patterns of aircraft operations and fuel burnouts with remarks on contrail formation over the United States. Preprints International Conference on Aerospace and Aeronautical Meteorology, May 22-26, 1972, Washington, D.C. Published by American Meteorological Society, Boston, MA, pp. 422-426.

Braham, R. R., Jr. and P. Spyers-Duran, 1967: Survival of cirrus crystals in clear air. J. Appl. Meteor., 6, pp. 1053-1061.

Briehl, D., T. J. Dudzinski and D. C. Liu, 1980: NASA Global Atmospheric Sampling Program (GASP): Data Report for Tape VL0014. NASA TM-81579, 41 pp.

Cohen, Ian D., 1979: Cirrus Particle Distribution Study, Part 5. AFGL-TR-79-0155, Air Force Surveys in Geophysics No. 414. NTIS, Springfield, Virginia, 81 pp.

Derr, V. E., 1980: Attenuation of solar energy by high thin clouds. Atmos. Env., 14, pp. 710-730.

Detwiler, A., 1980: Clear Air Seeding. PhD dissertation, SUNY Albany. (available from University Microfilms International, Ann Arbor, Mich.) 207 pp.

Dudzinski, T. J., 1979: Carbon Monoxide Measurement in the NASA Global Atmospheric Sampling Program. NASA TP 1526.

Englund, D. R., and T. J. Dudzinski, 1981: The Water Vapor Measurement System in the NASA Global Atmospheric Sampling Program, NASA Technical Paper (in press).

Hall, W. D. and H. R. Pruppacher, 1976: The survival of ice particles falling from cirrus clouds in subsaturated air. J. Atmos. Sci., 33, 1995-2006.

Heymsfield, Andrew J., (1973): PhD dissertation, U. Chicago, Chicago.

----(1975a): Cirrus uncinus generating cells and the evolution of cirriform clouds. Part I. Aircraft observations of the growth of the ice phase. J. Atmos. Sci., 32, pp. 799-808.

----(1975b): Cirrus uncinus generating cells and the evolution of cirriform clouds. Part III. Numerical computations of the growth of the ice phase. J. Atmos. Sci., 32, pp. 820-830.

London, J., 1957: A Study of the Atmospheric Heat Balance. Final Report, Project 131, Dept. Meteorlogy and Oceanography, New York University. (Referenced in Climatic Effects of Cirrus Clouds, by K. P. Freeman. PhD dissertation, U. of Utah. Available from University Microfilms International, Ann Arbor, Mich.)

Ludlam, F. H., 1980: Clouds and Storms. The Behavior and Effects of Water in the Atmosphere, The Pennsylvania State University Press, University Park, PA. 405 pp.

Nastrom, G. D., J. D. Holdeman, and R. E. Davis, 1981: Cloud Encounter and Particle Density Variabilities from GASP Data. NASA Technical Paper 1886, Langley Research Center, Hampton, VA.

Nyland, Ted W., 1979: Condensation Nuclei (Aitken particle) Measurement System used on the NASA Global Atmospheric Sampling Program. NASA TP-1415, Lewis Research Center, Cleveland, OH 25 pp.

Ohtake, Takeshi and Masayuki Inoue, 1980: Formation mechanism of ice crystal precipitation in the Antarctic Atmosphere. Communications a la VIIIeme Conference Internationale sur la Physique des Nuages, Clermont-Ferrand, 15-19 Juillet, 1980. pp. 221-224.

Palmen, E. and C. W. Newton, 1969: Atmospheric Circulation Systems. Academic Press, NY, 603 pp.

Perkins, Porter and Ulf R. C. Gustafsson, 1975: An Automated Atmospheric Sampling System Operating on 747 Airliners. NASA TM X-71790, Lewis Research Center, Cleveland, OH. 8 pp.

Pollack, James B. and Jeffrey N. Cuzzi, 1980: Scattering by nonspherical particles of size comparable to a wavelength: A new semi-empirical theory and its application to tropospheric aerosols. J. Atmos. Sci., 37, pp. 868-881.

Pruppacher, H. R. and J. D. Klett, 1978: Microphysics of Clouds and Precipitation, D. Reicel Publishing Company, Dortrechit, Holland, 714 pp.

Reiter, Elmar R., 1963: Jet Stream Meteorology. U. Chicago Press, 515pp.

Riehl, H., M. A. Alaka, C. L. Jordan, and R. J. Renard, 1954: The Jet Stream. Meteorological Monographs, V.2, no. 7. American Meteorological Society, Boston, MA, 100 pp.

Roewe, Douglas and Kuo-Nan Liou, 1978: Influence of cirrus clouds on the infrared cooling rate in the troposphere and lower stratosphere. J. Appl. Meteor., 17, pp. 92-106.

Scorer, R. S., 1978: Environmental Aerodynamics. Wiley, NY, 488 pp.

Shapiro, M. A., E. R. Reiter, R. D. Cadle, and W. A. Sedlacek, 1980: Vertical mass and trace constitutent transport in the vicinity of jet streams. Arch. Met. Geoph. Biokl., Ser B, 28, pp. 193-206.

Smiley, Vern N., Bruce M. Whitcomb, Bruce M. Morely, and Joseph A. Warburton, 1980: Lidar determinations of atmospheric ice crystal layers at South Pole during clear-sky precipitation. J. Appl. Meteor., 19, pp. 1074-1090.

Tiefermann, M. W., 1979: Ozone Measurement System for NASA Global Air Sampling Program. NASA TP 1451.

Varley, D. J., 1978a: Cirrus Particle Distribution Study, Part 1. AFGL-TR-78-0192, Air Force surveys in Geophysics No. 394. NTIS, Springfield, Virginia, 71 pp.

Varley, D. J. and D. M. Brooks, 1978: Cirrus Particle Distribution Study, Part 2. AFGL-TR-78-0248, Air Force Surveys in Geophysic No. 399. NTIS, Springfield, Virginia, 108 pp.

Varley, D. J., 1978b: Cirrus Particle Distribution Study, Part 3. AFGL-TR-78-0305, Air Force Surveys in Geophysics No. 404. NTIS, Springfield Virginia, 67 pp.

Varley, D. J. and A. A. Barnes, 1979: Cirrus Particle Distribution Study, Part 4. AFGL-TR-0134, Air Force Surveys in Geophysics No. 413. NTIS, Springfield, Virginia, 91 pp.

Viezee, W., R. M. Endlich, and S. M. Serebreny, 1967: Satellite-viewed jet stream clouds in relation to the observed wind field. J. Appl. Meteor., 6, pp. 929-935.

CHAPTER 3

OZONE VARIABILITY IN THE UPPER, TROPICAL TROPOSHERE

by Phillip Falconer* and Robert Pratt*

3.1 INTRODUCTION

Using data from the Spring of 1976, and continuing through the Autumn of 1978, ozone mixing ratio data from aircraft flights through the upper, tropical troposphere (20°N to 20°S at flight altitudes between 10 and 12.5 km) were extracted from the NASA-Global Atmospheric Sampling Program (GASP) data base. Analyses of the seasonal and inter-annual variations of ozone in the tropics for three geographic regions - South American (30°W - 100°W), the Pacific Islands (155°E - 145°W), and the Australasia region (95°E - 155°E) - show features that are not easily explained by the classical model (e.g., Pruchniewicz, 1974). Moreover, numerous instances of elevated ozone levels, perhaps exceeding their seasonal and geographic mean values by factors of 2 to 3, were encountered by the GASP aircraft. As will be pointed out later, the magnitude and seasonal frequencies of these sporadic "encounters" are merely symptomatic of the underlying, annual ozone oscillations in the tropics.

3.2 ANALYSIS METHODS

Ozone measurements from 563 flights between 20°S and 20°N were specified as part of the GASP tropical data set; all observations were made within the troposphere. This longitudinal coverage of the tropics cannot, however, be considered uniform because those aircraft participating in the GASP program (Pan Am and QANTAS) fly standard air corridors between irregularly-distributed ports of call (cf. Perkins, 1976). The most frequent coverage provided by the commercial aircraft includes the South and Central Americas; the Pacific Islands, east of Australia; and the Far East and Australia, as specified in the introductory remarks. Additionally, inter-hemispheric differences in the average, upper tropospheric ozone content were evaluated by calculating seasonal variations of 0 - 20°N, and 0 - 20°S.

The individual ozone mixing ratio measurements (in parts per billion by Volume, ppbV) reported on the GASP magnetic data

---

* Research Associates, ASRC

tapes generally required no corrections. However, during the period from April 9, 1977 to September 9, 1977, the Dasibi ozone sensor aboard the Qantas airliner apparently began to lose sensitivity due to scrubber fatigue. At the time of instrument recalibration at Lewis in early September, the recorded ozone values departed from their true values by nearly 37%. In order to "correct" for deterioration of the sensor, an empirical, daily correction term was applied to the reported ozone values, as follows:

$$\text{Corrected Ozone} = \text{Recorded Ozone} \times 1.91 \times (1-0.476 \exp(-(JD-99/153)^5)$$

where JD is the Julian Day (JD-99 is April 9). Two independent considerations were used in defense of this correction term: (1) engineers contacted at Dasibi Corporation and at the California Air Resources Division indicated that the likely scrubber lifetime would be 2-3 months, with a rapid deterioration ($\sim 0.5\%$ day^{-1}) thereafter for typical high altitude ozone concentrations; and (2) the time series of mean ozone abundance for selected, tropical flight corridors aboard the Qantas and the Pan American aircraft begin to visibly differ by the end of June, roughly 2 1/2 months after April 9. This high order, exponential equation effects only a slight increase in the recorded ozone through June, and a progressively larger increase (to 36.6%) by September 9.

3.3 OZONE "ENCOUNTERS" IN THE UPPER TROPICAL TROPOSPHERE

Recent evidence from the GASP tropical ozone data set, and the GAMETAG (Global Atmospheric Measurement Experiment on Tropospheric Aerosols and Gases) flight series over the Pacific (cf. Routhier et al., 1980), and from the important airborne experiments conducted by the Max-Planck-Institute for Aeronomy (Fabian and Pruchniewicz, 1977) nearly a decade ago, shows that extensive layering of ozone in the mid- to upper tropical troposphere may be more common than heretofore believed. Frequently, these ozone layers are first encounted as sharp ozone gradient discontinuities (analogous to mid-latitude weather fronts) and often persist for several hundreds of kilometers along the flight path. Nastrom (1979) gives two excellent examples of these ozone "encounters," based upon GASP measurements between New York and Rio de Janeiro, and concludes that the source of these high ozone levels (approximately 60-100 ppbv) is consistent with large-scale, meridional ozone transport from middle latitudes. Fabian and Pruchniewicz (1977) observed ozone "fronts" over tropical Africa on September 26-27 and, again, on October 2-4, 1972. Unfortunately, they did not suggest any interpretation on the source of these regions of high ozone other than possible instrument error.

We examined 141 tropical flights from the GASP data set during the two-year period 1976-1977 for the purpose of identifying the frequency and characteristics of ozone "encounters." In general, an encounter was defined as any occurrence of ozone mixing ratios in excess of 50 ppbV, at constant cruise altitude, between 20°N and 20°S. Although 50 ppbV is an arbitrary choice, we note that it departs significantly from the mean annual, tropical ozone abundance of 35 ppbV calculated from the 1976-1977 GASP data set.

One half of the 120 tropical ozone "encounters" lasted no more than approximately 30 minutes, or 400 km at typical cruising speeds of these commercial airliners. An additional 20% persisted for at least one-half hour. In both instances, these elevated ozone levels were observed deep in the tropics and away from the sub-tropical jet stream systems of either hemisphere. The remaining aircraft interceptions of anomalously higher ozone occurred near the poleward boundaries of the tropics, frequently in the vicinity (within 5° latitude) of high, sustained winds ($\geq$ 30 ms^{-1}). Although Nastrom (1979) was only able to conclude that "abnormally large ozone values of large areal extent are found near the equator (between 53° and 56°W at 12$\pm$0.5 km altitude) during autumn," we might add that our survey clearly indicates that ozone mixing ratios in excess of 50 ppbV lasting at least 30 minutes (4-6 successive ozone readings) are found over South America during the spring, and in other tropical regions, including Australasia, at other times of the year. Thus, we may extend Nastrom's observation by stating that these areas of unexpectedly large ozone values are episodic, but widespead throughout the tropics. Figures 3-1 and 3-2 indicate the nature of these ozone features.

Our analyses show that there is only a slightly greater number of ozone "encounters" in the northern tropics (0-20°N) than in its southern counterpart (0-20°S), by a 6:5 margin. Moreover, more than half of these are accompanied by coincident transitions in the (constant flight altitude) potential temperature, equivalent to at least 2°C per 100 km. These two factors appear consistent with the penetration of ozone-rich airmasses from higher latitudes into the tropics. Danielsen (1980) characterizes these instrusions as "thin laminae of dry, hydrostatically stable air...rich in ozone..." which leave the stratosphere during intense, middle latitude cyclogenesis, and subsequently spread, in sheets, equatorwards. Pruchniewicz suggests, alternatively, that the entrance zone for these laminae is primarily near the sub-tropical jet stream at 30°N. These intrusions may arrive from either hemisphere, as suggested in the trans-equatorial wind flow pattern shown in Figure 3-3. Unfortunately no air parcel trajectory analyses of the origin of these ozone fronts were

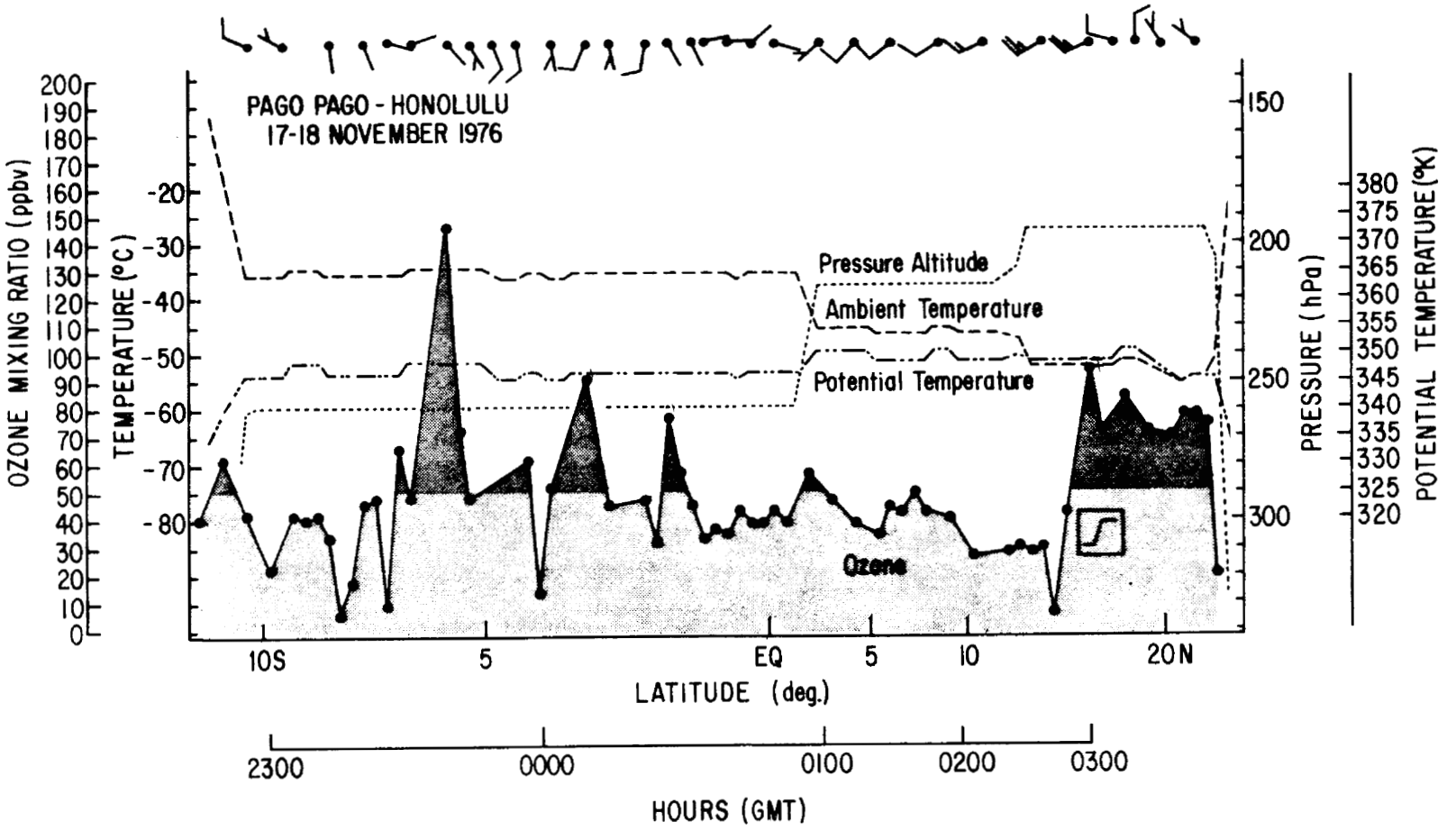

Fig. 3-1. Flight record within the tropical troposphere between Pago Pago and Honolulu. Ozone, pressure altitude, ambient temperature, and wind velocities are obtained from the GASP airliners. The symbol ⌐ refers to an "ozone wall", arbitrarily defined as a rapid increase of the ozone mixing ratio to above 50 ppbV near the poleward boundaries of the tropics. Typically the "wall" begins with at least a twofold increase and continues for at least 6 successive registrations into the sub-tropics.

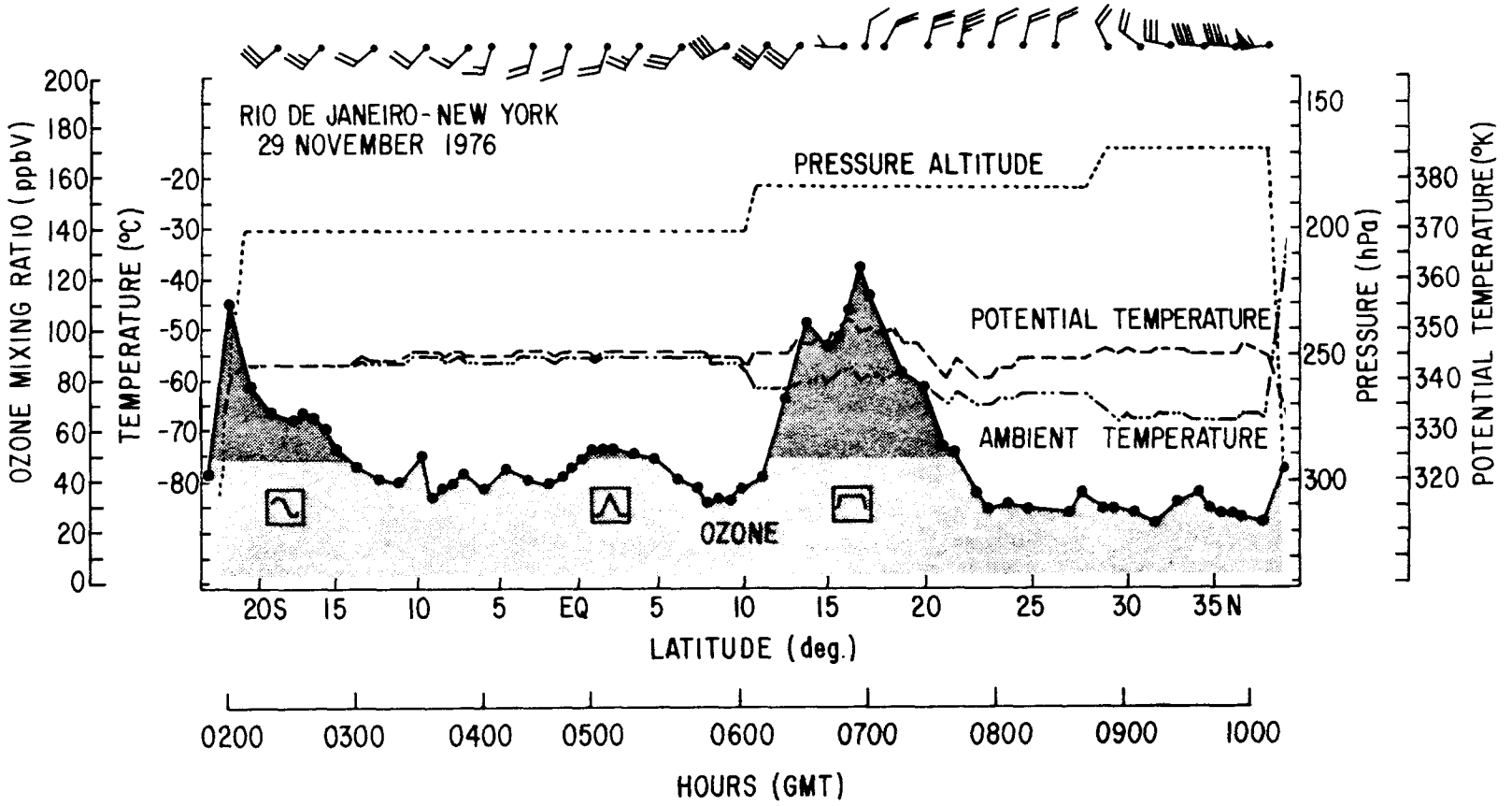

Fig. 3-2. Tropical flight record between Rio de Janeiro and New York City. The symbol ∿ refers to a gradual decrease of the ozone mixing ratio to levels below 50 ppbV near the poleward boundaries of the tropics. Λ refers to an "ozone peak" between 20°S and 20°N in which ozone levels greater than 50 ppbV do not last longer than 6 successive readings. The "extended ozone peak", ⌒, lasts longer than 6 successive registrations.

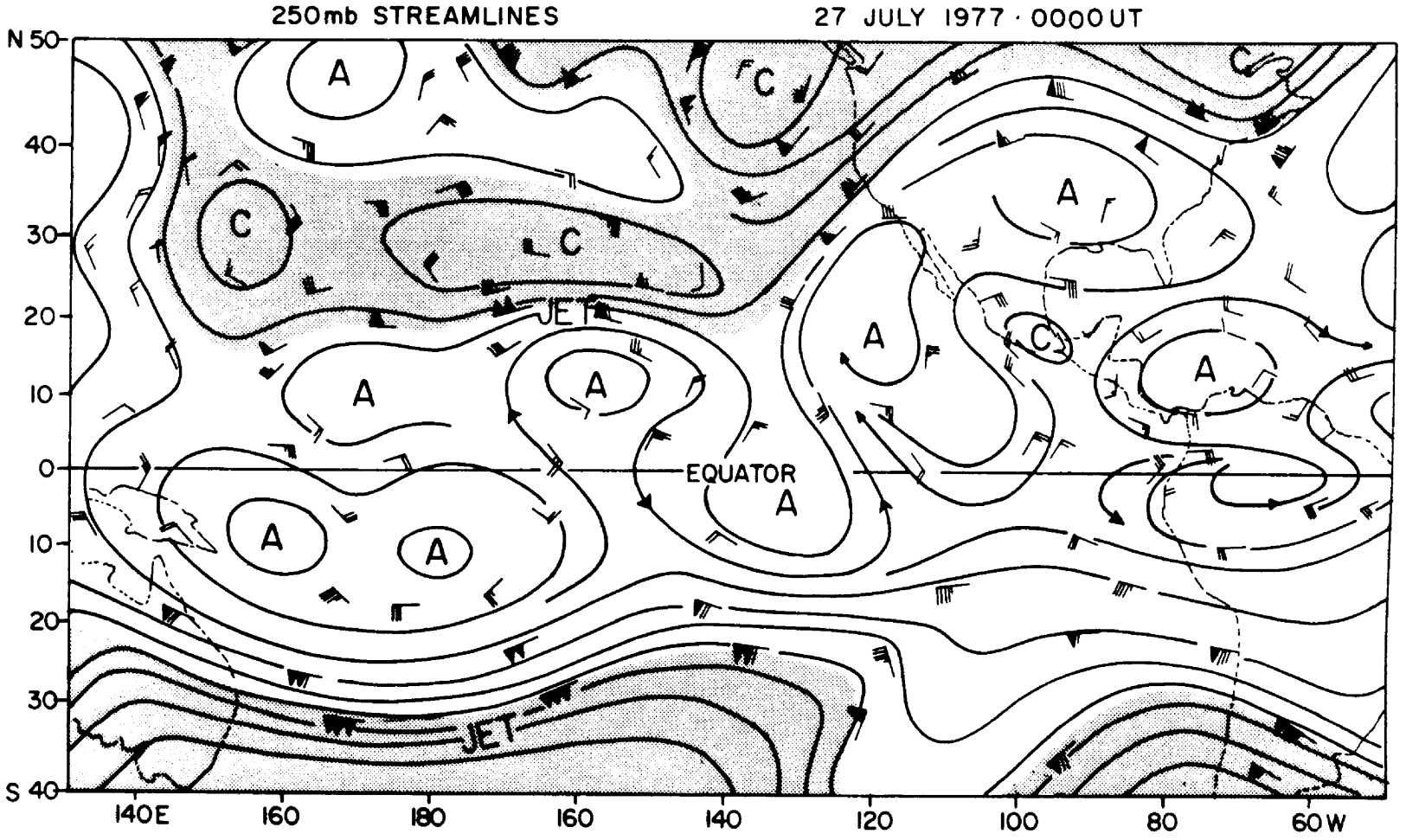

Fig. 3-3. Horizontal flow at 250 millibars on July 27, 1977 (A = Anticyclone, C = cyclone).

made because of an insufficient upper air (radiosounding) data base in the tropics, particularly over the Pacific.

3.4 TROPICAL OZONE "ENCOUNTERS" ALONG THE NEW YORK CITY - RIO DE JANEIRO TRANSECT

The tropical ozone distributions, which have been described in a climatological sense in the previous section, were also examined on individual flights for any obvious relation they bear to atmospheric thermal structure, observed wind, cloudiness, or character of the earth's surface. The majority of GASP tropical flights occurred over open ocean, for which the only wind and temperature data available were those measured by the aircraft itself. Evidence from some GASP data suggests that trace constituent concentrations at flight level may be related to convective activity, especially over heavily vegetated areas of the tropics (Pratt and Falconer, 1979). For most of the tropical flights, either measurements of light-scattering particles by the GASP instrument package or satellite pictures were the only available indications of the presence of cloudiness near the aircraft, when they were available.

Such case studies focused on flights over Central and South America. These flight corridors were usually oriented in such a way as to provide meridional transects through the tropics and subtropics. The flight paths also passed over both tropical jungle and open ocean. Fortunately a moderate number of upper air reports were available in the area. The most interesting example of these flights was along the New York City to Rio de Janeiro transect on November 21, 1976 (Figure 3-4). Nearly uniform ozone mixing ratios of about 40 ppbV were encounted as the plane flew south across the westerlies of the subtropical jet. At about 20°N, the winds at flight level became northeasterly, and ozone began to rise, reaching 90 ppbV as the winds again reversed to strong westerlies at 15°N. Ozone remained greater than 60 ppbV for the rest of the flight to Rio.

The meteorological situation is clarified by a vertical cross section along the flight (Figure 3-5). The three available upper air soundings, as well as the flight data show that the increase in ozone, which began at about 20°N, corresponded roughly to a sloping transition zone which also separated easterly winds (below and northward) from westerlies (above and southward). Humidity data from an aluminum ozide hygrometer, while they must be judged carefully, suggested that the transition zone consisted of a tongue of relatively dry air, with highest humidities found on the tropical side, along with the higher ozone. Although soundings were relatively scarce, signs of this transition zone were found to extend across the

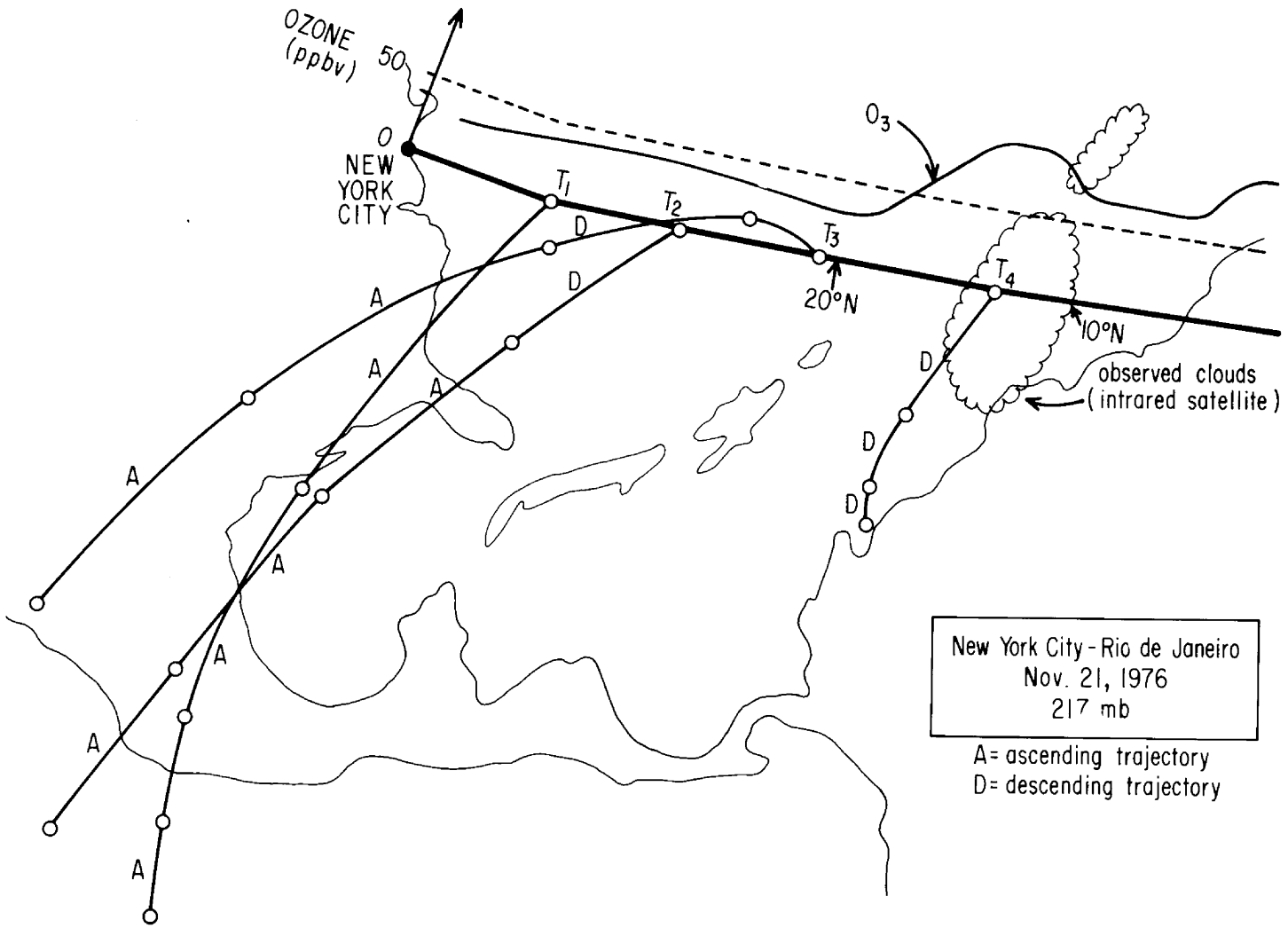

Fig. 3-4. Ozone measured on a flight from New York City to Rio de Janeiro on November 21, 1976. Flight path is the bold, straight line from New York; ozone mixing ratio is plotted using the flight path as the zero axis. Twelve hour isentropic trajectory computations are designated as either A (ascent) or D (descent). Trajectory endpoints lie on the

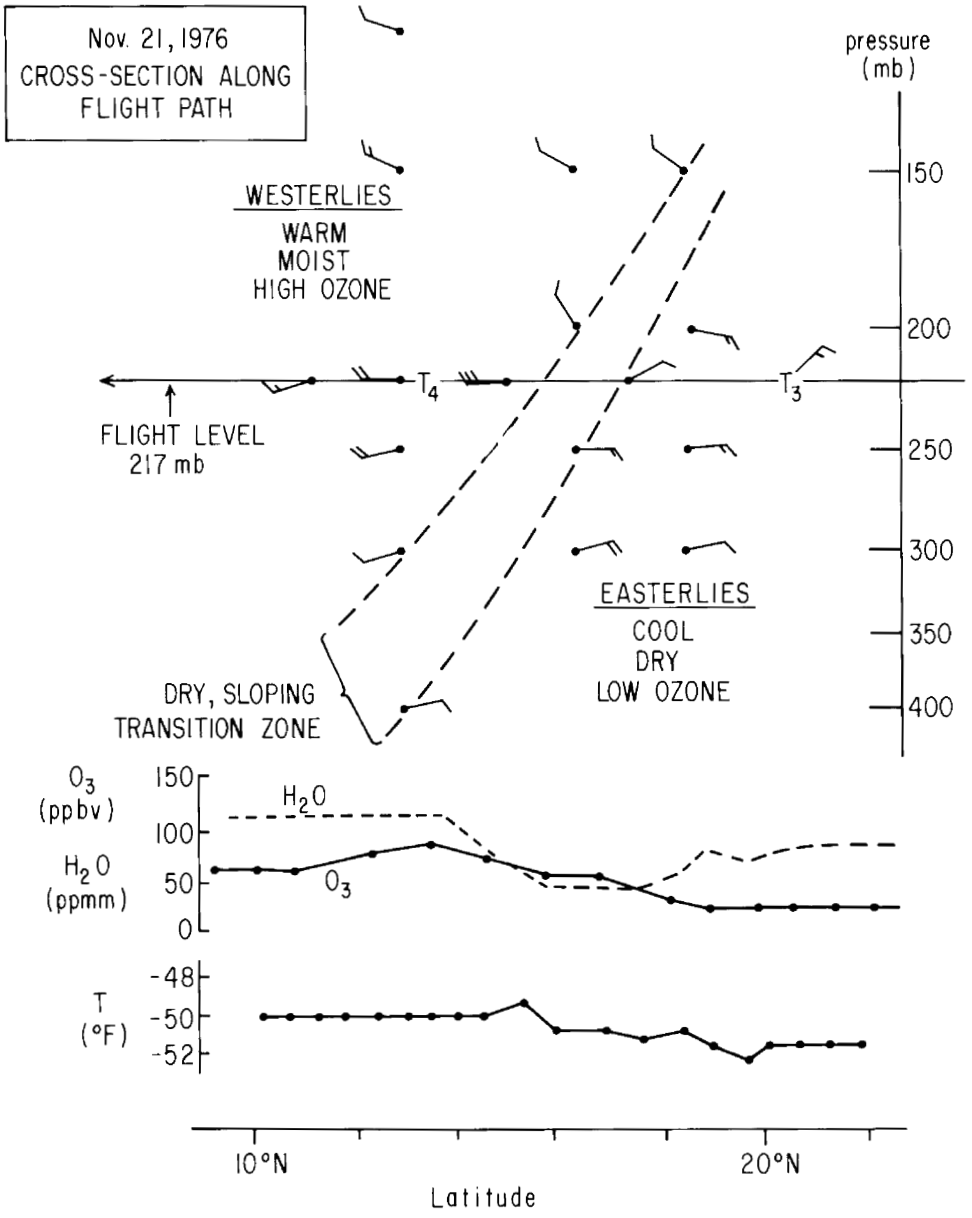

Fig. 3-5. Vertical meteorological cross-section along the flight path. Wind data, indicated by standard National Weather Service plotting convention, was obtained from 3 upper air soundings in the area, except for the wind reports at flight level which are recorded in the GASP data. Endpoints of trajectories 3 and 4 are indicated on the flight path.

Caribbean up to 20° of longitude to the west of the flight path. The temperature soundings also indicated that the transition zone consisted of a layer of enhanced static stability.

Since the origin of the air encountered by the aircraft is as important as the distribution measured at the time of the flight, isentropic back trajectories were obtained for several locations along the flight path. The trajectories were generously computed by Philip Haagenson at the National Center for Atmospheric Research, with the kind cooperation of Melvyn Shapiro. Four of the computer trajectories are indicated in Figure 3-4, in 12-hour segments labeled "A" for ascent or "D" for descent. Trajectories 1 and 2 show predominantly rising air which together with the observed tropospheric value of ozone, is consistent with the expected rising motion on the equatorward side of the subtropical jet (Palmen and Newton, 1979). The interpretation of trajectory 3 is uncertain, since the potential vorticity was observed to change greatly, violating the isentropic assumption. Trajectory 4 was chosen to end at the ozone maximum at 13°N. It shows that the high ozone air had descended for a least 36 hours prior to the flight (with tropospheric potential vorticity values). This trajectory is in possible conflict with the satellite observation of a cloud area surrounding the endpoint, although convective elements could have been imbedded within a broad area of descending motion on the synoptic scale of the trajectory computation.

The trajectory analysis indicates that the high ozone at 12°N, found above the transition zone in Figure 3-5, did not result from recent transport of stratospheric air in the vicinity of the subtropical jet. But it is impossible to tell whether it is a result of ozone-rich air carried a longer distance from high latitudes of either hemisphere, or of tropospheric chemistry within the tropics.

The north-south flights to South America frequently measured higher ozone deep in the tropics than in the subtropics on the anticyclonic side of the subtropical jet westerlies, as in Figure 3-4. Otherwise, no firm conclusions could be made from the individual flight examinations to relate ozone features to wind, temperature changes, cloudiness, or character of the earth's surface. The major problems were lack of upper air data, and lack of simultaneous GASP measurements of other trace constituents on most of the flights.

3.5 MULTI-SEASONAL, TROPICAL OZONE CLIMATOLOGY: 1976 - 1979

We are aware of only a few, detailed studies of the annual ozone cycle in the upper tropical troposphere which are based upon many years of observations. Ozone climatologies for individual years between 1963 and 1965 can be developed for Hilo, Hawaii (19.5°N); LaPaz, Bolivia (16°S); and Canton Island (3°S) from both the Air Force Cambridge Research Laboratory ozonesonde Network data base (cf. Hering and Borden, 1967 and references therein) and the NOAA Ozonesonde Program (Komhyr and Sticksel, 1967). The outstanding feature of these time series (composed of bi-weekly or monthly ballon ascents) is the noticeable lack of similarity in the timing of the annual ozone maxima* from one year to the next. This leads to some ambiguity in representing the local ozone cycle when the muti-year ozone records are composited at individual stations.

The reader is invited to compare, for instance, the "representative" annual, upper tropospheric ozone cycle at the Canal Zone (9°N) presented by Pruchniewicz (1973), based upon the 1963-65 chemiluminescent ozonesond releases by AFCRL: (Figure 3-6), and that presented by Chatfield and Harrison (1977), based upon electrochemical sondes released by the AFCRL between 1966-69 (Figure 3-7). The actual year-to-year variability at 200 hPa for the 1963-65 period, as interpolated from the ozonograms, is shown in Figure 3-8.

Ozone concentrations over Africa obtained from commercial airliners between the years of 1969 and 1974 (or portions thereof) have also been used to develop an annual, tropical ozone cycle. Using nearly 20 flights from the 1970-71 data base, Tiefenau et al. (1973) concluded that the tropical tropospheric ozone reservoir, while reasonably well-mixed within any one season betwwen 20°S and 25°N, undergoes a "remarkable seasonal variation between 0.03 g/g and 0.08 g/g...(which suggests)... a strong seasonal behavior asymmetery of the hemispheres, as for both regions between 20° to o°S and 0° to 25°N the highest values occur between May and June, the lowest values between October and December." Our own interpretation of their remaining ozone data from 1972-1974, although it frequently shows a reasonably uniform, inter-hemispheric ozone distribution within any given season, cannot be used in unequivocal support of a simple, annual ozone cycle whose maximum occurs during Spring in the northern hemisphere. For instance, from September-December 1972 through September-

---

* A semi-annual wave is frequently present in the tropical tropospheric ozone records.

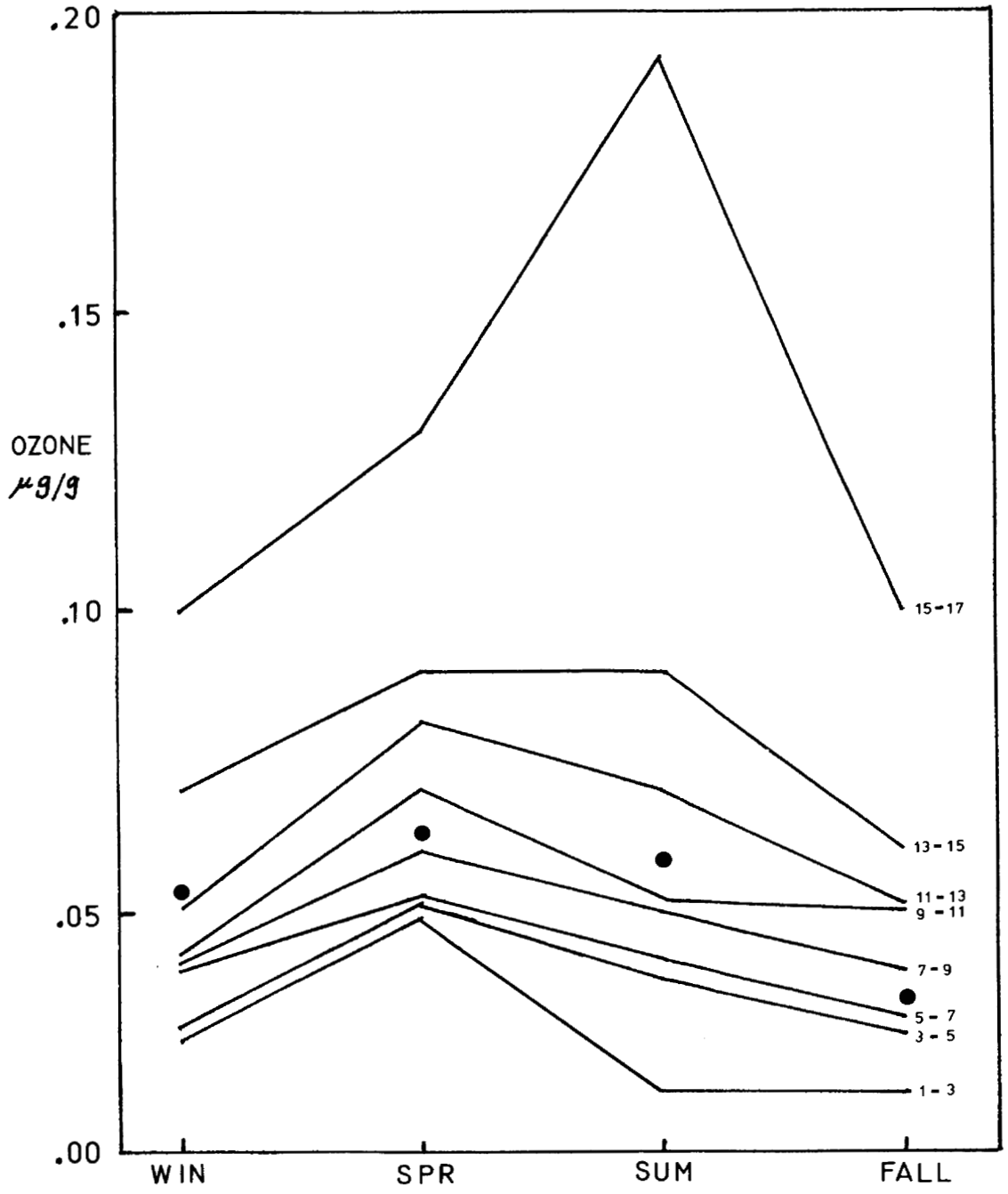

Fig. 3-6. Seasonal variation of tropical ozone for 2 km layers over the tropical station Canal Zone at 10 N. The data are an average of 3 years of ozonesonde observations from 1963 to 1965. Large solid dots are aircraft observations of Tiefenau, Pruchniewicz and Fabian (1973).

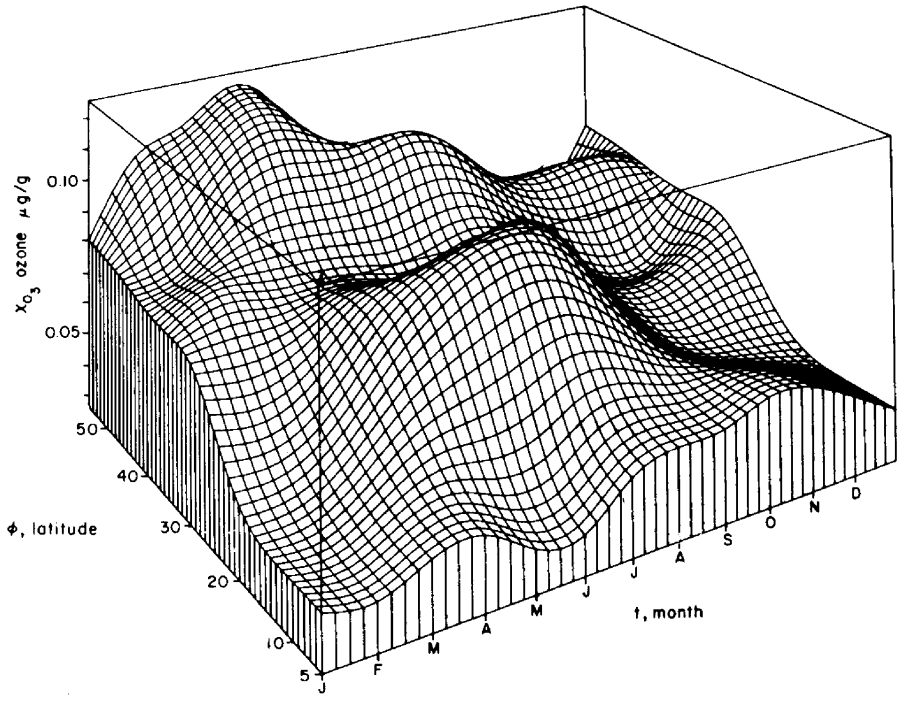

Fig. 3-7. Latitude-seasonal perspective for ozone mixing fractions at 7 km above six stations at 75°W longitude. (Reproduced from Chatfield and Harrison, 1977).

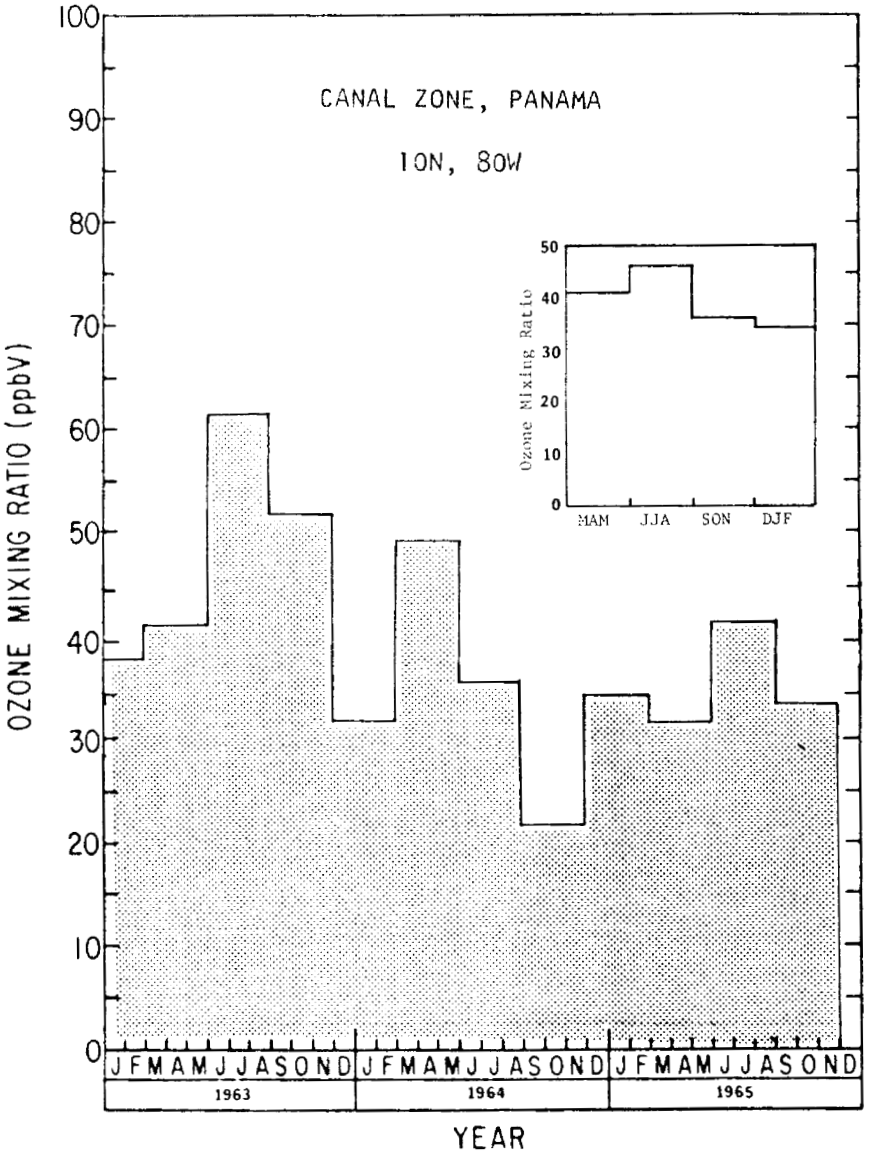

Fig. 3-8. Time series of ozone mixing ratios at the 200 hPa (also mb) level over the Canal Zone from the AFCRL Ozonesonde network. The insert shows the seasonal average ozone levels derived from the 1963-65 ozonesonde records.

December 1973 (the same 5 seasons used by Tiefenau, et al.), a semi-annual ozone wave, with equinoctal maxima, is evident.

Using the GASP aircraft data, seasonal (three month) ozone mixing ratios from three tropical zones, as described Section 3.1, were calculated for the latitude intervals 0-20°S, 0-20°N, and 20°S-20°N. These data are presented in Figures 3-9 to 3-11. The three year, hemispheric average ozone concentrations shown in Table 3-1 reveal a striking contrast between the western and eastern hemispheres, but little difference north and south of the equator. The absence of any significant meridional ozone gradient within the Pacific Island, Australasian or South American

	Pacific Islands	Australasia	South America
Equator to 20°S	28.6ppbv	28.4	49.6
Equator to 20°N	30.5	30.9	47.8

Table 3-1. Average tropical ozone mixing ratios from GASP commerical airliners in the years 1976-1979

flight files is interpreted as likely evidence for persistent north-south mixing of a quasi-conservative tracer gas, such as ozone, across the equatorial zone. Indeed, we have already indicated that the lack of long term, upper tropospheric ozone gradients along a meridional plane is a feature observed in repetitive aircraft flights (Tiefenau et al., 1973; Pruchniewicz, 1973) and from ozonesoundings over (approximately) 75°W at Canal Zone (9°N) and LaPaz, Bolivia (16°S).

The obvious east-to-west difference in the mean abundance of ozone aloft surely stands in support of favored zones of interhemispheric transport. For instance Wu (1978) shows that of the three geographic regions which we have selected for our analysis, the time averaged, vertically-integrated, meridional water vapor transport is 5 to 10 times stronger over the South American continent than over the Australasian-Pacific Islands sectors. This is clearly consistent with our higher ozone registrations in the western hemisphere. It might be noted, in conclusion, that the year-to-year differences in the annual ozone cycle recorded from GASP airliners precludes any simple interpretation of the behavior of the tropical ozone reservoir. On the whole, we are inclined to think that the tropics behave with unexpected complexity.

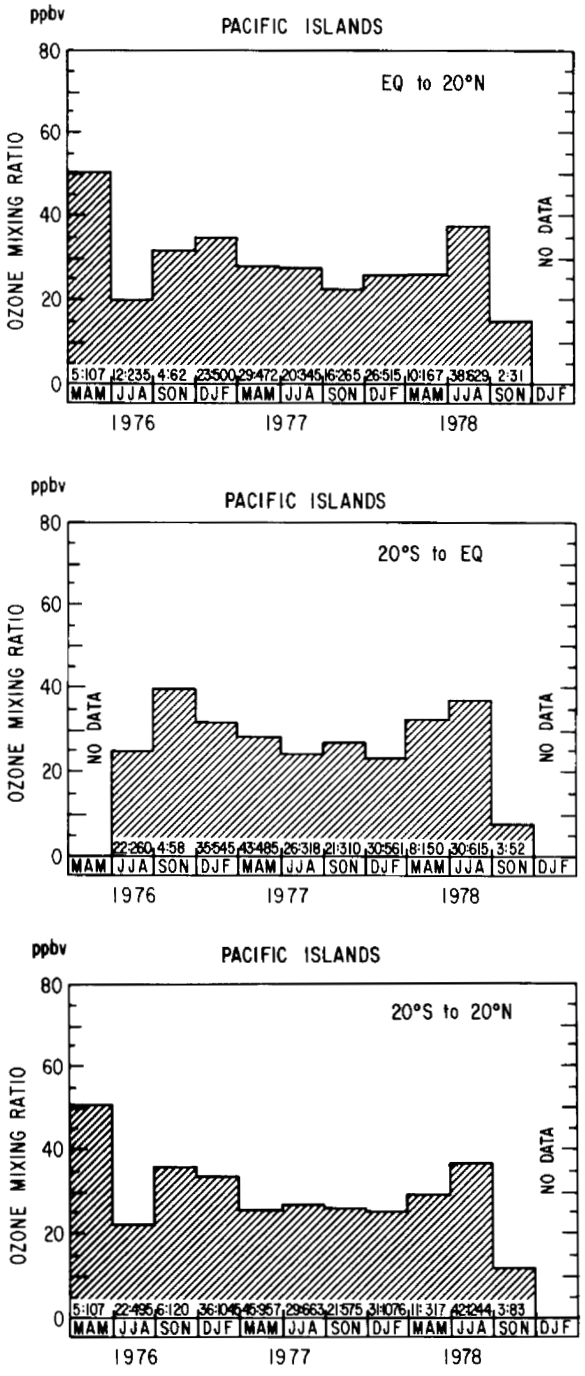

Fig. 3-9. Ozone variations in the upper tropical troposphere over Pacific Islands for the years 1976-79. Total number of GASP flights and of ozone observations are listed over each season.

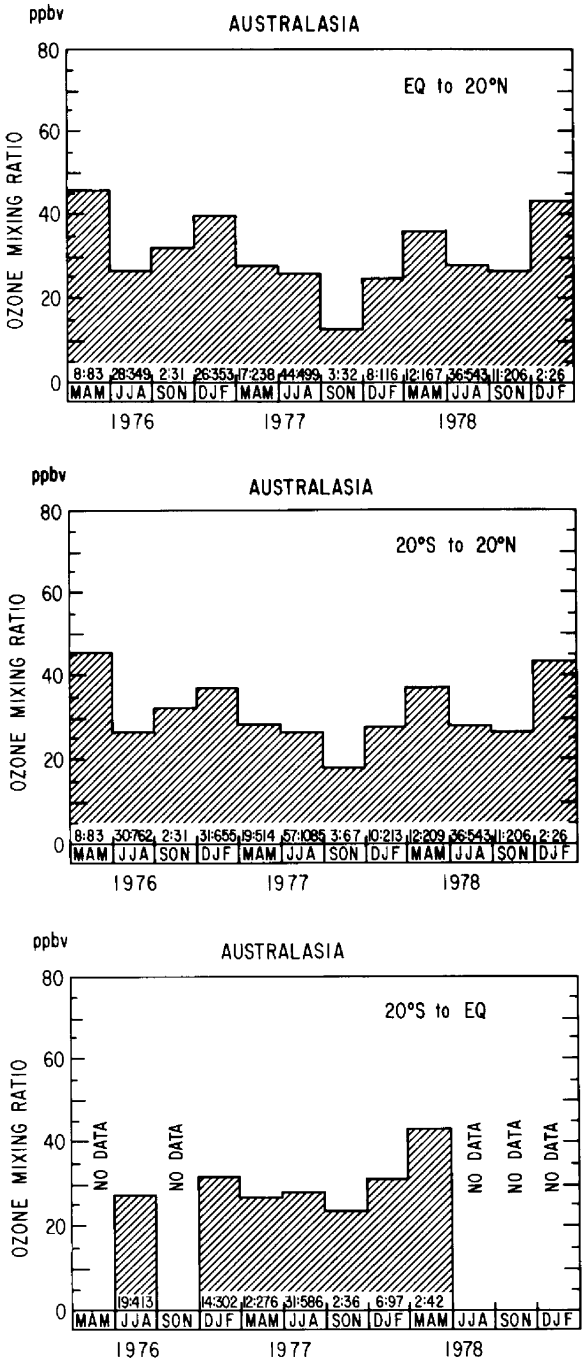

Fig. 3-10. Ozone variations in the upper tropical troposphere over the Australia-Asia region for the years 1976-79. Total number of GASP flights and of ozone observations are listed over each season.

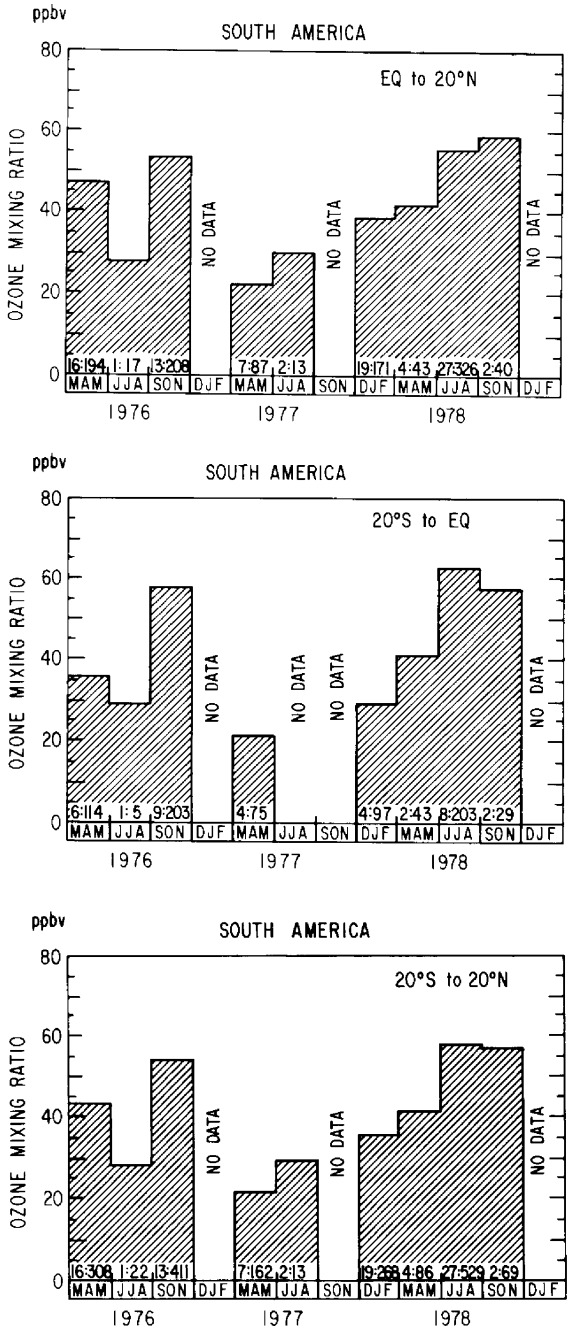

Fig. 3-11. Ozone variations in the upper tropical troposphere over South America for the years 1976-79. Total number of GASP flights and of ozone observations are listed over each season.

3.6 CONCLUSIONS

Frequent and widespread measurements of atmospheric ozone in the tropics 20°N to 20°S) indicate a more complex time and space behavior than has been presumed. Regions of ozone concentration in excess of 50 ppbV appear from time to time in both the northern and southern tropics, but with greatest frequency over the flight routes between the United States and South America. The origin of these regions of relatively high ozone could not be identified. However, case studies suggested the involvement of penetrations of middle latitude air masses, accompanied by distinct temperature gradients ($\geq 2^{o}C$ per 100 km) and, occasionally, abrupt wind direction changes.

By implication, these characteristics of ozone distribution in the tropics suggest a considerable role for the transport of ozone into and within the tropics by large scale air motions. This conclusion is consistent with the type of inter-annual and inter-regional variation of mean ozone concentrations shown in Figures 3-9 to 3-11, which is also an expected characteristic of large scale air patterns in both low and middle latitudes. It is also consistent with our observation that the frequency of ozone encounters was roughly proportional to the seasonal average ozone levels, which would be the case if the encounters represented intrusions of ozone rich air from higher latitudes.

The GASP data available for this study were sufficient to indicate such complexity in the tropical ozone distribution, which has generally remained unrecognized. Yet it was not sufficient to prove the role of long range transport, or of other possible factors such as local photochemistry, or lightning production of ozone in the intense convective storms common in the tropics. Examination of the later and more complete GASP data may shed more light on these mechanisms, but it appears that well-designed, dedicated observation programs are necessary to understand the apparently complex behavior of trace constituents in the tropics.

CHAPTER 3

Danielsen, E. F.: Notes on the meteorology of the Intertropical Convergence Zone during the July 1977 experiment. In: 1977 Intertropical Convergence Zone Experiment, NASA Tech. Memo. 78577, 1979.

Danielsen, E. F. : Stratospheric sources for unexpectedly large values of ozone measured over the Pacific During GAMETAG, August 1977. J. Geophys. Res., 85, 1980. pp. 401-412.

Fabian, P. and P. G. Pruchniewicz: Meridional distribution of ozone in the troposphere and its seasonal variations. J. Geophys. Res., 82, 1977. pp. 2063-2073.

Hering, W.S. and Borden, T. R., Jr.: Ozonesonde Observations Over North America. Volume 4, AFCRL-64-30 (IV), U.S. Air Force, Dec. 1967. (Available from DDC as AD666 436).

Komhyr, W. D. and P. R. Sticksel: Ozonesonde Observations 1962-1966. Volume 1. ESSA Tech. Rep., IER-IAS 1, U.S. Dept. of Commerce, 1967.

Nastrom, G. D.: Ozone in the upper troposphere from GASP measurements. J. Geophys. Res., 84, 1979. pp. 3683-3688.

Palmen, E. and E. Newton: Atmospheric Circulation Systems: Their Structure and Physical Interpretation. Academic Press, New York, 1969. 603 pp.

Perkins, P. J.: Global measurements of gaseous and aerosol trace species in the upper troposphere and lower stratosphere from daily flights of 747 airliners. NASA TM X-73544, Lewis REsearch Center, Cleveland, OH, 1976. 12 pp..

Pratt, R. and P. Falconer: Circumpolar measurements of ozone, particles, and carbon monoxide from a commercial airliner, J. Geophys. Res., 84, 1979. pp. 7876-7882.

Pruchniewicz, P. G.: The average tropospheric ozone content and its variation with season and latitude as a result of the global ozone circulation. Pure and Appl. Geophys., 106-108, 1973. pp. 1058-1073.

Routhier, F., R. Dennett, D. D. Davis, A. Wartburg, P. Haagenson, and A. C. Delany: Free-tropospheric and boundary-layer airborne measurements of ozone over the latitude range of 58°S to 70°N, J. Geophys. Res., 85, 1980. pp. 7307-7321.

Tiefenau, H. K., P. G. Pruchniewicz and P. Fabian: Meridional distribution of tropospheric ozone from measurements aboard commercial airliners, PAGEOPH, 106-108, 1973. pp. 1036-1040.

Wu, M. F.: Interannual variations of water vapor content and its flux components over the northern hemisphere, J. Meteor. Soc. Japan, 56, 1978, pp. 584-594.

CHAPTER 4

COMPARISON OF AEROSOL STANDARDS AND THE CALIBRATION OF THE NASA-LEWIS RESEARCH CENTER POLLAK COUNTER *

by W. Winters, S. Bernard, and A. Hogen

4.1 INTRODUCTION

The Atmospheric Sciences Research Center has maintained a working reference photo electric nucleus counter (Metnieks and Pollak, 1959; Pollak and Metnieks, 1960) in its laboratory for several years. The particular instrument used as a working reference is the twelfth in a series of about 30 instruments constructed by R. Gussman in accordance with drawings and specifications supplied to him by Prof. L. W. Pollak. This instrument was selected from a production lot of three, all of which were mutually compared and found to be in agreement within ± 1 scale division, throughout the full range of calibration.

The linearity of the electrical components of this instrument is frequently verified with neutral density filters, and a reference microammeter. The reference Pollak counter is compared with newly manufactured counters as they are acquired by ASRC. No serious discrepancies exist in the performance history of the reference (PG 12) nucleus counter.

4.2 CALIBRATION HISTORY OF THE WORKING STANDARD

The reference Pollak counter (Gussman-Pollak #12 or PG 12) was selected by convenience from the series PG 12, 13, 14 after intercomparison of the instruments. PG 13 was installed at the Mauna Loa Observatory in 1977 and is still in service there, serving as both a working reference standard, and as a climatological instrument. It has been thoroughly re-evaluated several times (B. Bodhaine, personal communication) and was recently compared with a photographic Aitken counter (Winters, Barnard, and Hogan, 1977).

---

* Research Associates, A.S.R.C.

Instrument PG 14 was simultaneously installed at the Woodcock-Blanchard tower on the northeast shore of Oahu. It was returned to ASRC after five years service and re-compared with instrument PG 12. There was no systematic difference in results between the initial and post experiment comparison.

Reference instrument PG 12 was taken to the Particle Technology Laboratory, University of Minnesota in 1973, for comparison with an electrostatic aerosol detection technique. The two techniques showed agreement to 20% throughout the range of calibration (Liu, Pui, Hogan, and Rich, 1974). Later that year, a calibration workshop was hosted by R. Cadle at the National Center for Atmospheric Research. This Pollack counter was compared with several instruments including the Stratospheric Aitken Nuclei Detection System (SANDS) and the balloon-borne system of J. Rosen. Again good agreement and comparable results were found among the several techniques (Cadle, et al., 1975).

The ASRC reference counter has been compared in the laboratory, with reference (or laboratory) Pollak counters, or Pollak replicas, including those built by: General Electric Co.; USAEC Health and Safety Lab; BGI, Inc.; Environment/One Corp.; Research Insitute of Atmospherics, Nagoya; Tokyo Institute of Science; Gardner Associates; and observatory instruments of NOAA-Geophysical monitoring for Climatic Change. In most cases, close agreement was found. In two cases the cause of disagreement was quickly located in two electrical components, and agreement achieved after replacing the components.

Comparison of other photoelectric nuleus counters with the ASRC reference counter appears to be a reliable technique for verifying the performance of such counters and detecting degraded counter performance.

4.3. CALIBRATION OF THE NASA LEWIS POLLAK COUNTER

A Pollak photoelectric nucleus counter was acquired by NASA Lewis as a working reference for the several Environment/One automatic nucleus photometers used in the Global Atmospheric Sampling Program. This instrument is number 23 in the series produced by R. Gussman, and is a very similar replica of the several instruments cited in the previous section.

This instrument was transported to the ASRC Laboratory at Schenectady Airport on December 7, 1976, by Ted Nyland. It was re-assembled in the calibration room and allowed to equilibrate overnight. A comparison was completed during the afternoon of December 8, 1976, using a sodium chloride aerosol generated by a DeVilbiss nebulizer. The results of the calibration are tabulated below as Table 4-1.

	Time	Gussman-Pollak #12 (ASRC Standard)	Gussman-Pollak #23 (NASA Lewis 119418)
#1	1415	Zero Check	99.9, 99.9
2	1550	51.9	51.7
3		52.2	52.8
4	1610	62.9	63.4
5		63.0	63.2
6	1625	72.8	73.1
7		73.1	72.0
8		74.0	73.7
9	1650	79.0*	81.0*
10		81.9	81.7
11	1715	91.0	93.4
12		90.2	90.2
13		90.9	90.2
14	1750	96.0	95.4
15		96.0	96.2

---

* Starred observation was attempted during line voltage transient which resulted in post-observation zero shifts.

Table 4-1 Comparison of photoelectric nucleus counters at ASRC Schenectady Laboratory on December 8, 1976. Sodium Chloride aerosol was produced from a DeVilbiss nebulizer.

Examination of the tabulated data shows that, in nearly every case, the agreement between the two instruments is within one scale division at the observed value. This is the criterion for agreement established by Pollack and Metnieks (1960) in deriving the "intrinsic calibration" of such photoelectirc nucleus counters. Two comparison points (#8 and #10) in the table are not within this criterion. The disagreement in point #8 appears to be due to a voltage transient in the laboratory at that time resulting in a subsequent zero shift. Repetition of the experiment (point #9) resulted in good correspondence. Point #10 was the first measurement after dilution of the aerosol supply in the test chamber. The disparity here may be due to incomplete mixing in the test chamber, as repetitive points #11 and #12 again show good agreement. This comparison sequence, showing 12 of 14 comparison points (86%) to be within $\pm$ 1 scale division when simultaneously observed with two Pollak counters, is typical of the performance of such instruments. The remaining 14% of points falling outside this band are usually attributable to random unknown error as in this case. The NASA Lewis instrument is shown to be a reliable replica of the Dublin nucleus counter, and to duplicate the intrinsic calibration of such counters established by Pollak and Metnieks (1960).

4.4 CONCLUSIONS

The NASA Lewis reference aerosol detector was compared to the reference aerosol detector of the Atmospheric Sciences Research Center in a test fixture (Hogan, 1980) shown to be capable of detecting degraded instrument performance. The NASA Lewis photoelectric nucleus counter met Pollak's accuracy criterion, reproducing the "intrinsic calibration" of such instruments, as established by the reference counter, to within 1 scale division in 86% of the trials.

The reference counter of the ASRC has been used to calibrate portable counters used on shipboard over the seas, on aircraft of NCAR and the U.S. Antarctic Research Program, on the Arctic and Antarctic ice, and at several island and mountain stations. This same reference instrument has been compared with the working standards of the major manufacturers of aerosol counters and several major laboratories. Data obtained by these several programs are directly comparable.

CHAPTER 4

References

Cadle, R. D., G. Langer, J. B. Haberl, A. Hogan, J. M. Rosen, W. A. Sedlacek, and J. Wegrzyn, 1975: A comparison of the Langer, Rosen, Nolan-Pollack and SANDS condensation nucleus counters. J. Appl. Meteor., 14, pp. 1566-1571.

Hogan, A. W., 1980: Recalibration of condensation nucleus counters. Atmos. Envir., 14, pp. 1335-36.

Liu, B. Y. H., D. H. Pui, A. W. Hogan, and T. A. Rich, 1974: Calibration of the Pollak counter with monodisperse aerosols. J. Appl. Meteor., 13, p. 46-51.

Metnieks, A. L. and L. W. Pollak, 1959: Instruction for use of photoelectric condensation nucleus counters. Geophys. Bull., No. 16, School of Cosmic Physics, Dublin Institute for Advanced Studies.

Pollak, L. W. and A. L. Metnieks, 1960: Intrinsic calibration of the photoelectric nucleus counter (Model 1957) with convergent light beam. Tech (Sci.) Note, No. 9, School of Cosmic Physics, Dublin Institute for Advanced Studies.

Winters, W., S. Barnard, and A. W. Hogan, 1977: A portable, photo-recording, Aitken counter. J. Appl. Meteor., 16, pp. 992-996.

CHAPTER 5

Aerosol Concentrations Over the Pacific

A. W. Hogan, S. Barnard, K. Krebschull

5.1 INTRODUCTION

The Atmospheric Sciences Research Center began a survey of aerosol concentrations over the surface of the seas, in cooperation with the State University Maritime College, in 1966. Initial observations were confined to the North Atlantic area and observations over the Pacific were made from 1969 to 1976. The Pacific observations are mainly confined to the great circle routes between the Panama Canal and Australia - New Zealand; California to Hawaii; California to Japan; and Hawaii to Japan. Additional north-south transects across the tropics, and east-west transects near the Antarctic convergence are available from single cruises of survey ships. The author made observations from 40° to 78°S, along the international date line from U.S.C.G.C. Northwind in 1979-80. The surface observations through 1976 were compiled and plotted on a mercator projection (Hogan, 1976); longer "climatologies" of surface aerosol observations have recently become available from island stations. The author has made aerial aerosol observations along the West Coast US - Hawaii - Samoa - New Zealand - McMurdo Sound - South Pole corridor at altitudes between 16000-26000 ft msl. These surface and mid tropospheric aerosol observations are examined, along with similar recordings obtained between 30,000-43,000 ft msl by the Global Atmospheric Sampling Program aircraft, in an attempt to determine the background of particles in the atmosphere, and their dispersion by the general circulation.

5.2 INSTRUMENTATION AND CALIBRATION

The initial aerosol observations from shipboard over the Pacific were made with the portable small particle detector of Rich (1955), as manufactured by Gardner Associates of Schenectady, NY. Observations from oceanographic ships were made with a similar photoelectric nucleus counter, modified to produce greater sensitivity to small changes in aerosol concentrations (Hogan, Winters and Gardner, 1975). Surface observations at Vito Levu, Fiji and Pitcairn island (Hogan and Christian, 1979) were made with these instruments. Measurements from 11,000 ft msl at Mauna Loa, Hawaii and from the southern tradewind zone in Samoa were obtained by the NOAA-Geophysical Monitoring for Climatic Change Program

(B. Bodhaine, private communication), using a Pollak counter. Additional Pollak counter data are available from the northern tradewind zone at Bellows Beach, Oahu, Hawaii (Hogan, 1976).

The aircraft observations taken at altitudes from 16,000-26,000 ft were obtained while ferrying the instrumented LC-130R of the US Antarctic Research Program (Renard and Foster, 1978) from the US to Antarctica. The airborne aerosol detector was the same (Hogan, Winters, and Gardner, 1975) as that used at the surface, but connected to either a compressor tap or isokinetic probe (Hogan, 1979). The aerosol information from higher altitudes provided by the Global Atmospheric Sampling Program was obtained with a pressurized automatic nucleus counters (Nyland, 1979). All of these instruments derive their calibration from the 1960 Pollak and Metnieks calibrtion of photoelectric nucleus counters, and are specifically referenced to instrument #12 of the Gussman series of Pollak replicas.

The photoelectric nucleus counter detects the total number concentration of particles in the air. While this is a fundamental parameter, it is desirable to know some of the other physical properties of the aerosol, such as diffusion coefficient (which is size dependent), fraction charged (which influences conductivity), and light scattering area. The mean diffusion-coefficient and reaction of particles charged were measured in many cases using the diffuser denuder of Rich (1966). Some light scattering parameters were measured by a commercial instrument (Royco) at the surface. A Royco light scattering detector was also used as part of the GASP instrumentation package.

Vertical profiles near Hawaii (Hogan, 1976) indicate that, although the total number concentrations of aerosol particles measured at the surface, and above the trade wind inversion are quite similar, the size (as determined by light scatter, fraction charged and diffusion coefficient) of the aerosol at the two altitudes is very different. Experiences at South Pole showed that very dry subsiding air contained large numbers of particles of very small size (Hogan, 1975).

These experiences led to our suggestion to Lewis Research Center that the GASP program incorporate a simple sizing technique into the airborne observations, which would yield some information relative to particle sizes encountered. This technique is based on the intial calculations of Spurny (1969), who suggested that membrane filters could be used as size selective diffusion batteries. Twomey (1981) has recently described a more complete Nuclepore - based membrane filter size measurement technique.

A second automatic nucleus counter was aspirated through a Nuclepore filter, in parallel with the primary unaltered nucleus counter during the last year of the GASP program. The aerosol concentration measured by the primary, unaltered nucleus counter represents the total number concentration of all particles present greater than the minimum detectable size. The number of particles measured by the second counter represents those transmitted through the size-selective "window" of the nuclepore filter.

Two types of Nuclepore filters were used during this portion of the program, both of 47 mm diameter. The first, with a nominal pore size of 8.0 μm, will transmit nearly all particles greater than 10^{-6} cm radius, but will effectively remove all particles with radii less than 5×10^{-7} cm. The second, with a nominal pore size of 1.0 μm, removes most particles, but transmits more than half of the particles through its "window" region of $.05\mu m < r < \mu m.2$.

The total concentration of aerosol particles is compared to the transmitted through either filter. If, for example, the 8 μm pore size is used and the difference in concentration across the filter is great, then one must conclude that the majority of the number concentration consists of very small particles. If the 1.0 μm pore size is used and there is little difference across the filter, then the aerosol consists mostly of particles of small diffusion coefficient. If either filter transmits 25 to 75% of the total aerosol, the aerosol contains a mixture of many sizes.

This technique, in conjunction with meteorological analysis and ozone and water vapor mixing ratio data can be used to determine whether the aerosol material has recently formed via gas conversion (large loss of small particles, which would be short-lived in nature due to coagulation), or has been aged for a long period without the addition of new material (narrow size range with little loss of "small" particles through the filter), or has recently been brought up from the surface by convection (broad size range). These solutions are not unique, but do prove of some benefit in our understanding of aerosol sources and sinks.

5.3 METEOROLOGICAL ANALYSIS

The surface aerosol data collected during 1966-76 showed that the mean aerosol concentration varied with climatic region over the open seas. Our preliminary analysis of GASP and mid-tropospheric data indicates a relatively strong variation in mean aerosol concentration with latitude and altitude. Stratospheric air is generally lower in total particle concentration than tropospheric air. We have selected these meteorological parameters to categorize aerosol concentrations:

1. Temperature profiles during climb or descent are used to determine if lapse or inversion is present at, and enroute to, that altitude.
2. When two distant temperature profiles indicate the tropopause may have been interested in level flight, temperature gradient wind direction, and ozone data are used to estimate the location ($\pm 2^{o}$) whre the tropopause was crossed.
3. Wind, temperature, and ozon profiles are used to identify extrusions of stratopsheric air around jet streams and over troughs.

5.4 RESULTS OF EXPERIMENTS

5.4.1 Surface Aerosol Concentrations

The mean aerosol concentrations as measured over the Pacific Ocean surface from ships and island stations, during the period 1966-1974 is shown in Figure 5-1. More recent data, from the Mauna Loa Observatory (11,000 ft msl) and American Samoa (sea level) is enclosed in boxes. The most frequently followed great circle routes over the Pacific are shown by arrowed lines.

As a general characterization, the North and South temperate regions have mean values of aerosol concentration of 300-500 n/cm^3. The trade wind region, and the region of polar easterlies experience mean aerosol concentrations of less than 300 n/cm^3. No marked increase in aerosol concentrations is found near the ITCZ in the surface observations. This may, in part, be due to observer bias, resulting from delaying observations during showers or thunderstorms.

5.4.2 Observations Along the Great Circle Route from California to Hawaii

The rarity of severe storms in the eastern Pacific, and the absence of ice in these waters, allows both ships and aircraft to follow a direct great circle route from Los Angeles or San Francisco to Hawaii. The tropopause is normally quite high over the tropical Pacific, so that all of the data obtained

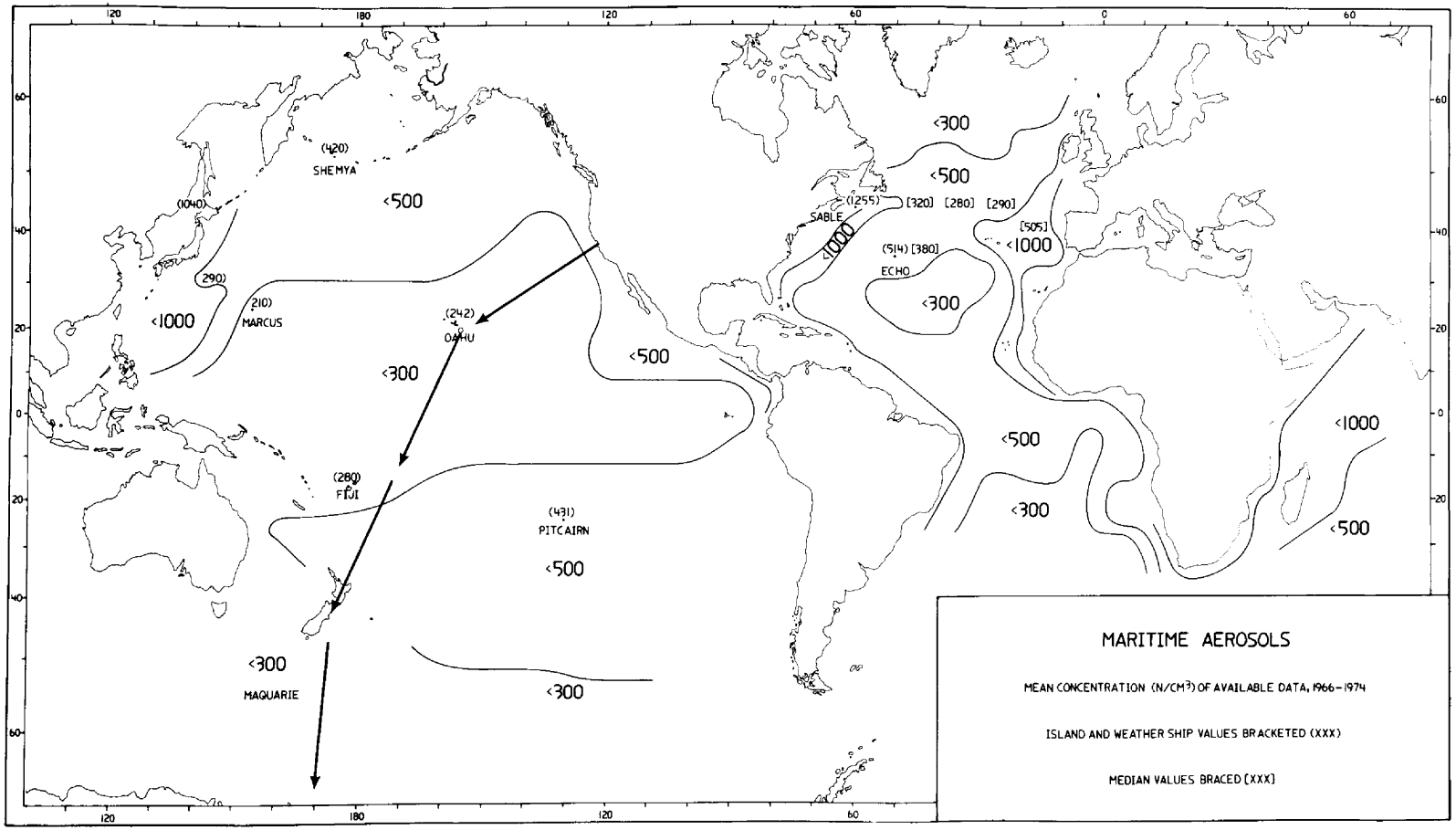

Fig. 5-1. Mean values of aerosol concentration over the seas, measured from shipboard during 1966-1974. The approximate great circle air routes covered by GASP and USARP aircraft are plotted.

along this route in the layers between 550-300 mb by the U.S.A.R.P. Hercules represent tropopsheric air. Most of the GASP data from the 300-200 mb layer is also from tropospheric air, except that stratospheric air may be encountered along the northern most portion of the route, near the North American coast, when returning from Hawaii. The clockwise circulation of air about the semi-permanent high pressure systems at 30°N latitude often results in easterly winds in the lower troposphere along the northern half of this route. Westerlies are frequently found above 500 mb over the trade wind zone. The air above 700 mb is usually quite dry, and cloudless except for cirrus, along this route.

The mean surface values of Aitken nucleus concentration measured along this route from 1966-1974 ranged from 220-360 n/cm^3 (Table 5-1). There was a slight latitudinal tendency, possibly reflecting influence of continental air from the west coast of North America.

A flight from Point Mugu, California, to Honolulu at altitudes below 700 mb (6,000-8,000 ft msl) aboard the Naval Research Lab Constellation in 1972 found concentrations of 150-300 n/cm^3 over this same route. Vertical profiles, from the surface to approximately 500 mb upwind of the island of Hawaii, showed that the total aerosol concentration above the trade inversion was numerically comparable to the concentration near the sea surface. The particles were, however, much smaller. Very low concentrations (30 n/cm^3) were found in air recently occupied by cumulus turrets.

Data from three transects from Point Mugu to Hawaii are available from the USARP-VX6 record. The most recent data obtained October 9, 1980, is illustrative of typical conditions, and plotted as Figure 5-2. The aircraft departed Point Mugu, climbed to 16,000 ft (530 mb) and proceeded westward in dry air with following winds. There was an air pollution alert in Los Angeles at this time, and the sea below was obscured by stratus with no clouds above. There was a following wind of 15 to 25 kt from ENE to SE at this altitude, an ozone mixing ratio of .040 ppm v/v (supplied by E. Robinson) and a total aerosol concentration of 500 n/cm^3.

The airplane climbed to approximately 470 mb at 128°W longitude, where it encountered more moist air with winds still from SE, at 20 to 35 kt. The sea surface was still covered by stratus; altostratus and cummulus cloud cover was present to just below the aircraft's altitude; and cirrostratus were presented above. The aerosol concentration decreased slightly to 280-430 n/cm^3, while ozone increased to .050 ppm v/v in this layer.

Table 5-1. Mean Surface Aerosol Concentrations Along the Los Angeles to Honolulu Great Circle Route from 1966-1974

Longitude Band	Mean Concentration
120-130W	360 n/cm^3
130-140W	260 n/cm^3
140-150W	220 n/cm^3
150-160W	280 n/cm^3

Table 5-2. Aerosol Concentrations Observed from Shipboard along a Track from Hawaii to Samoa

1966 - 1974

Latitude Band	Mean Concentration
20N-10N	250 n/cm^3
10N-0	180 n/cm^3
0-10S	150 n/cm^3
10S-20S	170 n/cm^3

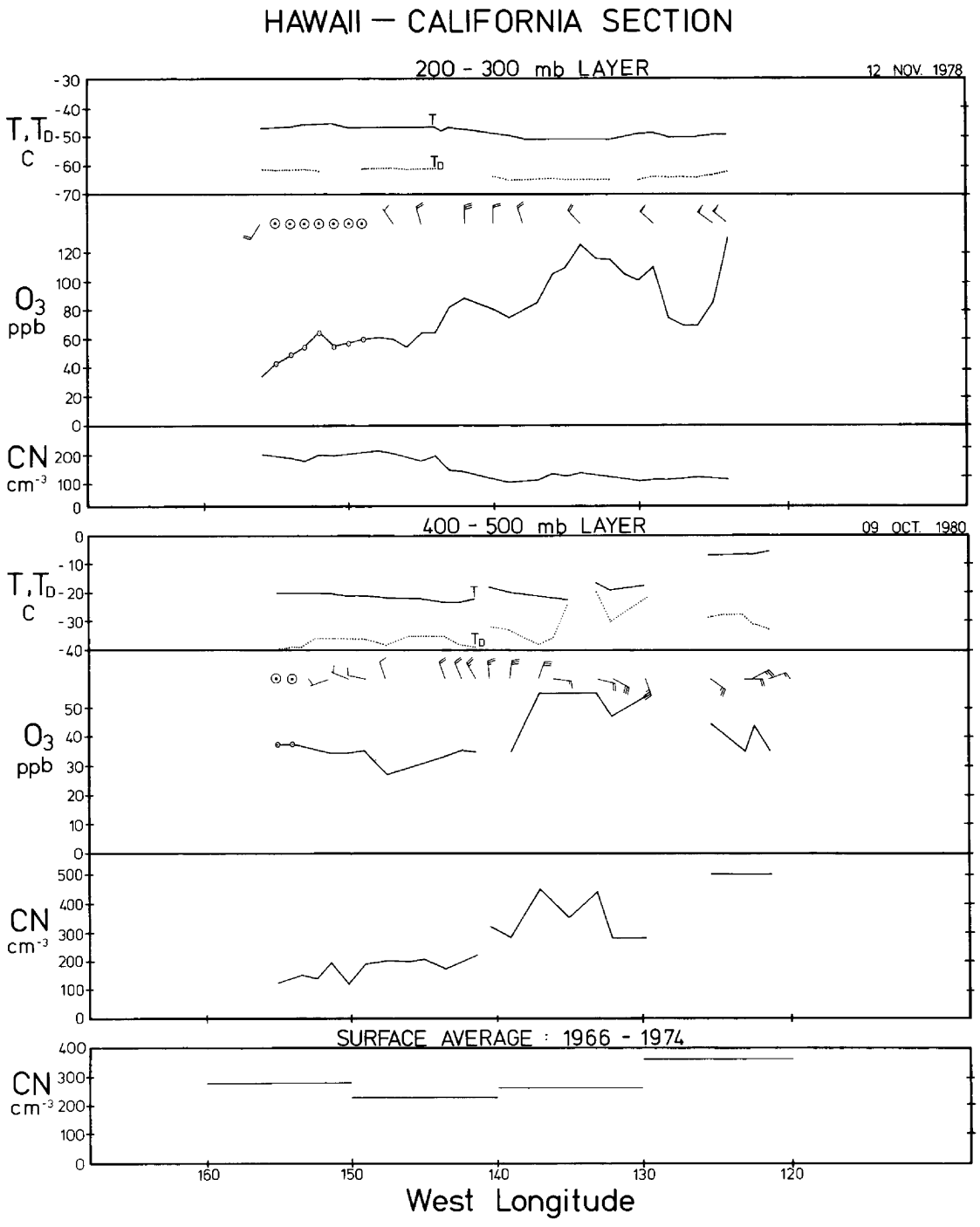

Fig. 5-2. Comparison of meteorological variables, ozone and aerosol concentration observed along a great circle from southern California to Hawaii at the surface, near 500 mb and near 250 mb standard pressure levels. The great circle route enters the Trade Wind Zone at about 140° west longitude.

Another climb to drier air at 420 mb was completed at 135°W longitude, over cumulus clouds. A light easterly was present, ozone was .055 ppm and total aerosol concentration 350-450 n/cm^3. At 137°W longitude the wind shifted to north at 30 kt, the air became slightly more humid, and both ozone and aerosol concentrations decreased, to 0.35 ppm and 300 n/cm^3 respectively. A final climb to 385 mb at 141°W found dry air, well above cumulus tops, and the winds light, but more westerly. The winds continued to become more westerly, and diminished in speed as the aircraft approached Hawaii. Ozone concentrations typical of the tropics (.025-.040 ppm v/v) persisted at this altitude. The aerosol concentrations were quite constant at 200 n/cm^3 in the weak northwesterlies, and decreased to 150 n/cm^3 in calm air near the Hawaiian Islands.

The data from flight record indicate that:

1) There was a weak flow of air slghtly contaminated with continental aerosol, above the stratus just west of the North American Coast.

2) A weak front in the vicinity of 130° - 135°W promoted mixing of sea level aerosol up to, and higher altitude ozone down to, the 500 mb level.

3) The troposphere between 700-400 mb over the trade wind zone is rather homogeneous with respect to ozone and aerosols, as the values found by the aircraft are quite comparable to those reported by the Mauna Loa Observatory at 680 mb (3.4 km, 11,000 ft.).

A transect along the same great circle was obtained on November 12, 1978 by GASP aircraft at 220 mb. The air was quite dry all along the route. Relatively strong northwest winds were encountered just west of the North American coast. The winds became weaker, and more northerly west of 130°W longitude, and gently diminished, to light and variable west of 145°W longitude.

The accelerating winds east of 130-135°W indicate that a jet stream was probably over the continent, with corresponding subsidence bringing ozone laden air down to the 220 mb level. The calm tropical troposphere, above the trades, west of 145°W is again relatively low in ozone. There is a noticeable out-of-phase relationship between ozone and total particle concentration. The concentration of 200 n/cm^3 measured over the tradewind zone indicates that particle concentrations are rather uniform throughout the tropical troposphere, above the trade inversion. The Nuclepore sizing device quite constantly transmits 50 to 60 percent of the total

aerosol concentration, indicating that the aerosol is a mix of many sizes, probably in coagulation equilibrium. Were this aerosol of smaller size, indicative of recent transport from its source, very little would be transmitted; were it depleted of small particles (i.e. similar to stratospheric aerosol) almost all particles would be transmitted.

The greatest variability in size and concentration of aerosol particles over this section of the Pacific occurs beneath the trade inversion, where clouds rapidly modify the characteristics of the aerosol (Hogan, 1976). Aerosol concentrations show a slight out-of-phase relationship with ozone concentration and diminish slowly with altitude. Some continental influence may be present in easterly flow along the coast of North America, to as far offshore as 130^{o}W longitude.

Although aerosol concentrations observed were markedly uniform from 700 - 200 mb and from 130^{o}W to 155^{o}W longitude along cloudless tracks, very different aerosol characteristics may accompany storms and cloudiness in this region.

5.4.3 Transects of the Troposphere Over the Tropical Pacific From Hawaii to Samoa

Surface observations of aerosol concentration in this zone are available from shipboard surveys of 1966-1974, island observations from Vitu Levu, Fiji during the early 1970's, the north shore of Oahu at the same time, and continuous records from the NOAA-GMCC observatories at American Samoa and Mauna Loa, Hawaii (700 mb level). The mean values obtained at these observatories are remarkaly consistent, approximately 250 n/cm^{3} at all locations.

Mean values obtained from ships along this great circle route are the result of far fewer observations, and are somewhat less than the long term concentration. Table 5-2 indicates that surface aerosol concentrations in the tropics are slightly lower south of the ITCZ, which usually lie in the vicinity of 10^{o}N.

Airborne observations along the Hawaii-Samoa Great Circle Route are interesting because they present both a transect of the inter-tropical front and also allow comparison of aerosol concentrations in the northern and southern hemispheres in close time proximity.

Two transects obtained in October 1977 by the USARP aircraft and the GASP Pan Am 747 SP (Flight 50) are shown in Figure 5-3. The USARP C130 was proceeding south at 18,000 ft in very dry air above the trade inversion. At 13^{o}N, the air became

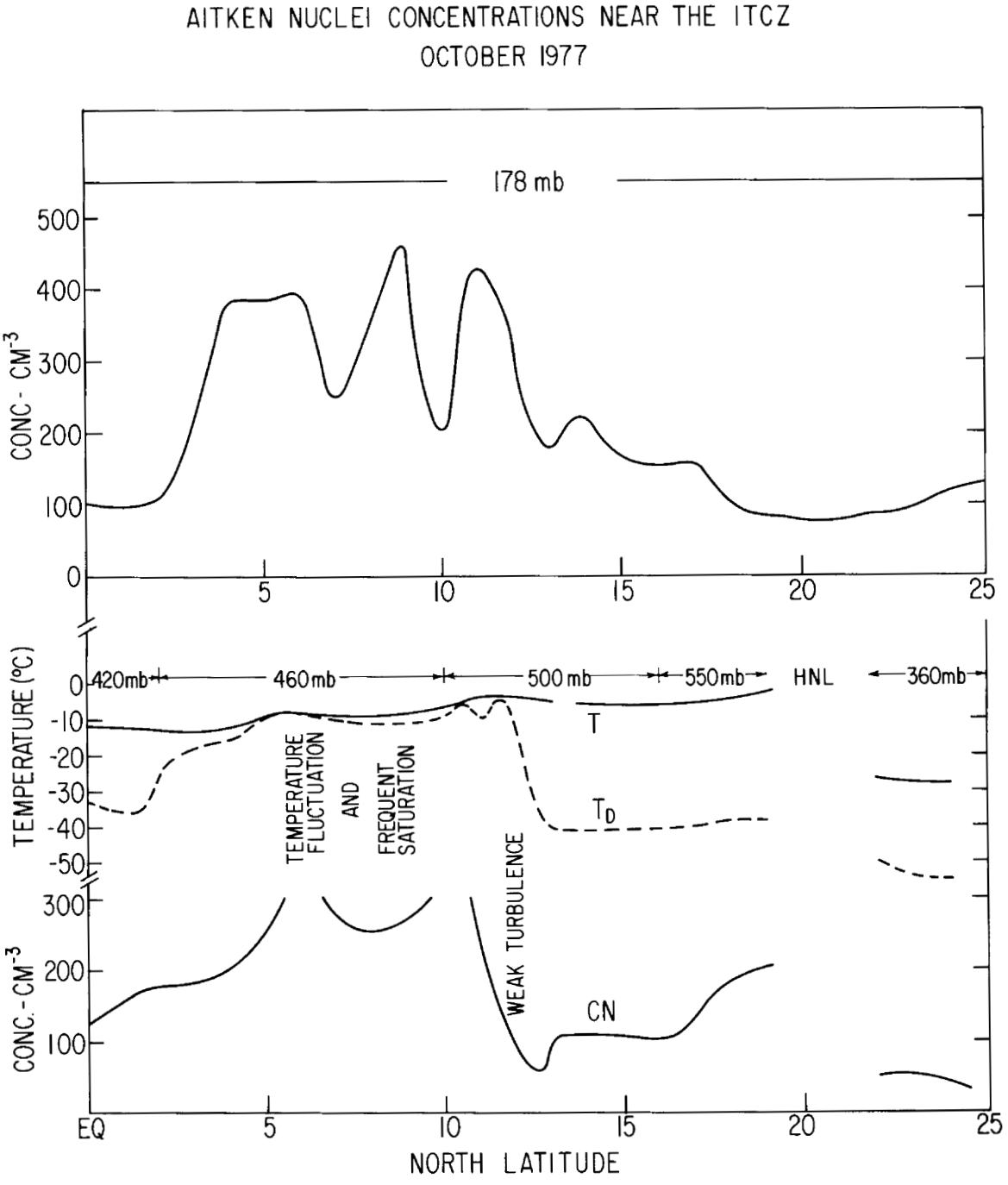

Fig. 5-3. Cross sections through the intertropical convergence zone, over the Pacific Ocean, obtained near 500 mb by the USARP aircraft, and above 200 mb by the GASP-Pan Am Flight 50. Enhanced particle concentrations are found in the ITCZ at both altitudes.

slightly turbulent, more humid and occasionally saturated in the vicinity of cummulus turrets. The aerosol concentration increased from 120 n/cm^3 to several hundred per cm^3, with wide fluctuations in the moist air. Concentrations then diminished to about 180 n/cm^3 coincident with departure from the moist air at 4^o - 5^{o}N latitude.

A few days later, Flight 50 transected the same region, at 178 mb and encountered a similar rise in aerosol concentration, with similar fluctuations between 5^o and 12^{o}N latitude.

A similar transect between approximately 18,000 and 20,000 ft made by the C130 aircraft in October 1980 shows a similar pattern (Figure 5-4). The ozone record from this flight, supplied by E. Robinson, varies inversely with aerosol concentration. This is indicative that moist, ozone-depleted surface air carries great quantities of aerosol material to the mid and upper troposphere when strong vertical motion in cumulus towers is present along the ITCZ. An interesting question arises, however, as concentrations measured aloft are greater than surface concentrations. This same phenomenon is also found near, and over, Antarctica and will be discussed in subsequent sections.

The particulate material transported upward by cumulus turrets near the ITCZ seems to spread out more uniformly over a latitude band of at least 10^o at higher altitudes. A GASP aircraft traversed this same flight route, between Honolulu and Auckland on November 13, 1978, at flight levels between 290-230 mb pressure altitude. Humidity records indicate that the air may have been near ice saturation at the flight level between 5^o-6^{o}N latitude, and south of 9^{o}S latitude but that generally dry air was encountered in the vicinity of the equator. Winds were fairly strong and southwesterly near Hawaii, light and variable from 13^{o}N to 5^{o}N (a doldrum) and southwesterly at about 30 kt south of the equator. Ozone concentrations seem typical of the tropics through most of the flight, but show a minimum in still air at 10^{o}N altitude. Total aerosol concentrations were very low (less than 100 n/cm^3) in the calm air between 9^o and 14^{o}N latitude but rose to 300-500 n/cm^3 in a broad band of dry air surrounding the equator. The concentrations fell below 100 n/cm^3 upon entering moister air south of 8^{o}S latitude.

Preliminary analysis of the recorded data would seem to indicate that surface air had been transported to the flight level and above by cumulus turrets or cumulonimbus anvils prior to passage of the GASP aircraft. Upon cessation of convection, the air began to subside, reducing the relative humidity but not destroying the particles transported to this altitude along with the water. This analysis may not be precise, but this

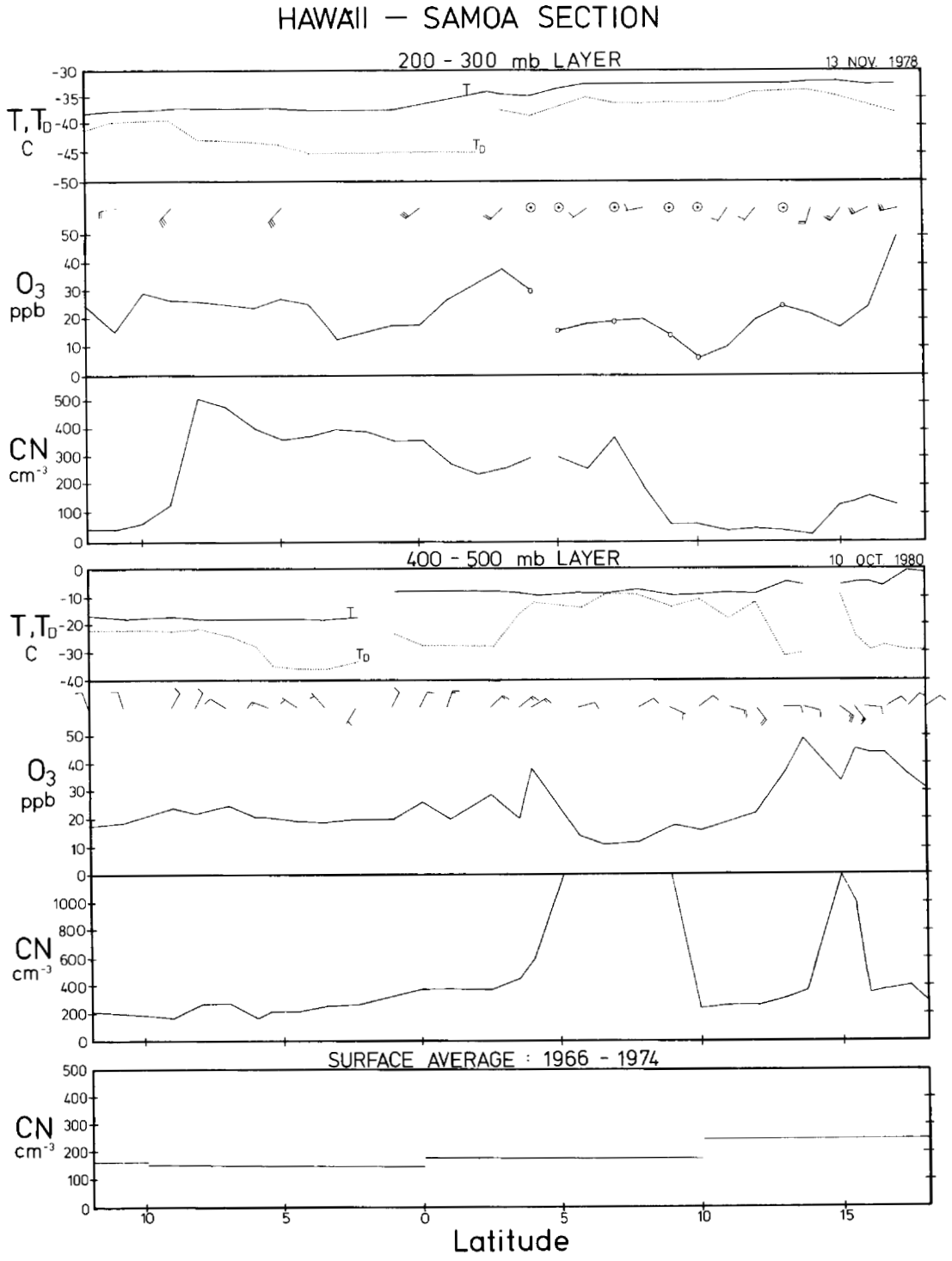

Fig. 5-4. Measurements from Hawaii to Samoa near 500 mb and 250 mb. Ozone is out of phase with aerosol in the 500 mb layer. At both altitudes the rising air of the ITCZ is characterized by 1) less dewpoint depression, 2) reduced ozone, 3) increased particle concentration.

"dry air" flight data does indicate that enriched aerosol layers exist over the equatorial zone in the absence of clouds. The presence of such high concentrations in the upper tropical troposphere near the ITCZ may very well account for the uniform aerosol concentrations in the troposphere between 20° and 35°N, where this air is strongly subsiding.

5.4.4 Transects of the Sub Tropical Front Along a Route from Samoa to New Zealand

A similar number of transects at flight levels between 550 mb and 360 mb have been made by the USARP aircraft between American Samoa and Christchurch, New Zealand. A frequent meteorological feature along this flight route is a subtropical jet stream at 25°-30°S latitude.

The aircraft departed Samoa and climbed to 550 mb in relatively moist air. The air began drying as the flight proceeded south at this pressure altitude. Very light westerly winds were encountered; ozone concentrations were again typical of the tropics; and aerosol concentrations diminished in concert with diminishing dewpoint.

A climb to 470 mb was completed at 20°S latitude, stronger west northwesterly winds were encountered at this level as were higher ozone concentrations. At 24°S latitude, ozone concentrations increased sharply to .080 - .1 ppm and westerly winds strengthened just before initiating another climb to 425 mb. A westerly jet was encountered between 25° and 30°S with a 100 kt core at 28°S. Ozone concentrations oscillated from .040 to .080 ppm in the high winds, and diminished rapidly with decreasing wind speed at 30°S.

A final climb to 400 mb was completed at 30°S latitude. winds were westerly at 30-40 kt at this altitude, and the air relatively dry, although an undercast was present. Cirro-stratus thickened and was present just below the aircraft at 38°S, where the air rapidly became moister. Ozone concentrations varied from .040 - .070 ppm in this region, diminishing as the air became moister. Aerosol concentrations remained quite constant at about 200 n/cm^3, all along the route south of 20°S, which seems to be a characteristic of the cloudless southern hemisphere temperate troposphere.

The continuation of the HNL-AKL GASP flight described in the last section shows somewhat similar features in Figure 5-5. "Spring comes" as a layer of fairly dry, calm, ozone rich air subsides between strong northwesterly winds at 22°-25°S. The subtropical jet at 22°S was not well developed at this altitude (230 mb) on the day of this flight, and the airplane

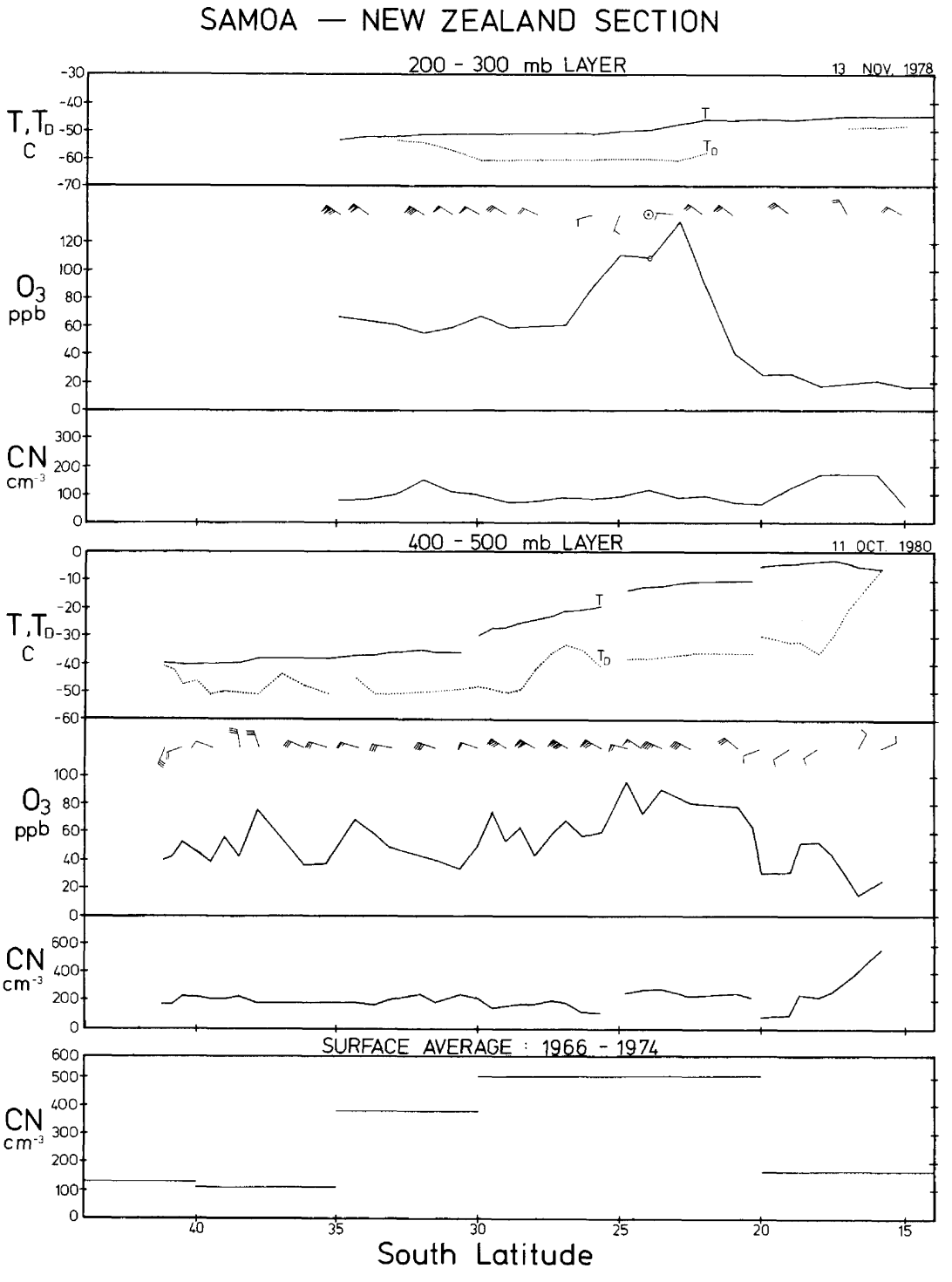

Fig. 5-5. Measurements along a great circle from Samoa to New Zealand. The maximum ozone concentration at both altitudes correlates well with minimum wind speed. Aerosol concentrations have rather steady values at both altitudes in Southern Hemisphere air south of 20°S.

was just beginning to enter the core of the circumpolar jet as descent began to Auckland. Aerosol concentrations were 200 n/cm^3 in moist tropical air north of 20^oS, and very consistent, near $100/cm^3$ in the dry air south of 20^oS latitude.

5.4.5. Aerosol Observations South of 45^oS Latitude

Very few aerosol observations have been made south of 45^oS latitude. A continuous series of surface observations began at South Pole in 1975, which had been preceded by a year long series of such observations at Mirnii (Voskresenskii 1968). The first upper tropospheric and lower stratospheric aerosol measurements were made by the USARP VX6 aircraft in late October of 1977, and a transect of the polar stratosphere, near the 200 mb level was accomplished by a Pan American World Airways B747 aircraft in late October of 1977 (Hogan and Mohnen, 1979; Pratt and Falconer, 1979). Consistently low aerosol concentrations, on the order of tens per cubic centimeter, were found above 200 mb poleward of 45^oS latitude by GASP instruments aboard Pan Am's Flight 50. The measurements are quite consistent with those from the surface to 270 mb over Antarctica by USARP VX6 aircraft.

A strong circumpolar vortex is present near 60^oS during the southern hemisphere winter and early spring. This vortex usually breaks up in early to mid November, promoting mixing of upper air from Antarctica to the lower latitudes and vice versa. The extremely low concentrations of aerosol measured over Antarctica and south of 50S enroute to New Zealand during Flight 50 probably reflect typical aerosol levels poleward of the vortex. Aerosol concentrations of 60 n/cm^3 were found near the 400 mb level by the USARP VX6 aircraft in this region on November 1, 1977, when no jet was encountered. This transect showed strong downward mixing of ozone rich stratospheric air on the poleward side of the jet near 62^oS, but a continuum of aerosol concentration at about 100 n/cm^3 on both sides, and in, the jet at 400 mb on November 11, 1977. This may indicate that the polar vortex had collapsed during early November 1977, because it appeared as though ozone-rich low latitude statospheric air reached high southern latitudes, and upper level mixing generally increased the aerosol concentration in the layer above 400 mb.

A series of surface aerosol observations, made by the author, between Wellington, New Zealand and McMurdo, Antarctica, during December 1980 - January 1981 is shown as Figure 5-6. Seas were not stormy during this period, and general surface transport was from low to high altitude, as shown by the wind flags.

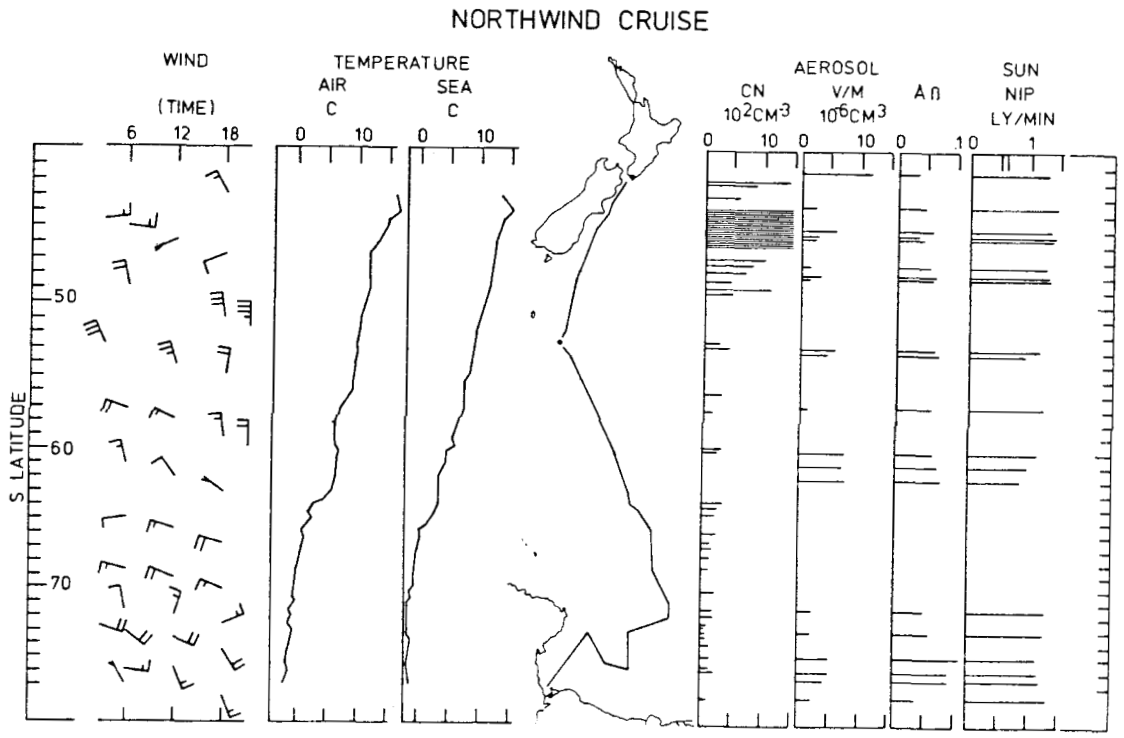

Fig. 5-6. Surface observations, from USCGC Northwind, along the date line from 40°S to 75°S latitude. The lowest concentrations of particles were measured at the surface in the easterlies south of the Antarctic Circle. Haze and relatively high aerosol concentration were found from 50-65°S.

Aerosol concentrations were generally from 300 - 500 n/cm^3 in westerly windflow and less than 200 n/cm^3 were found over pack and fast ice, where winds were from off the ice shelf.

The two transects of USARP VX6 instrumented aircraft from New Zealand to McMurdo as previously cited were in relatively dry air, although the prevailing weather conditions were much different. The transit of this aircraft form Christchurch to McMurdo on October 24, 1980 explored an entirely different regime, probably more representative of southern hemispheric stormy periods (Figure 5-7). No well defined jet was encountered at flight levels, but winds were steadily out of the west at speeds above 50 kt along the flight route. Cirrus were present at flight level over the southern coast of the South Island (48^{o}S) and were present at, and above, flight altitude (and the air at, or near, water saturation) until a descent was made for ice reconnaisance in the Polar easterlies at 67^{o}S. Ozone concentrations were uniformly low and aerosol concentrations exceeding 200 n/cm^3 were found in all observations with several measurements of 400-500 n/cm^3 or more in saturated air. These results may be interpreted as evidence that the stormy region of the Great Southern Ocean may not only be a strong source of aerosols near the surface, but that the strong mixing accompanying these storms may disperse this aerosol through the lower two-thirds of the atmosphere, in a 20^o wide belt, which may at times encircle the earth. There is no evidence of encountering air of recent stratospheric history at any point along this flight route.

5.5 SUMMARY AND CONCLUSIONS

This work is a preliminary analysis of aerosol concentrations obtained at three levels over the Pacific Ocean in an attempt to define the source and sink regions for aerosol material, and to discover some of the meteorological mechanisms which may result in the transport of this aerosol material away from its source region at several levels. Completion of a "climatology" of GASP aerosol data, similar to the climatology of surface aerosol data which served as a basis for this program will undoubtedly refine, or even contradict, some of these preliminary conclusions:

1. Circulation about the semi-permanent high pressure system located off the West Coast of the US at approximately 30^{o}N can often cause continental aerosol to be advected seaward to at least 130^{o}W longitude over the Pacific in clear air.

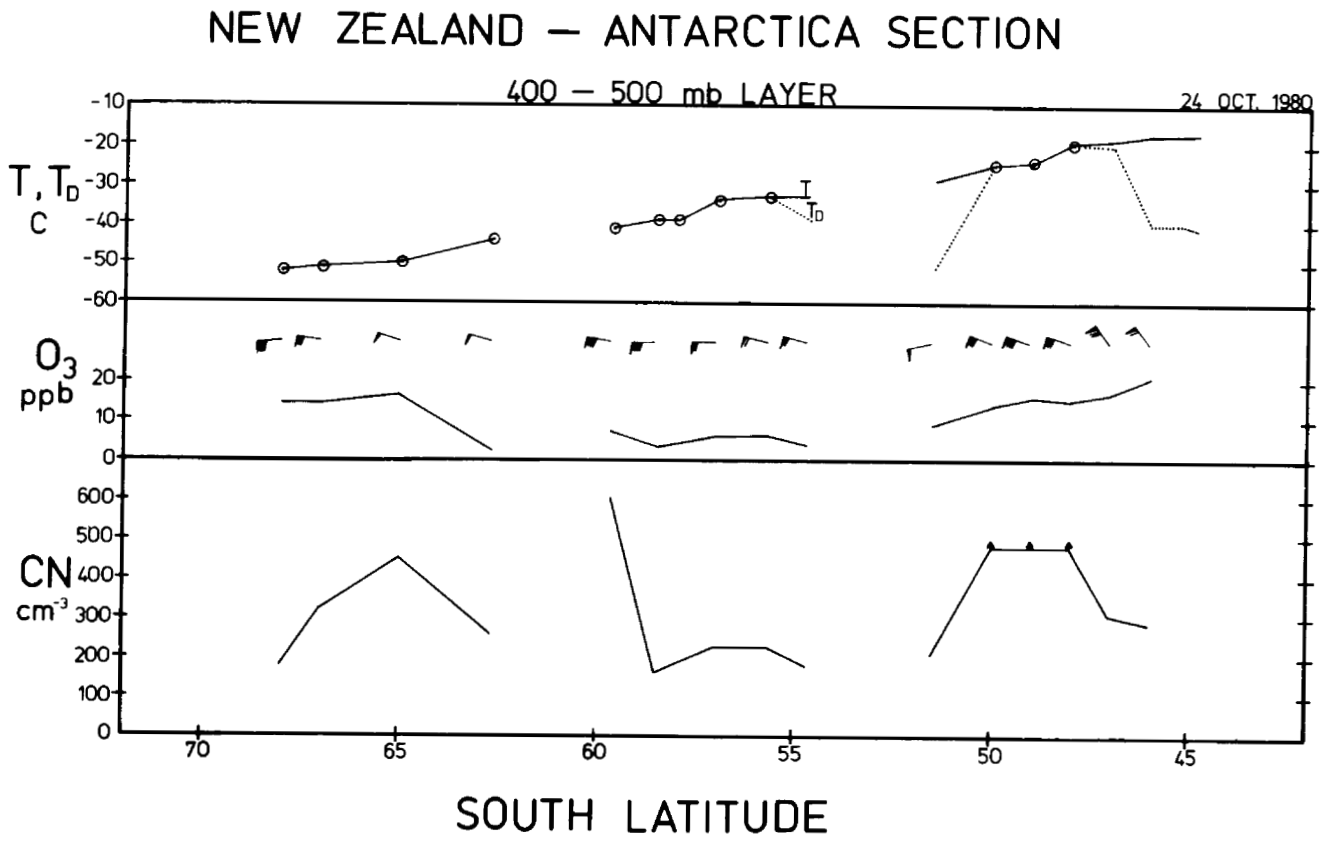

Fig. 5-7. Measurements along a great circle route approximately above the ship route of Fig. 5-6. The region was quite stormy on this date, with no real jet core at the flight level. Ozone concentrations were quite low and aerosol concentrations relatively high and variable in the moist air, which probably had been in recent contact with the sea surface.

2. Aerosol concentrations are rather uniform in clear air, over the Pacific Ocean in the latitude band between approximately 10^{o} and 30^{o}N from the top of the trade inversion to near the 200 mb level.

3. While some aerosol may enter the layers adjacent to the trade wind inversion when occasional cumulus turrets penetrate the inversion, it appears that the major source of clear air aerosol in the band 10^{o}-30^{o}N is located in the ITCZ. the aerosol spreads outward above the trade inversion.

4. Aerosol concentrations seem to change very little across fronts and jet streams in the dry air of the southern hemisphere. The seasonal changes in concentration, especially those accompanying the breakdown of the circumpolar vortex, seems to exceed air mass differences in aerosol concentration.

5. Aerosol concentrations south of 40^{o}S latitude are from 5-20 n/cm^3 in the lower stratosphere and about 60 n/cm^3 in the upper troposphere before breakdown of the polar vortex. After breakdown of the polar vortex, both layers have a concentration of about 100 n/cm^3.

6. The lower two-thirds of the atmosphere over the stormy band of the Pacific, from 47^{o}-67^{o}S, may contain total aerosol concentrations of 500 n/cm^3. The frequency with which the upper layers of high aerosol concentration mix into the lower stratosphere, is unknown.

7. The aerosol concentrations observed aloft, in clear weather by aircraft, during the GASP and associated programs, is comparable to, or less than, surface observations of aerosol which made up the initial data base. Aerosol observations at altitudes in moist and cloudy conditions often greatly exceed the values obtained at the surface beneath these points. Similar phenomena have been noted in Antarctica, when moist air arriving at South Pole contains more aerosol material than that measured over the Ross Sea by Hogan or over the Weddell Sea by Meszaros and Vissy (1974). This may be due to incomplete or inaccurate observations over the seas in stormy conditions where source strength is greatest, or to particle multiplication mechanisms in moist air. Aircraft profiles in Hawaii showed tropical cumulus to be sinks, or scavengers of aerosol, in line with theories of Junge, Mohnen and Vonnegut. This poses an important question relative to the aerosol balance of the troposphere.

CHAPTER 5

REFERENCES

Hogan, A. W.; 1975: Antarctic Aerosols. J. Appl. Meteor., 14, 550-559.

Hogan, A. W.; 1976: Aerosols of the trade wind region. J. Appl. Meteor., 15, 611-619.

Hogan, A. W; 1979: Meteorological transport of particulate material to the South Polar plateau. J. Appl. Meteor., 18, 741-749.

Hogan, A. W. and T. Christian, 1979: Aitken nuclei observations at Pitcairn Island. Presented at IUGG meeting, Canberra.

Hogan, A. W. and V. A. Mohnen, 1979: On the global distribution of aerosols. Science, 205, 1373-1375.

Hogan, A. W. W. Winter and G. Gardner, 1975: A portable aerosol detector of high sensitivity. J. Appl. Meteor., 14, 39-45.

Meszaros, A., and K. Vissy, 1974: Concentration, size distribution, and chemical nature of atmospheric particles in remote oceanic areas. Aerosol Science, 5, 101-109.

Nyland, T. W., 1979: Condensation Nuclei (Aitken Particle) Measurement System used on the NASA Global Atmospheric Sampling Program. NASA TP-1415, 25 pp.

Pratt, R., and P. Falconer, 1979: Circumpolar measurements of ozone, particles, and carbon monoxide from a commercial airliner. J. Geophys. Res., 84, 7876-7882.

Renard, R. J. and M. S. Foster, 1978: The Airborne Research Data System (ARDS). Description and an Evaluation of Meteorological Data Recorded During Selected 1977 Antarctic Flights. Naval Post-graduate School Technical Report 63-78-002, Dept. of Meteorology, Monterey, CA, 90 pp.

Rich, T. A., 1955: Photo electric nucleus counter with size discrimination. Geofis. Pura. Appl., 31, 60-65.

Rich, T. A., 1966: Apparatus and method for determining particle size. J. Recherche Atmos., Vol. III, 2nd Year, 65-69.

Spurney, K. R., J. Lodge, Jr., E. Frank, and D. Sheesly, 1969: Env. Science Tech., 3, 464-468.

Twomey, S., and R. Zalabasky, 1981: Multifilter technique for examination of the size distribution of the natural aerosol in the submicrometer size range. Env. Science and Tech., 15, 177-184.

Voskresenskii, A. I., 1968: Condensation nuclei in the Mirnii Region. Tr. Sov. Antarktcheskia Eksped, No. 38, 194-198.

1. Report No.	2. Government Accession No.	3. Recipient's Catalog No.
NASA CR-3691		

4. Title and Subtitle	5. Report Date
AIRCRAFT MEASUREMENTS OF TRACE GASES AND PARTICLES NEAR THE TROPOPAUSE	June 1983
	6. Performing Organization Code

7. Author(s)	8. Performing Organization Report No.
P. Falconer, R. Pratt, A. Detwiler, C-S. Chen, A. Hogan, S. Bernard, K. Krebschull, and W. Winters	None
	10. Work Unit No.

9. Performing Organization Name and Address	11. Contract or Grant No.
State University of New York at Albany Atmosphere Sciences Research Center 1400 Washington Avenue Albany, New York 12222	NSG-3138
	13. Type of Report and Period Covered
12. Sponsoring Agency Name and Address	Contractor Report
National Aeronautics and Space Administration Washington, D. C. 20546	14. Sponsoring Agency Code 505-40-22 (E-1599)

15. Supplementary Notes

Final report. Project Manager, James D. Holdeman, Aerothermodynamics and Fuels Division, NASA Lewis Research Center, Cleveland, Ohio 44135.

16. Abstract

This final report contains five independent contributions describing research activities at the Atmospheric Sciences Research Center of the State University of New York at Albany, which were performed using atmospheric constituent data obtained by the NASA Global Atmospheric Sampling Program. Chapter 1 surveys the characteristics of the particle size spectrum in various meteorological settings from a special collection of GASP data taken near the end of the program. Chapter 2 describes further analysis of that subset which examine the relationship between humidity and cloud particles. Chapter 3 reports on climatological and case studies of tropical ozone distributions measured on a large number of flights over the course of the entire program. Finally Chapters 4 and 5 discuss particle counter calibrations as well as the comparison of GASP particle data in the upper troposphere with other measurements at lower altitudes over the Pacific Ocean.

17. Key Words (Suggested by Author(s))	18. Distribution Statement
Clouds; Atmospheric particles; Particle counters; Atmospheric ozone; Tropical ozone; Aircraft measurements; Global Atmospheric Sampling Program (GASP); Meteorological parameters	Unclassified - unlimited STAR Category 47

19. Security Classif. (of this report)	20. Security Classif. (of this page)	21. No. of Pages	22. Price*
Unclassified	Unclassified	147	A07

* For sale by the National Technical Information Service, Springfield, Virginia 22161

NASA-Langley, 1983